

Abstract

Title of Document: THE CELL WALL LIPID PDIM MEDIATES PHAGOSOMAL ESCAPE AND HOST CELL EXIT OF *MYCOBACTERIUM TUBERCULOSIS*

Jeffrey Quigley, Doctor of Philosophy, 2016

Directed by: Associate Professor, Volker Briken, PhD
Cell Biology and Molecular Genetics

Mycobacterium tuberculosis (Mtb) has a complex interaction with host cell death signaling pathways. Mtb inhibits apoptosis at early stages of infection but transitions to promote necrosis at later stages of infection to allow for host cell exit. Mtb phagosomal escape has proven to be a crucial step in the transition to the pro-necrotic phase of infection. However, Mtb phagosomal escape is poorly understood. Previously, we described a transcriptional repressor, Rv3167c that regulates Mtb phagosomal escape and necrosis induction. Mtb Δ Rv3167c demonstrates increased phagosomal escape accompanied by increased necrosis induction in infected macrophages. Here, we show that Mtb Δ Rv3167c over expresses the Mtb virulence lipid phthiocerol dimycocerosates (PDIM) and the over expression of PDIM is responsible for the increased necrosis seen in Mtb Δ Rv3167c. Further, we demonstrate that PDIM contributes to the phagosomal escape of Mtb. This work ascribes a novel, and crucial, role of PDIM in Mtb pathogenesis.

THE CELL WALL LIPID PDIM MEDIATES PHAGOSOMAL ESCAPE AND HOST
CELL EXIT OF *MYCOBACTERIUM TUBERCULOSIS*

By

Jeffrey Quigley

Dissertation submitted to the Faculty of the Graduate School of the
University of Maryland, College Park, in partial fulfillment
of the requirements for the degree of
Doctor of Philosophy
2016

Advisory Committee:

Associate Professor Volker Briken, PhD, Chair

Professor Najib El-Sayed, PhD

Professor Kevin McIver, PhD

Professor Daniel Stein, PhD

Professor Lyle Isaacs, PhD, Deans Representative

© Copyright by

Jeffrey Quigley

2016

Table of Contents

Table of Contents	ii
List of Figures	iv
List of tables	v
List of abbreviations	vi
Chapter 1: Introduction	1
1.1 Tuberculosis	1
1.1.2 Causative agent	1
1.1.3 Disease Progression	2
1.1.4 Treatment	3
1.2 Immune response to Mtb	6
1.3 Mtb-mediated evasion of phagosomal defense mechanisms	7
1.3.1 Mtb phagosomal escape	8
1.4 Host cell death modulation by Mtb	10
1.4.1 Mtb targeted innate immune signaling	10
Apoptosis	10
Autophagy	11
Necrosis	16
1.5 Mtb Transcriptional Regulation	18
1.5.1 TetR-like family of transcriptional regulators	20
1.6 Mycobacterial cell wall	23
1.6.1 Virulence lipids of Mtb and their role in pathogenesis	24
1.6.2 PDIM	29
PDIM Synthesis	29
PDIM contributions to cell wall integrity	32
PDIM contributions to Mtb virulence	34
1.7 Summary	36
Chapter 2: Materials and Methods	37
Chapter 3: Rv3167 regulates the virulence lipid PDIM	44
3.1 Introduction	44

3.2 Results	45
3.2.1 Establishing the Rv3167c regulon	45
3.2.2 RNAseq reveals up-regulation of PDIM synthesis genes in MtbΔ <i>Rv3167c</i>	47
3.2.3 PDIM is responsible for the increased necrosis induction of MtbΔ <i>Rv3167c</i>	50
3.2.4 PDIM contributes to autophagy induction and phagosomal escape in Mtb	51
3.3 Discussion	57
Chapter 4: Rv3167c is a TetR-like transcriptional regulator	60
4.1 Introduction	60
4.2 Results	61
4.2.1 Rv3167c has the characteristics of a typical TetR-like transcriptional regulator	61
4.2.2 Identification of Rv3167c binding sites	64
4.2.3 Identifying the Rv3167c inducing ligand	70
4.2.4 Genes directly regulated by Rv3167c do not contribute to increased necrosis	74
4.2.5 MtbΔ <i>Rv3167c</i> is resistant to kanamycin	75
4.3 Discussion	82
Chapter 5: Discussion and Future Directions	88
5.1 Rv3167c regulation of the PDIM operon	88
5.2 PDIM contribution to Mtb phagosomal escape	90
References	96
Appendix A: Primers used in this study	107
Appendix B: Rv3167c regulated genes list-as determined by RNAseq	110

List of Figures

Fig. 1: Possible outcomes of Mtb infection.....	5
Fig. 2: Apoptotic signaling pathways.....	13
Fig. 3: Overview of non-selective and selective autophagy.....	15
Fig. 4: Regulation of <i>E. coli</i> TetR.....	22
Fig. 5: The mycobacterial cell wall.....	25
Fig. 6: Localization of Mtb virulence lipids.....	27
Fig. 7: Structure of mycobacterial PDIM and PGL.....	31
Fig. 8: PDIM operon and synthesis.....	33
Fig. 9: RNAseq analysis reveals an extensive Rv3167c regulon.....	46
Fig. 10: Mtb Δ Rv3167c over expresses the Mtb virulence lipid PDIM.....	49
Fig. 11: PCR confirmation of <i>mmp17</i> knockouts.....	52
Fig. 12: PDIM contributes to induction of host cell necrosis by Mtb.....	53
Fig. 13: PDIM is necessary for host cell autophagy induction and phagosomal escape of Mtb.....	55
Fig. 14: EsxA secretion is maintained in Mtb <i>mmp17::TN</i>	56
Fig. 15: Rv3167c is a TetR-like transcriptional regulator.....	62
Fig. 16: <i>Rv3168</i> and <i>Rv3169</i> are up-regulated in Mtb Δ Rv3167c.....	65
Fig. 17: Identification of additional Rv3167c binding sites.....	68
Fig. 18: Luciferase based reporter system to identify Rv3167c ligand.....	71
Fig. 19: Confirmation of <i>Rv3168-Rv3169</i> and <i>moeW</i> knockouts and MetS over-expression.....	76
Fig. 20: Genes directly regulated by Rv3167c do not contribute to increased necrosis.....	77
Fig. 21: Mtb Δ Rv3167c demonstrates resistant to kanamycin.....	79
Fig. 22: Possible mechanisms of PDIM contribution to Mtb phagosomal escape.....	94

List of tables

Table 1. Regulated cell death modes.....	12
Table 2: GO term enrichment of <i>MtbΔRv3167c</i> differentially regulated genes.....	48
Table 3: Gel filtration chromatography analysis of Rv3167c dimerization.....	63
Table 4: Putative Rv3167c binding sites as determined by ChIPseq.....	67
Table 5: Summary of Rv3167c binding sites based on EMSA	69
Table 6: Summary of potential Rv3167c ligands tested	73
Table 7: <i>MtbΔRv3167c</i> antibiotic resistance is limited to the aminoglycosides.....	80

List of abbreviations

BCG	Bacille Calmette Guerin
CLR's	C-type lectin receptors
CpnT	Channel protein with necrosis inducing toxin
DAMP's	Danger associated molecular patterns
DAT	Di-acyltrehalose
DHFR	Dihydrofolate reductase
DISC	Death inducing signaling complex
EEA1	Early endosomal antigen 1
EMSA	Electromobility Shift Assay
FPLC	Fast Protein Liquid Chromotography
GO	Gene ontology
HTH	Helix-turn-helix
IFN γ	Interferon γ
iNOS	Inducible nitric oxide synthase
ITC	Isothermal Titration Calorimetry
LAM	Lipoarabinomanna
LXA4	Lipoxin A4
ManLAM	Mannose capped lipoarabinomannan
MDR-TB	Multi-drug resistant
MPFC	Mycobacterial Protein Fragment Complementation
Mtb	<i>Mycobacterium tuberculosis</i>
MTBC	<i>Mycobacterium tuberculosis</i> complex
NLR's	NOD like receptors
PAMP's	Pathogen associated molecular patterns
PAT	Poly-acyltrehalose
PDIM	Phthiocerol dimycocerosates
PGE2	Prostaglandin E2
PGL	Phenolic glycolipid
PI	Propidium Iodide
PIM	Phosphoinositol mannosides

PKS	Polyketide synthases
RIPK1	Rest in peace kinase 1
RIPK3	Rest in peace kinase 3
RNI	Reactive nitrogen intermediates
ROS	Reactive oxygen species
SL-1	Sulfolipid-1
STPK	Serine threonine protein kinases
TB	Tuberculosis
TCS	Two component systems
TDM	Trehalose dimycolate
TDR-TB	Totally drug resistant Tuberculosis
TEM	Transmission electron microscopy
TFTR	Tetracycline Repressor like family of transcriptional regulators
TLC	Thin Layer Chromotograh
TLR's	Toll like receptors
TNF	Tumor necrosis factor
XDR-TB	Extremely drug resistant Tuberculosis

Chapter 1: Introduction

1.1 Tuberculosis

Tuberculosis (TB) is an ancient disease, plaguing mankind for centuries. Archaeological remains support the ancient association of TB with humanity as DNA from the *Mycobacterium tuberculosis* complex has been recovered from approximately 9000 year old neolithic remains (1). Otherwise known as the white plague, TB was the leading cause of death by an infectious agent in pre-antibiotic 19th and 20th century industrialized countries. With the emergence of vaccines and antibiotic strategies to combat the disease, TB became manageable. However, the WHO estimates that currently one third of the world's population is infected with TB resulting in 1.8 million deaths (WHO). Most of these deaths occur in developing countries without access to proper treatment, where the disease remains endemic.

1.1.2 Causative agent

Human TB is caused by the bacterium *Mycobacterium tuberculosis* (Mtb) first described by Robert Koch in 1882 (3). Mtb is a Gram positive organism, with a genome rich in guanine and cytosine, belonging to the phylum actinobacteria. Among the genus *Mycobacterium*, Mtb belongs to a subgroup collectively referred to as the *Mycobacterium tuberculosis* complex (MTBC). Members of this complex include the human pathogens *Mycobacterium canetti* and *Mycobacterium africanum*, *Mycobacterium bovis*, which is the cause of bovine tuberculosis, and *Mycobacterium microti* and *Mycobacterium pinnipedii*, which afflict voles and seals, respectively (4). While *Mycobacterium marinum* (*M. marinum*) is not a member of the MTBC, it has nonetheless proved useful as it causes disseminating disease in its natural host, fish and frogs, informing research about Mtb

pathogenesis (5,6,7). Mtb was thought to have arisen from a zoonotic transmission of *M.bovis* from cows to humans based on evidence that human TB was coincident with animal domestication around 10,000 years ago. However, more recent comparative genomic analysis studies indicate that Mtb arose approximately 70,000 years ago, co-evolving and dispersing along with humans (8).

1.1.3 Disease Progression

Mtb is spread from host to host through aerosol droplets when a person with active TB coughs or sneezes. Following inhalation, the pathogen gains access to the relatively sterile lower lobes of the lung where it encounters and infects neighboring phagocytes (9). The dose needed to result in a successful Mtb infection is estimated to be as low as a single bacillus. Alveolar macrophages are widely considered the preferred host cell for Mtb and as such are the predominant lung cell initially infected. However, there have been reports suggesting that Mtb can infect dendritic cells in the murine lung (10). After the initial infection of an alveolar macrophage, there are several possible outcomes. The first being clearance of the pathogen early on by the innate immune response. This typically occurs when the first encountered phagocyte is not naïve, *i.e.* it has been activated and producing reactive nitrogen species. This outcome results in no symptoms of infection and does not initiate an adaptive immune response. The second possible outcome is the establishment of a latent form of the disease. In this case, the innate immune response is unable to eliminate Mtb. A localized inflammatory response is induced which recruits immune cells to the site of infection. This allows for cross presentation of Mtb antigens to recruited lymphocytes and results in the activation of an adaptive immune response. The ultimate outcome of this form of the disease is the

formation of the granuloma, the hallmark of tuberculosis infection. The granuloma is a compact aggregate of immune cells. At its core are infected macrophages. Surrounding the core are cells in varying degrees of differentiation, including foamy lipid rich macrophages, epitheloid cells (a uniquely differentiated macrophage), and multinucleate giant cells (11). The entire structure is enclosed in a ring of lymphocytes. The granuloma is regarded as a last defense and a way to ‘wall-off’ the infection as the granuloma does not actually lead to the elimination of the pathogen. Within the granuloma, Mtb enters a low replicative state of persistence and can remain in this state for decades. Latency is the most common form of the disease and occurs in a majority of TB cases. These individuals show no outward signs of infection and are generally considered to be non-infectious. The final form is active disease. This can occur soon after initial exposure to Mtb in immunocompromised individuals or can be a result of reactivation of latent infection. In this state of infection, Mtb is actively dividing. The granuloma becomes necrotic and begins to break down in a process known as caseation. This allows Mtb access to the airways whereby infected individuals can disseminate the pathogen through coughing and sneezing, and are considered infectious. Transition to active disease is associated with changes in immune status of the host from healthy to a number of immunocompromised states, most notable HIV infection, old age, or malnutrition (Figure 1). (12,9,10,13).

1.1.4 Treatment

The first effective drug against Mtb infection was streptomycin, discovered by Selman Waksman during the Second World War (3). Streptomycin gave way to isoniazid in the 1950’s, the first oral antibiotic effective against Mtb. The current treatment,

adopted in the 1970's, comprises four first line drugs-isoniazid, rifampicin, pyrazinamide and ethambutol. Treatment consists of a two month intensive phase where all four drugs are administered, followed by a continuation phase with isoniazid and rifampicin lasting an additional 6-9 months. Isoniazid and ethambutol target the mycobacterial cell wall, inhibiting production of mycolic acid and arabinogalactan, respectively. Rifampicin targets RNA polymerase and inhibits protein synthesis, while pyrazinamide is believed to target fatty acid synthesis (14). The prolonged treatment regime and high toxicity of the drugs leads to issues with patient compliance. While direct observational therapy is mandated for TB treatment, in the parts of the world where TB is endemic this is hard to enforce. This ultimately leads to the emergence drug resistance in the form of Mtb causing multi-drug resistant (MDR-TB) and extremely drug resistant (XDR-TB) infections (14). Treatment of either of these forms of TB require the use of third line drugs, which are expensive and associated with more side effects than both the first and second line treatments (14). More recently, totally drug resistant TB (TDR-TB) strains resistant to all available first and second line drugs have been reported in Iran and India (15). In the face of the growing prevalence of drug resistant strains, there has been a significant effort to develop new antibiotics effective against TB.

There is only one current vaccine in use for TB, the Bacille Calmette Guerin (BCG) vaccine. BCG is a live attenuated vaccine and was generated by Albert Calmette and Camille Guerin in 1919 at the Institute Pasteur in France by the repeated subculturing of *M.bovis in vitro* (16). BCG prevents pediatric complications from Mtb infection in children. However, it fails to prevent TB in adults. This is believed to be the result of a waning of the cellular immune response over time as the individual ages. BCG is also

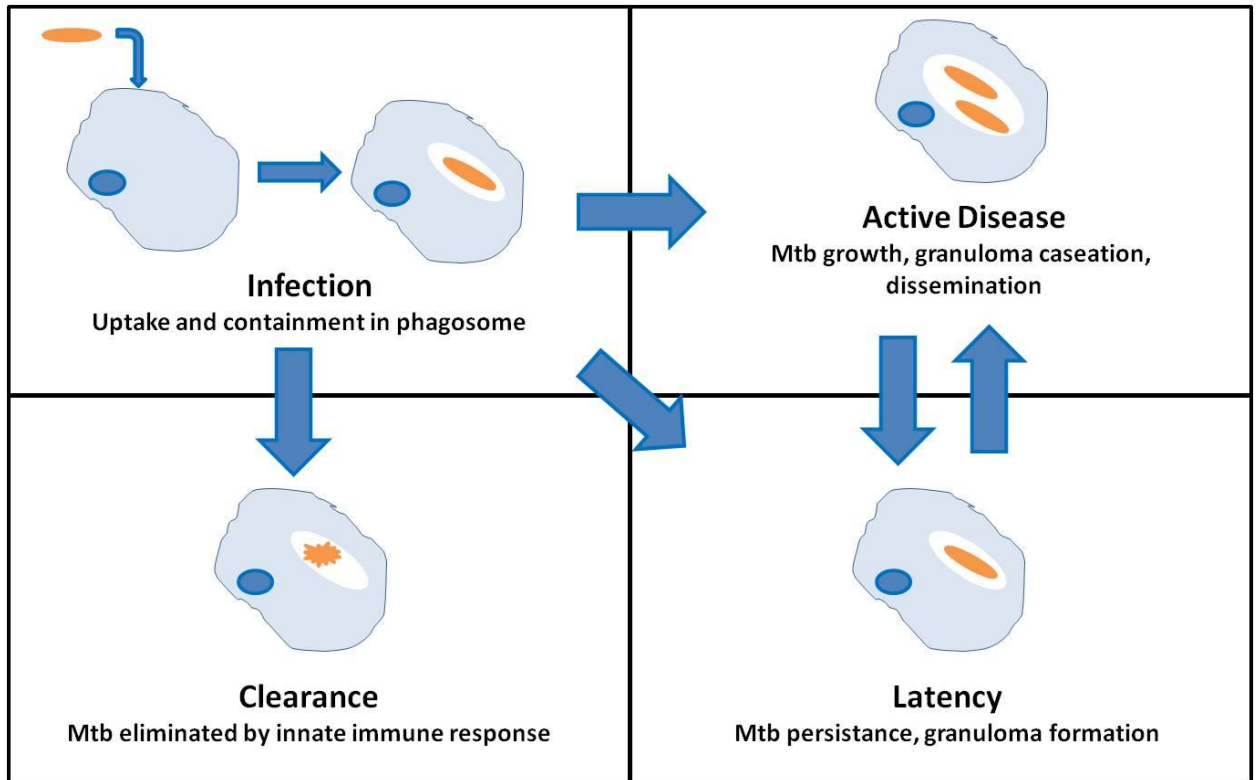


Fig. 1: Possible outcomes of Mtb infection

Three possible outcomes may follow infection of the host by Mtb. In some cases, the innate immune response may successfully eliminate the pathogen leading to clearance of infection. More commonly, the bacteria multiply within the host cells leading to development of a localized inflammatory response, immune cell recruitment and eventually activation of the adaptive immune response. These events lead to formation of the granuloma. Bacteria located within the granuloma enter into a persistent state and a latent, asymptomatic infection develops. In about 5-10% of latently infected individuals disease reactivation occurs, characterized by multiplication of bacteria located within the granuloma and tissue necrosis. Under some conditions (*eg*: immunodeficiency), active disease may develop immediately after infection bypassing the latent stage.

Adapted from (12).

ineffective in individuals that have been previously exposed to mycobacteria in the environment or through prior vaccination, the latter ruling out the possibility of booster doses of the vaccine in older individuals. With the emergence of HIV, another issue that has arisen is the increased risk of HIV positive children developing disseminated disease following BCG vaccination (3). Current efforts are aimed at improving the long term protection afforded through the current BCG vaccine as well as attenuated Mtb based and subunit based vaccines (12,3).

1.2 Immune response to Mtb

Mtb infection can hardly be considered immunologically silent. In fact, infection with active Mtb results in a hyperinflammatory response both locally and globally (17). Mtb is recognized by macrophage mannose receptor and complement receptor leading to the engulfment of the bacterium (18). In addition to these receptors, Mtb is also recognized by various toll-like receptors (TLR's), C-type lectin receptors (CLR's) and NOD-like receptors (NLR's). The Mtb ligands heat shock protein 65 KDa (Hsp65), 19 KDa lipoprotein and lipoarabinomanna (LAM) are recognized by TLR2 present on the macrophage surface. TLR2-mediated recognition of Mtb leads to the production of pro-inflammatory cytokines such as tumor necrosis factor (TNF) and IL6. Recognition by TLR's is a crucial component of the host immune response to Mtb as mice deficient in the downstream signaling adaptor MyD88 are extremely susceptible to Mtb infection (18). Activation of cytosolic NLR's has also been shown to be extremely important in the host response to Mtb. NLR's form part of complexes known as inflammasomes assembled in response to detection of pathogen associated molecular patterns (PAMP's) and danger associated molecular patterns (DAMP's) present in the cytosol and are

required for activation of caspase1 and subsequent cleavage of the pro-inflammatory cytokines IL1 β and IL18 into their active forms. A plethora of cytokines are released in response to Mtb infection. However, few play as dominant a role as TNF, IL1 β , and interferon γ (IFN γ). Animals deficient in TNF or IL1 β exhibit increased mortality to Mtb infection (19,20).

The adaptive immune response against Mtb is driven mainly by T-lymphocytes. Both CD4⁺ helper T cells and CD8⁺ cytotoxic T cells are involved in the control of Mtb infection, deficiency of either of the cell types results in mortality of infected mice (18,13). The cytokine response elicited by Mtb shapes the adaptive immune response against the pathogen. Following antigen presentation in association with Class II MHC molecules, CD4⁺ T cells can acquire a Th1 or a Th2 phenotype. Both CD4⁺ and CD8⁺ cells migrate to the lungs and produce the cytokine IFN γ . IFN γ activates the infected macrophages leading to increased killing of phagocytosed mycobacteria. This is achieved by upregulating expression of the enzyme inducible nitric oxide synthase (iNOS) and increasing generation of reactive nitrogen intermediates (RNI) in the infected macrophages. Antigen presentation by infected cells is also enhanced following exposure to IFN γ as it upregulates expression of MHC genes (18,13,9).

1.3 Mtb-mediated evasion of phagosomal defense mechanisms

Mtb has several ways whereby it can inhibit host immune responses. The key first step in this process is gaining access to the relatively sterile distal lobes of the lung. Co-infection studies of *M. marinum* with *S. aureus* or *P. aeruginosa* demonstrated that the presence of commensals and environmental microbes in the upper airways leads to the recruitment of microbicidal macrophages with increased iNOS activity. In contrast, more

permissive macrophages are recruited actively by mycobacteria in the distal regions of the lungs (5). During phagocytosis of Mtb, macrophages generate reactive oxygen species (ROS) in the phagosome (21). Mtb produces antioxidants such as superoxide dismutases SodA and SodC, and the catalase KatG, to counter phagosomal ROS. ROS may exert direct microbiocidal effects on Mtb making controlling ROS generation essential. Following uptake by phagocytic cells, Mtb resides in a compartment that resembles the early endosome. Mtb-mediated phagosomal arrest is dependent on inhibition of Rab7 recruitment. The secreted Mtb effectors PtpA and Ndk prevent Rab7 activation and convert active GTP bound Rab7 to its inactive GDP bound form (18,13,22). Recruitment of the host protein coronin1 to live Mtb-containing phagosomes is also implicated in inhibition of phagosome fusion with lysosomes (23). Mtb also secretes the phosphatase SapM that dephosphorylates host phosphatidylinositol-3-phosphate, resulting in phagosomal maturation arrest (24). While inhibition of host phagolysosome fusion is obviously beneficial to Mtb survival, recent studies using *M. marinum* suggest *Mycobacterium* experience acid stress *in vivo* and can survive in the lysosome. In resting macrophages, a significant portion of *M. marinum* get delivered to the lysosome, but are not killed as a direct result of the membrane serine protease MarP (25).

1.3.1 Mtb phagosomal escape

While classical literature supported the view that Mtb remained within the modified early endosome-like compartment at all times, more recent reports have emerged demonstrating that Mtb eventually escapes from the phagosome to the cytosol (26). The intracellular location of bacteria has important consequences for their

recognition by the host and the generation of innate and adaptive immune responses. Mtb was long thought to reside exclusively within a vacuole that has the characteristics of an early endosomal compartment (13,18). However, it is now evident that Mtb also escapes the phagosome to reach the host cell cytosol (27-29). In the common laboratory strain H37Rv, phagosomal escape occurs later in infection, between 4-5 days, than what is reported for other intracellular pathogens (30). However, this isn't the case for all strains of Mtb. A study of various clinical isolates determined that the kinetics of phagosomal escape are variable, with some strains escaping the phagosome almost immediately after establishing infection (31). This process was shown to involve the host phospholipase A2 (31). Interestingly, necrosis induction by Mtb was shown to closely follow escape to the cytosol (27,32), suggesting escape from the phagosome is a pre-requisite to Mtb dissemination. Phagosomal escape is not unique to Mtb. In fact it has been known for some time that the closely related *M. marinum* accesses the cytosol early in infection (33). Perhaps the pathogen with the most well characterized escape mechanism is *L. monocytogenes*, which coordinately uses the pore-forming toxin LLO as well the secreted phospholipases PlcA and PlcB to escape the phagosome (34). *S. flexneri* also encodes a pore forming toxin, IpaBC, that is involved in phagosomal escape, while the intracellular pathogen *R. prowazekii* secretes multiple phospholipases that aid in cytosolic translocation (34). The effector molecules that facilitate Mtb cytosolic translocation remain largely undefined. The Mtb type VII secretion system ESX-1 and the secreted pore forming effector EsxA are required for Mtb phagosomal escape (27). Mtb also expresses multiple phospholipases that may play a role in phagosomal membrane rupture (28).

1.4 Host cell death modulation by Mtb

Elimination of infected host cells by apoptosis is yet another innate immune mechanism that Mtb interferes with to avoid clearance. Mtb inhibits cell death via apoptosis to avoid both direct bactericidal effects of the process and via efferocytosis (35). Additionally, uptake of Mtb antigens via phagocytosis of apoptotic bodies by dendritic cells allowed for the presentation of extracellular antigens to CD8+ T cells through cross presentation (36). While it inhibits apoptosis, Mtb induces cell death via necrosis. Discussion of host cell death pathways and their modulation by Mtb is discussed below.

1.4.1 Mtb targeted innate immune signaling

The earliest classification of cell death was based on morphology and three types of cell death were identified; type I, type II and type III, which today are referred to as apoptosis, autophagy associated cell death and necrosis, respectively (37). Historically, apoptosis was considered to be the only regulated cell death mechanism, while necrosis was thought to be an accidental form of cell death. Accumulated evidence now suggests this was a severe over simplification of cell death modalities. The most recent classifications of cell death are based on biochemical parameters with five categories of cell death recognized (Table 1) (38,39).

Apoptosis

An apoptotic cell is defined by a set of distinct morphological features. Nuclei of apoptotic cells undergo condensation and fragmentation (40). Apoptotic cells shrink and plasma membrane blebbing is observed; however, plasma membrane integrity is not affected. Because cell contents are contained within apoptotic bodies, apoptosis is

generally considered to be immunologically silent (41,42). Apoptosis pathways can be classified into two categories – extrinsic and intrinsic. Extrinsic apoptotic pathways are initiated in response to interaction of death receptors belonging to the TNF receptor superfamily with their cognate ligands. Intrinsic apoptotic pathways are activated in response to changes in the equilibrium between pro and anti-apoptotic members of the Bcl2 family induced by stimuli such as oxidative stress, genotoxic stress, UV light etc. Both pathways lead to the activation of initiator caspases. In the extrinsic pathway, a death inducing signaling complex (DISC) is formed that recruits the initiator caspase 8 leading to its oligomerization, autoprocessing and activation. In the intrinsic pathway, the preponderance of pro-apoptotic Bcl2 family members leads to mitochondrial outer membrane permabilization and release of cytochrome C from the mitochondrial intermembrane space to the cytosol ultimately resulting in activation of caspase 9. Activated initiator caspases lead to the cleavage and activation of the effector caspases 3, 6 and 7 that target a vast array of proteins and lead to execution of apoptosis (Figure 2) (36,38,41).

Autophagy

Autophagy is an evolutionarily conserved catabolic process that involves sequestration of cytosolic contents into *de novo*-generated double membrane vesicles termed autophagosomes. Subsequent fusion of autophagosomes with lysosomes leads to degradation of autophagosomal contents (44,45). Autophagy induction is achieved by both intracellular and extracellular stresses such as amino acid starvation, growth factor deprivation, reduced ATP levels, ER stress, hypoxia, oxidative stresses and microbial invasion (46). Autophagy can be non-selective where random areas of the cytosol are

Alternate names	Caspase requirement	Biochemical features	
Extrinsic apoptosis	+	Death receptor signaling, activation of caspases 3,6,7,8	
Intrinsic apoptosis	+	MOMP, activation of caspase 3,6,7,9	
Autophagic cell death	-	Accompanies autophagy, LC3 lipidation	
Mitotic catastrophe	-	Mitotic arrest, caspase 2 activation in some cases	
Regulated necrosis			
RIPK1 and RIPK3 dependent	Necroptosis	-	RIPK1 & RIPK3 phosphorylation and activation.
Inflammasome dependent cell death	Pyroptosis	+	Caspase 1 activation, accompanied by IL1 β and IL18 secretion
Inflammasome dependent cell death	Pyronecrosis	-	Dependent on cathepsin activity and activation of inflammasomes but independent of caspase 1 activity, accompanied by IL1 β and IL18 secretion
PARP1 dependent cell death	Parthanatos	-	PARP1 activation, PAR generation, Translocation of mitochondrial AIF to nucleus
NETosis		-	NADPH oxidase activation, release of extracellular traps composed of histones and chromatin
Ferroptosis		-	Reported to occur in tumor cells via inhibition of Cys/Glu antiporter, dependent on decreasing concentration of glutathione and ROS generated by Fenton reactions occurring in lysosomes
Oxytosis		-	Reported to occur in neurons via inhibition of Cys/Glu antiporter, dependent on glutathione and mitochondrial ROS
CypD dependent necrosis		-	Dependent on CypD mediated opening of MPTP, loss of mitochondrial membrane potential
Entosis		-	RHO and ROCK activation

Table 1. Regulated cell death modes

Abbreviations: MOMP- mitochondrial outer membrane permeabilization; RIPK – rest in peace kinase; PARP1 – poly ADP ribose polymerase 1; PAR – poly ADP ribose; AIF – apoptosis inducing factor; CypD – cyclophilin D; MPTP – mitochondrial permeability transition pore; ROCK1 – RHO associated coiled coiled containing protein kinase.

Adapted from (38,39).

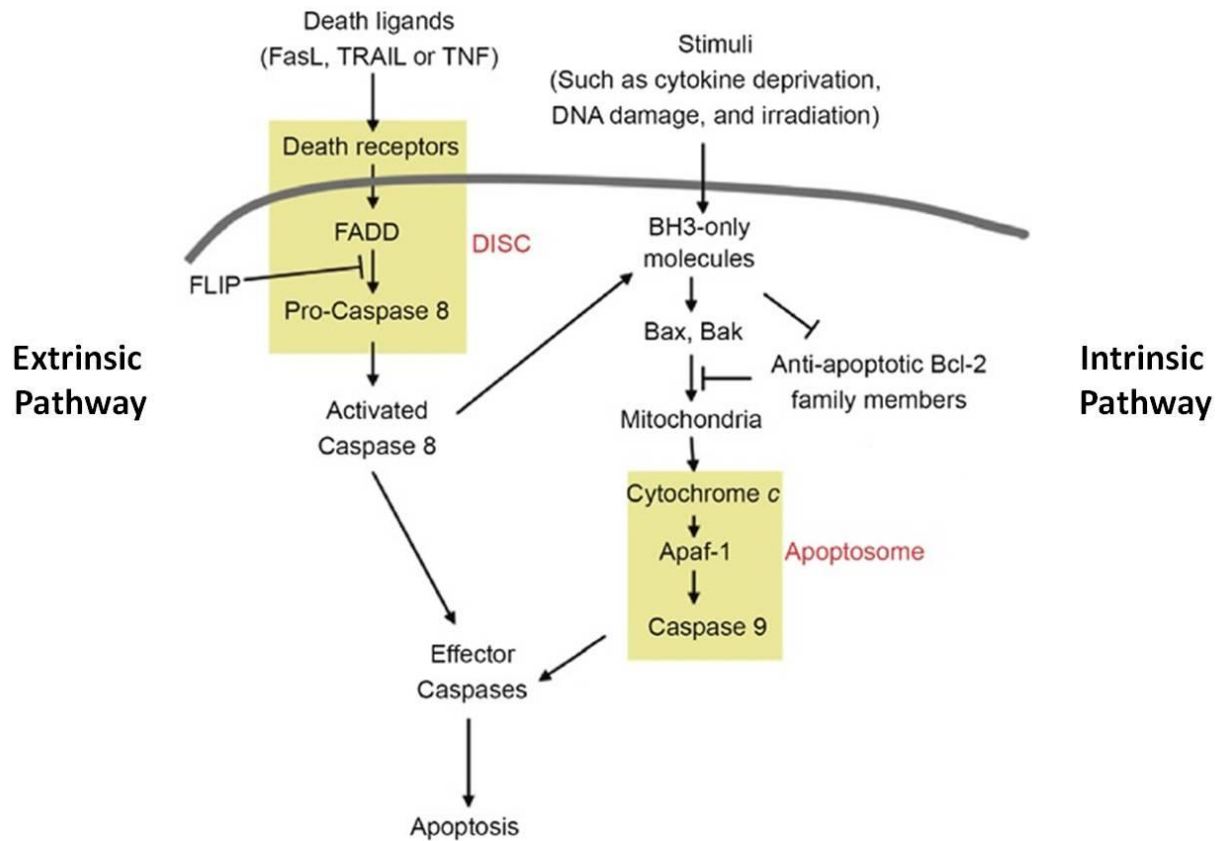


Fig. 2: Apoptotic signaling pathways

The extrinsic apoptotic pathway is activated following recognition of death ligands by their cognate receptors. This results in formation of DISC and cleavage and activation of the initiator caspase 8. The intrinsic apoptotic pathway is activated in response to stimuli that lead to a preponderance of the pro-apoptotic Bcl2 family members. This leads to cytochrome C leakage from mitochondria, formation of apoptosome complex in the cytosol and cleavage and activation of the initiator caspase 9. Activated initiator caspases cleave and activate the effector caspases 3, 6 and 7 that in turn target different host molecules and lead to development of characteristic features of apoptotic cell death.

Abbreviations: FasL-fas ligand, TRAIL-TNF related apoptosis inducing ligand, DISC-death inducing signaling complex, FADD-Fas associated death domain, Apaf1-apoptosis associated factor 1

Adapted from (43).

engulfed within the autophagosome in a process termed macroautophagy. Alternatively, cargo may be specifically targeted to the autophagosomes in selective autophagy. Based on the cargo, selective autophagy may be of different types – mitophagy (mitochondria), reticulophagy (ER membranes), xenophagy (micro-organisms) (Figure 3)(47). Apart from directly killing micro organisms by directing them to lysosomal compartments, autophagy also serves to deliver cytosolic PAMP's to endosomes harboring cytosolic PRR's, resulting in generation of innate immune responses (48). Recent studies have shown that Mtb in the absence of other stimuli induces autophagy. A comparative study of autophagy induction by mycobacterial species demonstrated an inverse relationship between autophagy induction and bacterial virulence in macrophages (49). Autophagy induction is associated with anti-mycobacterial effects. Treatment of infected macrophages with autophagy inducing stimuli results in increased killing of mycobacteria (50-52). The ability of autophagy to overcome the phagolysosome biogenesis block exerted by Mtb and to deliver bacteria to the lysosomal compartments is thought to underly the mycobactericidal effects of autophagy (49,52). The ability of Mtb to induce autophagy in macrophages was linked to EsxA production; a lower percentage of *esxA* mutant bacteria colocalized with autophagosomal markers compared to wild type Mtb (32). The mycobacterial lipoprotein LpqH has also been implicated in Mtb-mediated autophagy induction in human macrophages (51,53). While evidence exists demonstrating that Mtb induces selective autophagy, there are reports that indicate that the pathogen possesses the ability to inhibit autophagy. The Mtb protein Eis has been implicated in this process as an *eis* mutant induces higher levels of autophagy compared

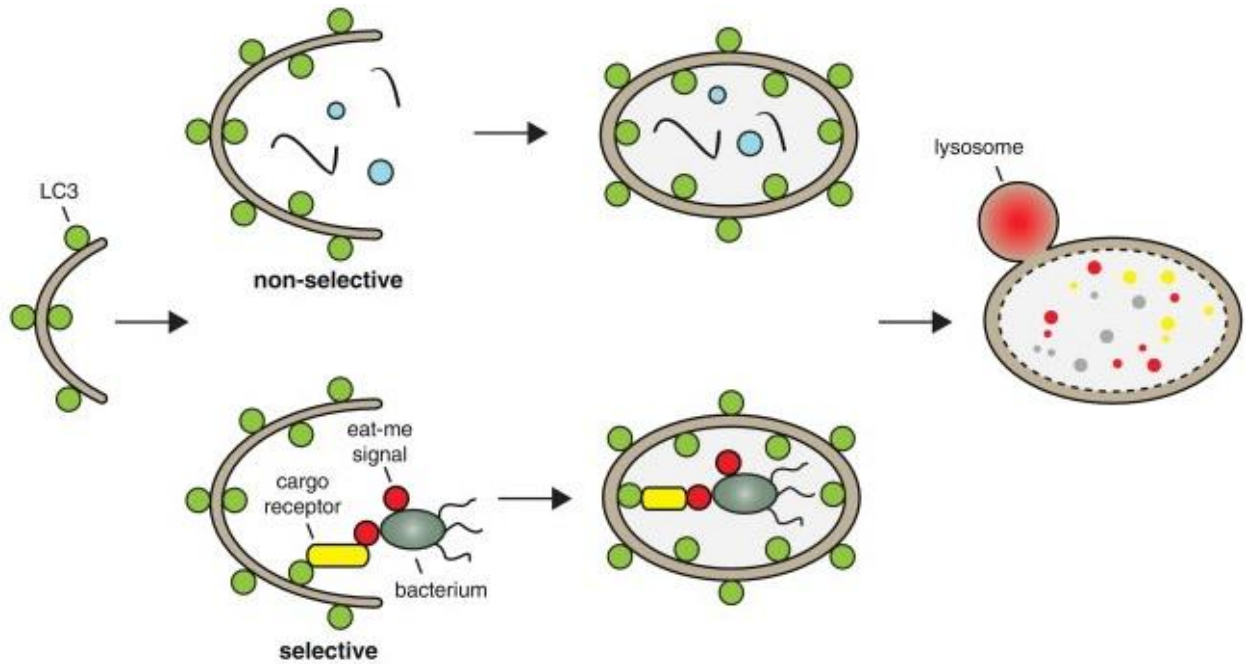


Fig. 3: Overview of non-selective and selective autophagy

Cytosolic material is captured in a non-specific manner in non-selective or macroautophagy. Specific cargo receptors are involved in selective autophagy with xenophagy of a bacterium being depicted in this image. The captured material is encapsulated in a double membrane autophagosome that eventually fuses with a lysosome leading to degradation of autophagosomal contents.

Adapted from (47).

to the WT control in a ROS- and JNK-dependent manner (54).

Necrosis

In contrast to apoptotic cells, nuclei of necrotic cells remain mostly unchanged. Transmission electron microscopy (TEM) studies show minor chromatin condensation to small irregular patches in necrotic cells, while in the case of apoptotic cells complete condensation to crescent shaped forms is observed. Necrosis is not considered immunologically silent as plasma membrane integrity is compromised resulting in release of cytosolic contents (41,42). Necrosis induction is independent of caspase activation (42). Historically, necrosis is thought of as an unregulated process akin to cell lysis due to some catastrophic event. However, this view has changed significantly as evidence has accumulated showing necrosis is indeed a regulated process. Several signaling modules leading to necrotic cell death have emerged in recent years with some signaling pathways being initiated in response to specific stimuli in certain cell types. Regulated necrosis is dependent on RIPK1 (rest in peace kinase 1) and/or RIPK3 (rest in peace kinase 3). It has been reported to be induced in response to signaling by death receptors, pattern recognition receptors as well in response to viral infections, and was called necroptosis (55).

While apoptosis induction is associated with a decrease in Mtb viability, cell death by necrosis does not affect Mtb viability. No changes in Mtb recovery from infected macrophages was observed following treatment with the necrosis inducer hydrogen peroxide, while apoptosis induction with ATP leads to loss of bacterial viability (56). Studies on susceptibility to Mtb of mouse mutants that lack genes contributing to necrosis induction or inhibition also indicate that necrosis induction is beneficial for the

pathogen rather than the host (57). Mtb-mediated necrosis has been shown to be dependent on production of the lipid mediator lipoxin A4 (LXA4) and consequent inhibition of prostaglandin E2 (PGE2) in infected macrophages (58). Mice made deficient in LXA4 production were found to be more resistant to Mtb infection. Conversely, deficiency in PGE2 rendered the mice more susceptible to Mtb infection (59,60). Modulation of eicosanoid (LXA4 and PGE2) production by Mtb leads to necrosis via three mechanisms – loss of mitochondrial membrane potential, inhibition of plasma membrane repair and inhibition of apoptotic envelope formation. Mtb infection results in production of LXA4 and subsequent inhibition of PGE2 synthesis favoring necrosis (61).

Mtb has two specialized secretion systems encoded by the ESX loci, ESX1 and ESX5 that transport proteins across its cell wall. EsxA, secreted through the ESX1 system, has been shown to form pores in artificial lipid bilayers as well in red blood cell membranes resulting in hemolysis (62-64). Both *ESX1* and *esxA* mutant strains have been shown to induce much lower levels of necrosis in infected macrophages compared to the wild type Mtb strain (65,66). It must be noted that EsxA is required for the secretion of other ESX1 substrates as well. Therefore, it is difficult to determine the contribution of EsxA itself in Mtb-mediated necrosis. The ESX5 locus is required for the transport of PE-PPE proteins and an Mtb ESX5 mutant strain was found to be deficient in necrosis induction (65). The requirement of the ESX5 locus to induce necrosis could possibly be due to its role in the secretion of the PE25/PPE41 complex as macrophages treated with the recombinant protein complex undergo necrosis (67). Ectopic expression of PE-PGRS33 protein in mammalian cells led to mitochondrial localization of the protein and

induction of necrosis (68). A recent study has implicated the Mtb CpnT (channel protein with necrosis-inducing toxin) protein encoded in necrosis induction. Increased levels of caspase 1, caspase 3 and RIPK1 independent cell death was observed in Jurkat T cells overexpressing the C terminal fragment of CpnT compared to control cells (69).

1.5 Mtb Transcriptional Regulation

Whether a bacterium is free living, symbiotic, or an opportunistic or professional pathogen, the key to survival is the ability to monitor and respond appropriately to varying external stimuli. In most bacteria, adaptation to a changing environment is mediated primarily through transcriptional regulation (70). Being an obligate intracellular pathogen, Mtb faces a tough uphill battle defending itself against various host innate and adaptive immune mechanisms, while at the same time attempting to shape the host environment into one suitable for replication and transmission. Transcriptional profiling indicates that intracellular Mtb faces a phagosomal environment that is oxidative, nitrosative, hypoxic, carbohydrate poor, and able to induce membrane stress (71). Mtb's ability to manage and interpret these varying signals and respond in a timely fashion is vital to successful infection. Mtb encodes roughly 214 putative DNA binding proteins (72). Recent efforts have been conducted to study the DNA-binding and transcriptional impact of each of these proteins (73). These studies demonstrated, perhaps unsurprisingly, that Mtb gene regulation is highly interconnected and redundant (72), hinting at a fine tuned transcriptome. Mtb, like many other bacteria, makes extensive use of sigma factors, two component systems (TCS), serine threonine protein kinases (STPK), and transcription factors to shape its transcriptome (74).

Mtb encodes 13 sigma factors that provide promoter specificity to the core RNA polymerase. The house keeping or principal sigma factor is SigA with a second principal sigma factor like SigB is almost identical to SigA. The other 11 sigma factors are extracytoplasmic sigma factors, which respond to external stimuli (75) and are proposed to be needed for varying responses to the intracellular host environment. The sigma factors themselves form an interconnected network of regulation defined by autoregulation and trans-regulation of other sigma factors (2). While sigma factors E, F, G, H, and J were all shown to be up-regulated in macrophages, only SigE and SigG were shown to be required for survival in macrophages (75). Also, deletion mutants of sigma factors C, D, E, F, and L have been shown to be attenuated to some degree in a mouse infection model (76-79).

Mtb also directly monitors its environment through the use of TCS, which consist of a membrane spanning sensor histidine kinase and a cytosolic response regulator (74). Mtb encodes 12 complete TCS of which two, MtrAB and PrrAB, are essential (74). Deletion of the TCS *senX3/regX3*, *dosRST*, *phoPR*, and *mprAB* results in attenuation in the mouse model of infection (74). Another method in which Mtb senses its environment is through STPK. Mtb has 11 known STPK of which none have had their stimulating ligand defined and only PknA and PknB are essential (80). The remaining STPKs have all been associated with virulence to some degree. Most notably, PknB, which phosphorylates the transcription factor EmbR resulting in a change in the ratio of LAM (81). Another Mtb STPK of note is PknE. PknE was shown to respond to changing NO conditions to influence host cell apoptosis (82).

By far the largest and most diverse group of transcriptional regulators in Mtb are the transcription factors. Mtb is predicted to encode 161 proteins with a helix-turn-helix (HTH) DNA binding motif (83). Of the 161 HTH containing proteins, 52 are predicted to be TetR-like transcription factors, making this group the most abundant group of transcription factors in Mtb, a characteristic shared by many other *Mycobacterial* species (83).

1.5.1 TetR-like family of transcriptional regulators

The Tetracycline Repressor (TetR)-like family of transcriptional regulators (TFTR) is well represented and widely distributed among bacteria (84). They are one of the most abundant types of transcriptional regulators utilized by bacteria (85). TFTR are broadly identified as having an N-terminal HTH DNA-binding domain and a C-terminal domain involved in dimerization and ligand binding (85,86). The N-terminal HTH DNA-binding domain is highly conserved and is what classifies a transcriptional regulator as a TFTR (84). Conversely, the dimerization and ligand binding domain is extremely diverse (86) owing to the broad range of ligands these regulators can respond too. TFTR typically act as repressors of transcription when not bound to their cognate ligand (87). Binding of an effector molecule at the c-terminal pocket induces a structural change in the protein resulting in release of the protein from DNA (86). Regulation of *E. coli* TetR is depicted in Figure 4, which represents the typical function of TFTR. TFTR typically bind small molecule ligands (84), although there are examples of binding to peptide (88) and lipid ligands (89). While many inducing ligands of TFTR are known, the vast majority of TFTR have no known ligand. Of the ~200,000 known bacterial TFTR in sequence databases, we know the inducing ligands for only 61 (83). TFTR act as homodimers,

binding palindromic operator sequences upstream of regulated genes restricting RNA polymerase from access to the genes promoter (84). TFTR are typically auto-regulatory in nature in addition to regulating genes that are usually in close proximity and divergently encoded in the genome although this is not always the case (152). TFTR originally were very closely associated with antibiotic resistance and regulation of antibiotic efflux pumps as is the case the namesake of the family, *E. coli* TetR (84). However, it is becoming clear that while these transcriptional regulators share a high degree of structural homology, they are extremely diverse in function (83). As more TFTR are being characterized, it is clear they control a diversity of regulated functions ranging from cellular and lipid metabolism to quorum sensing (83). There are examples of TFTR serving as activators of transcription, as is the case for DhaS from *L. lactis* (155), as well as TFTR that serve as local or global regulators such as AmtR from *C. glutamicum* (156). TFTR transcriptional regulators are as diverse in function as they are numerous throughout the bacterial kingdom.

As mentioned above, Mtb encodes 52 TFTR making them the most abundant family of transcriptional regulators in Mtb (83). As is the case within the broader family, TFTR in Mtb have broad functions such as antibiotic resistance, carbon metabolism, nitrogen metabolism, co-factor metabolism, and virulence. EthR behaves similarly to TetR and is associated with activation of ethionamide, a drug used in treatment of tuberculosis (90). The TFTR Rv3066 controls the expression of the gene *mmr*, encoding a multi-drug efflux pump conferring resistance to erythromycin and thioridazine (91). Interestingly, Mtb encodes a number of TFTR associated with the regulation of lipid metabolism. Two of the most well studied TFTR in Mtb are KstR and KstR2.

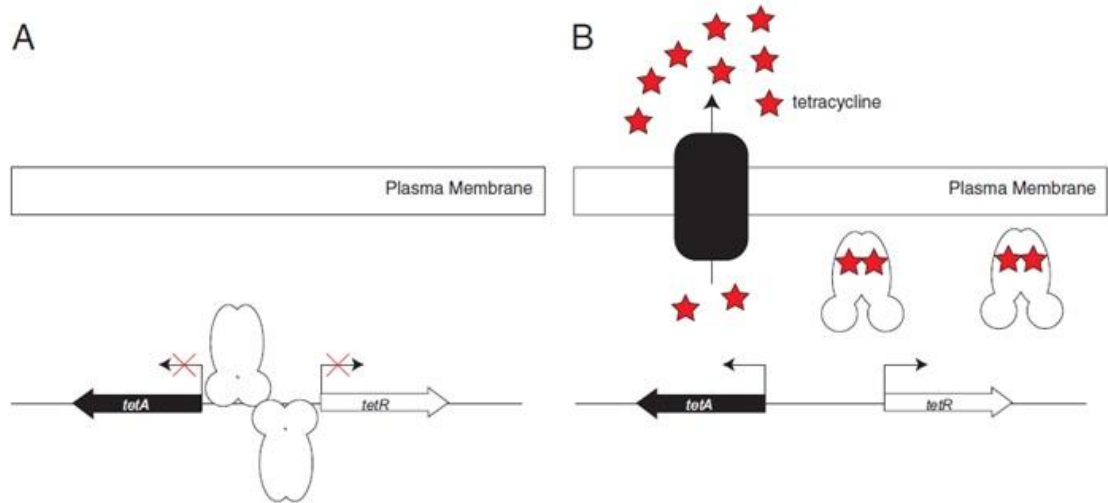


Fig. 4: Regulation of *E. coli* TetR

E. coli TetR is the founding member of the TFTR and demonstrates typical TFTR transcriptional regulation. A) When the inducing ligand tetracycline (red star) is not present, TetR binds to operator sequences within its own promoter and that of the neighboring gene TetA repressing transcription from both promoters. B) When tetracycline is present it binds to TetR inducing a structural change resulting in release of DNA and expression of both TetR and TetA, an efflux pump, which pumps the tetracycline out of the cell.

Adapted from (84).

Intracellular Mtb relies heavily on host lipids as a carbon source, specifically host cholesterol (92). KstR and KstR2 control the expression of genes needed for the catabolism of cholesterol (89). KstR has been shown to be up-regulated upon infection in macrophages as well as growth on cholesterol and is essential for virulence in a murine model of infection (89). The TFTR Mce3R controls a number of genes involved in lipid metabolism and redox reactions (93). The TFTR Rv0302 controls the expression of several mycobacterial membrane protein large (Mmpl) proteins known to be involved in transporting Mtb virulence lipids to the outer membrane (94). Rv0302 is one of six TFTR encoded by Mtb not found in the closely-related veterinary pathogen *M. bovis* including Rv0328, Rv0330c, Rv1534, Rv2160A, and Rv3160c (83). This suggest these transcriptional regulators control functions specific to Mtb pathogenesis and are thus interesting targets for future studies. Despite much work, the vast majority of TFTR in Mtb still have no assigned function.

1.6 Mycobacterial cell wall

While technically classified as a Gram-positive organism, Mtb cannot be stained by traditional gram-staining. Instead it must be stained using acid fast techniques such as Ziehl-Neelson staining. This is due in large part to the presence of an unusually lipid rich cell wall unique to the order *Actinomycetes*, which includes the genera *Mycobacterium*, *Rhodococcus*, *Corynebacterium* and *Nocardia* (95). When discussing *mycobacterial* species, this lipid rich cell wall structure is termed the mycomembrane (96). The mycomembrane is largely comprised of three distinct macromolecules-peptidoglycan, arabinogalactan, and mycolic acids-surrounded by a non-covalently linked capsule of protein, polysaccharides, and lipids unique to TB complex (Figure 5). The peptidoglycan

layer surrounds the plasma membrane much like other gram-positive bacteria and is comprised of long polymers of repeated N-acetyl glucosamine-N-acetyl muramic acid disaccharide linked by peptide bridges (95). Surrounding the peptidoglycan layer is the arabinogalactan layer. Repeating units of the disaccharide galactan are covalently linked to the N-acetylglucosamine subunits of the peptidoglycan layer. Galactan is subsequently modified with long arabinan polymers. There is variability in arabinosylation and some galactan chains remain free. Arabinan chain termini are branch and modified in the case of pathogenic mycobacteria by a galactosamine residue. Finally, most arabinan polymers are ligated to long chain mycolic acids which are responsible for the characteristic thick waxy coat of Mtb and are major contributors to cell wall permeability and virulence (98). Non-covalently embedded in the outer membrane, mycolic acid layer are Mtb-specific glycolipids with varying contributions to virulence (Figure 6). These lipid species are discussed further below.

1.6.1 Virulence lipids of Mtb and their role in pathogenesis

From the earliest investigations into the virulence of Mtb, it was recognized that the unique cell envelope of this organism confers the fundamental basis of its ability to modulate host immunity (99). The effectiveness of Mtb as an immunological adjuvant was found to result from properties of components of the cell envelope. The adjuvant referred to as Freund's adjuvant is comprised of heat killed Mtb. Most of the lipids found in the mycomembrane have been shown to modulate the host immune response to one extent or another, sometimes with overlapping functions highlighting the importance of the Mtb mycomembrane in the pathogens success. It's important to note that in addition to their immunomodulatory role, most if not all of the lipids species found in the

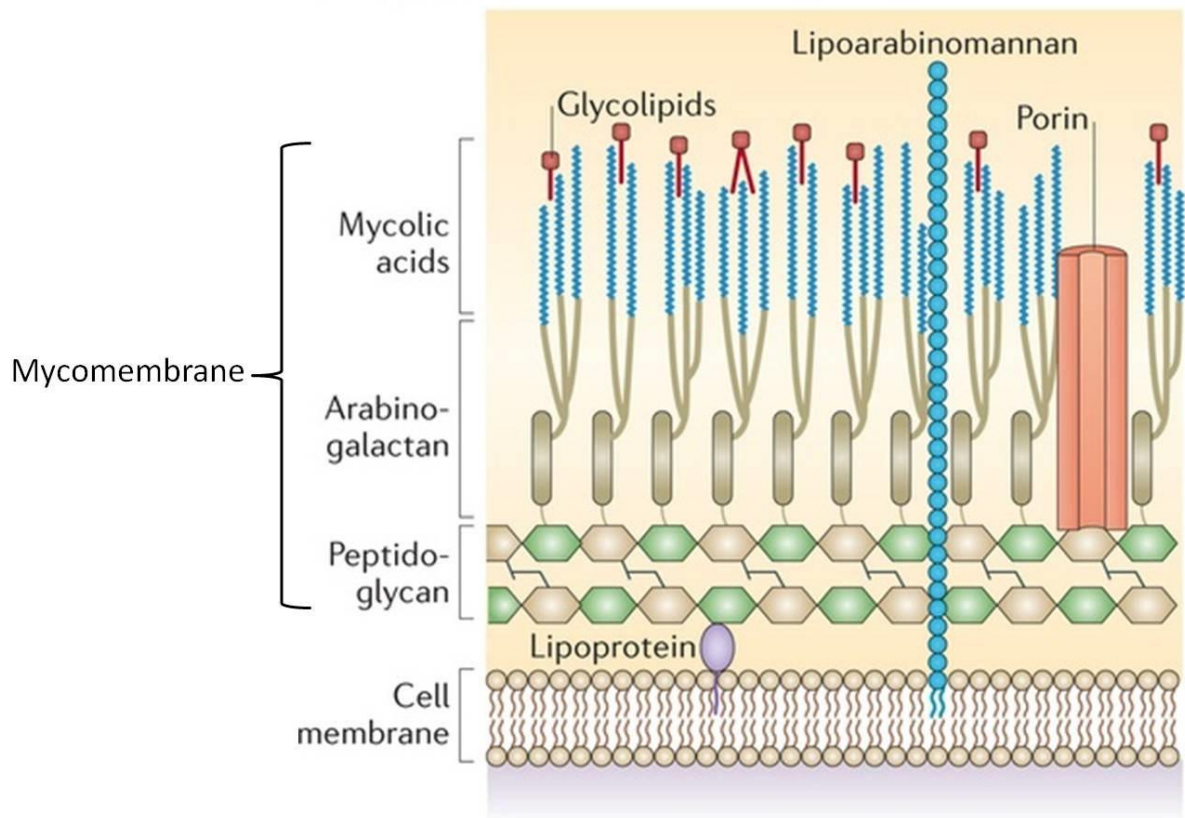


Fig. 5: The mycobacterial cell wall

Mtb is classified as a Gram-positive bacterium. However, due to the presence of a lipid-rich outer cell wall, Mtb cannot be Gram stained. Mtb's membrane consists of a typical plasma membrane surrounded by a peptidoglycan layer. Surrounding the peptidoglycan layer is a layer of arabinogalactan consisting of the disaccharide galactan covalently linked to long arabinin polymers. The arabinin polymers are linked to long chain mycolic acids which are responsible for the lack of gram staining. Non-covalently embedded in the mycolic acid layer are varying glycolipids associated with Mtb virulence. The peptidoglycan, arabinogalactan, mycolic acid layers are collectively referred to as the mycomembrane.

Adapted from (97)

mycomembrane serve a structural role as well as a role in maintaining a permeability barrier to toxic compounds. Mtb deficient in the production of any of these lipids often become more susceptible to antibiotic compounds as well as reactive oxygen and nitrogen species (98,100-103).

One of the most extensively studied Mtb lipids is LAM and the derivative mannose-capped lipoarabinomannan (ManLAM). LAM is produced not only by mycobacteria but other closely related species while ManLAM is only produced by pathogenic mycobacteria. LAM and ManLAM are recognized by mannose receptor, DC-SIGN, Dectin-2, and TLR2 on the surface of macrophages and dendritic cells, implicating the lipids in the invasion process (103). LAM has been implicated in phagosomal arrest through the inhibition of recruitment of late endosomal markers required for phagolysosomal fusion, most notably early endosomal antigen 1 (EEA1) indirectly through calcium flux into the cell (105). Mtb defective in the expression of LAM have been shown to induce a hyper-inflammatory cytokine response (106). Of particular interest, the Mtb complex restricted lipid ManLAM has the ability to inhibit apoptosis induction by limiting calcium flux, activating the pro-survival kinase AKT, and inhibiting the pro-apoptotic mitochondrial protein Bad (107). A precursor for the production of LAM and one of the most abundant lipids in the mycomembrane is phosphoinositol mannosides (PIM). PIM, as with LAM, has been shown to interact with DC-SIGN, hinting at a role in the invasion process (22). PIM has been implicated in the prevention of phagosomal acidification most likely through its role in promoting the fusion of the phagosome with early endosomal membranes (108). LAM and PIM have

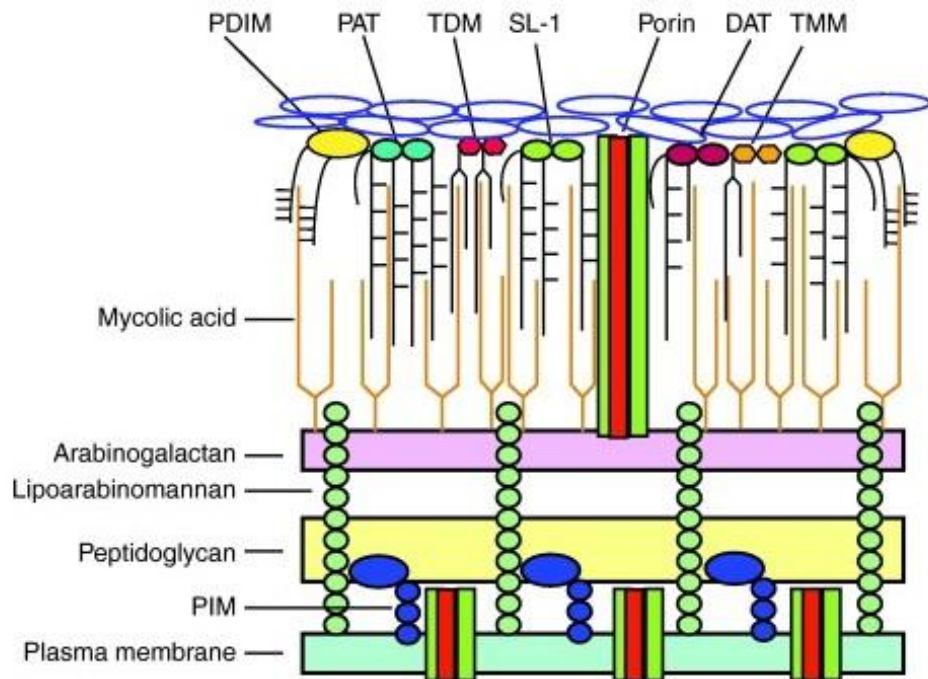


Fig. 6: Localization of Mtb virulence lipids

Mtb produces a number of virulence lipids with varying effects on virulence. Most of these lipids are non-covalently embedded in the mycolic acid layer of the Mtb mycomembrane. Being at the interface of Mtb and the host cell, these lipids unsurprisingly demonstrate a number of immunomodulatory effects including the prevention of phago-lysosome fusion (PIM) and the induction of pro-inflammatory cytokines (TDM and PDIM).

Abbreviations: DAT-Diacylated trehalose, PAT-polyacylated trehalose, PDIM-phthiocerol dimycocerosates, PIM-phosphoinositol mannosides, SL-1-sulfolipid 1, TDM-trehalose dimycolate, TMM-trehalose monomycolate.

Adapted from (104)

also been demonstrated to have the ability to traffic within intracellular compartments of the host cell (109) as well as incorporate into the membranes of uninfected neighboring bystander macrophages (110). This could explain Mtb's ability to manipulate the environment beyond the infected cell.

Another well studied Mtb lipid, related to mycolic acid and only produced by virulent mycobacteria, is trehalose dimycolate (TDM). TDM consists of two mycolic acid chains covalently linked to a trehalose sugar residue (22). Mtb in which TDM has been removed from the surface, or "delipidated", are attenuated in mice as compared to wild type bacilli (17). TDM has also been implicated in arresting phagosome maturation. However, the mechanism by which this occurs is still unclear (111). TDM, as with mycolic acid, has pro-inflammatory activity. Mtb delipidated in TDM showed less robust production of IL1 β and TNF α (112). Most surprisingly, polystyrene beads coated in purified TDM elicited a similar pro-inflammatory phenotype when injected into rats. Additionally, TDM coated beads alone were able to induce the formation of the granuloma in rats injected with the beads (113).

Mtb also produces many methyl-branched fatty acids including, di- and poly-acyltrehalose (DAT, PAT), sulfolipid-1 (SL-1), and phthiocerol dimycocerosates (PDIM). All of the methyl-branched lipid species are specific to the Mtb complex. DAT, PAT, and SL-1 are structurally related and form a sub-group within the methyl-branched family termed the acyltrehalose family (100). Little is known about the function of DAT/PAT in Mtb pathogenesis. However, initial studies indicated a role in inhibiting phagosomal acidification as well as the impairment of cytokine production in activated macrophages (22). While its exact mechanistic role remains elusive, SL-1 has been

shown to play a significant role in *Mtb* virulence (114). *Mtb* deficient in SL-1 localization to the outer membrane are attenuated in both the guinea pig and mouse model of infection (115).

1.6.2 PDIM

In 1976, while comparing virulence of varying strains of *Mtb* in a guinea pig model of infection, Goren and colleagues made note of a particular strain that was severely attenuated compared to others (116). As it turns out, this strain was a variant of the common laboratory strain H37Rv that was deficient in the production of the surface glycolipid PDIM. Several decades later, with the benefit of the sequenced *Mtb* genome, two independent groups using signature tagged-transposon mutagenesis identified insertions in the PDIM genetic locus that resulted in attenuation in the mouse model of infection (117,118). Together, these studies identified PDIM as one of the first known virulence factors of *Mtb*, igniting years of research into the synthesis and virulence mechanisms of this important lipid mediator.

PDIM Synthesis

Structurally, PDIM consists of a methyl branched glycol moiety termed phthiocerol esterified to two long chain methyl branched lipids termed mycocerosic acid (119)(Figure 7a). Both molecules are produced through large proteins termed polyketide synthases (PKS)(119). The phthiocerol group is produced by a type II fatty-acid synthase encoded by the genes *ppsA-E* and is a modular PKS. Synthesis begins with a short chain fatty acid precursor (C22-C24) followed by condensation reactions adding either methyl-malonyl-CoA or malonyl-CoA (119). The mycocerosic acid are synthesized by a type I fatty-acid synthase and iterative PKS encoded by the gene *mas* (119). Synthesis again

begins with a short chain fatty acid but is followed by iterative additions of propionate(119). The mycocerosic acids are esterified to the phthiocerol group through the action of the acyltransferase encoded by *papA5* (119). Fully synthesized PDIM is then exported to the outer mycomembrane through the coordinated action of an ABC transporter encoded by the genes *drrA-C* (118) and an RND family membrane transporter encoded by the gene *mmp17* (118). Schematic depiction of PDIM synthesis and export is show in Figure 8b. Genetic deletions of *drrA-C* or *mmp17* in Mtb still make complete PDIM but fail to properly localize the glycolipid to the cell surface (118). A structurally related glycolipid synthesized by the same proteins is phenolic glycolipid (PGL) (119). PGL is structurally nearly identical to PDIM, the exception being the presence of a sugar modified phenol group (119). All members of the Mtb complex produce PGL albeit with strain-specific sugar modifications (Figure 7b and c). However, with the exception of the Beijing sub-clade (120), Mtb does not produce PGL as a result of a seven base pair deletion in the gene *pks15/1*, which is responsible for the addition of the phenol group to the short chain fatty acid building block of the glycolipid (120). Aside from the phenol group addition, PGL is synthesized by the PpsA-E and Mas PKS systems and exported via DrrA-C and Mmp17 (119). The genes necessary for the synthesis and export of PDIM and PGL are encoded in one 50 kb locus of the Mtb genome (Figure 8a). Given the size of the PKS genes needed to produce PDIM, it is not surprising that the production of PDIM is an energetically expensive process. As a result, PDIM production is lost when grown for extended periods of time *in vitro* (122). This is presumed to be a result of the transcriptional down regulation of the PDIM operon. However, there is little known about PDIM transcriptional regulation. The transcriptional regulator EspR was shown to have a

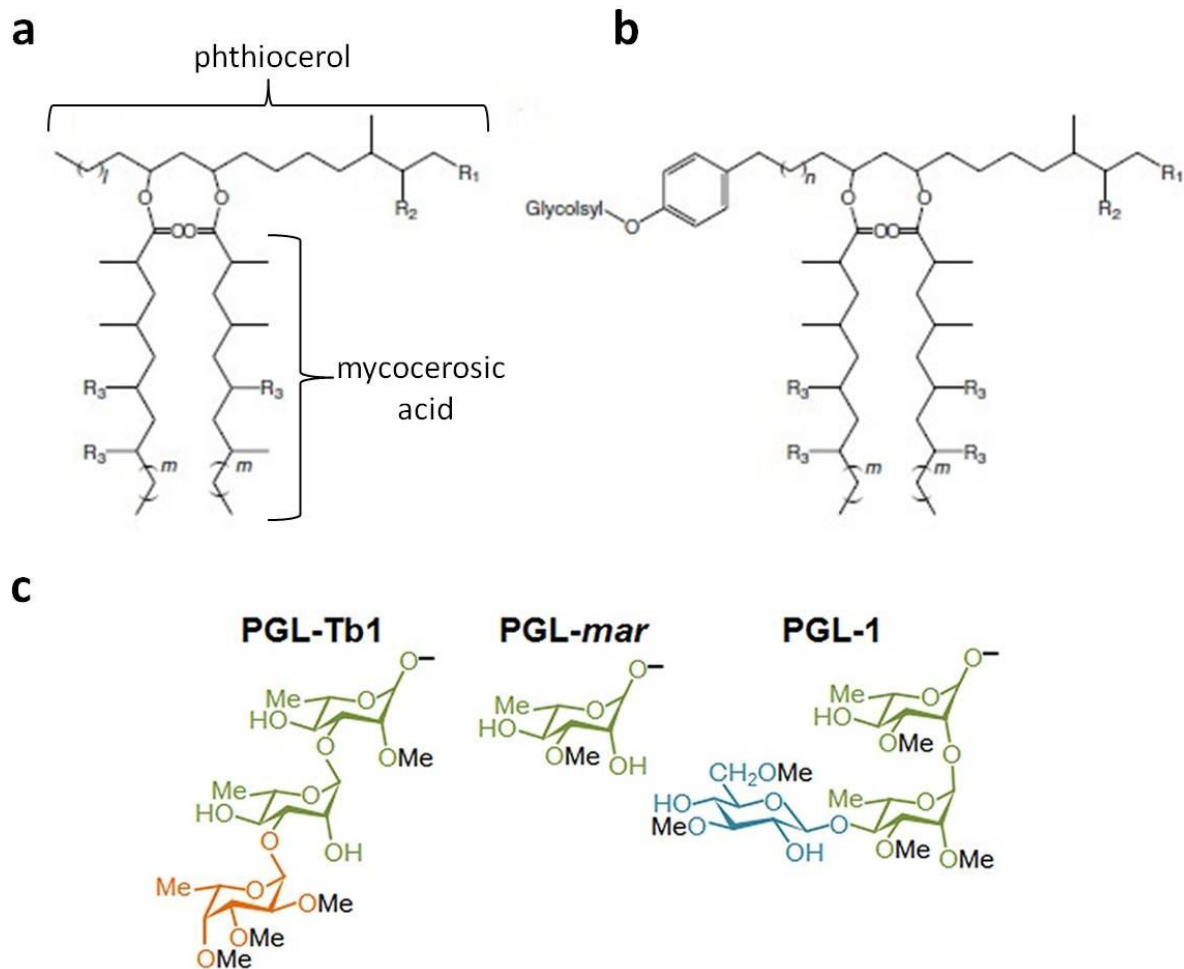


Fig. 7: Structure of *mycobacterial* PDIM and PGL

a) Structure of PDIM consists of a methyl-branched glycol moiety termed phthiocerol esterified to two long chain methyl-branched lipids termed mycocerosic acid. b) Structurally related membrane lipid PGL that is almost identical to PDIM except for the addition of a phenol group to the end of the phthiocerol, group which is modified with species specific methylated sugar moieties. c) Structures of the sugar moieties attached to the phenol group of PGL in *Mtb* (PGL-Tb1), *M. marinum* (PGL-mar), and *M. leprae* (PGL-1).

Abbreviations: PDIM-phthiocerol dimycocerosates, PGL-phenolic glycolipid

Adapted from (119,121)

binding site upstream of the PDIM operon, but overexpression of *espR* in wild type Mtb had little effect on PDIM operon expression (123). The deletion of the RNA polymerase beta subunit *rpoB* in Mtb resulted in over production of PDIM (124) whereas the deletion of the serine threonine protein kinase *pknH* resulted in a reduction in PDIM production (125), although these effects are speculated to be indirect. PDIM is reported to be expressed from a promoter requiring the alternative sigma factor SigL (74). Down regulation of PDIM production is transient as mouse infection will induce the production of PDIM again (126), highlighting its importance to Mtb pathogenicity.

PDIM contributions to cell wall integrity

As with most glycolipids of the mycomembrane, PDIM plays a role in the structural integrity and permeability barrier of Mtb. Deletion of the gene *fadD26*, an acyl-transferase involved in PDIM synthesis, resulted in increased susceptibility to detergent stress and nitric oxide stress *in vitro* (127). In the Mtb vaccine strain *M. bovis* BCG, PDIM deficiency increased the susceptibility to the antibiotic vancomycin (101). Increased antibiotic susceptibility was also seen in the PDIM and PGL producing fish pathogen *M. marinum* deficient in the production of both glycolipids. Of note, the PDIM/PGL-deficient *M. marinum* strain used in that study was more susceptible to the first line Mtb drug rifampicin (128). The same study went on to show that PDIM/PGL deficient strains demonstrated increased uptake of hydrophilic ethidium bromide as well as the hydrophobic dye Nile red (128). Taken together these findings highlight the substantial contributions of PDIM to the structural integrity and resistance to toxic intermediates of Mtb. An additional function of PDIM is to serve as a metabolic sink for the accumulation of toxic propionate during intracellular infection (130). It has been

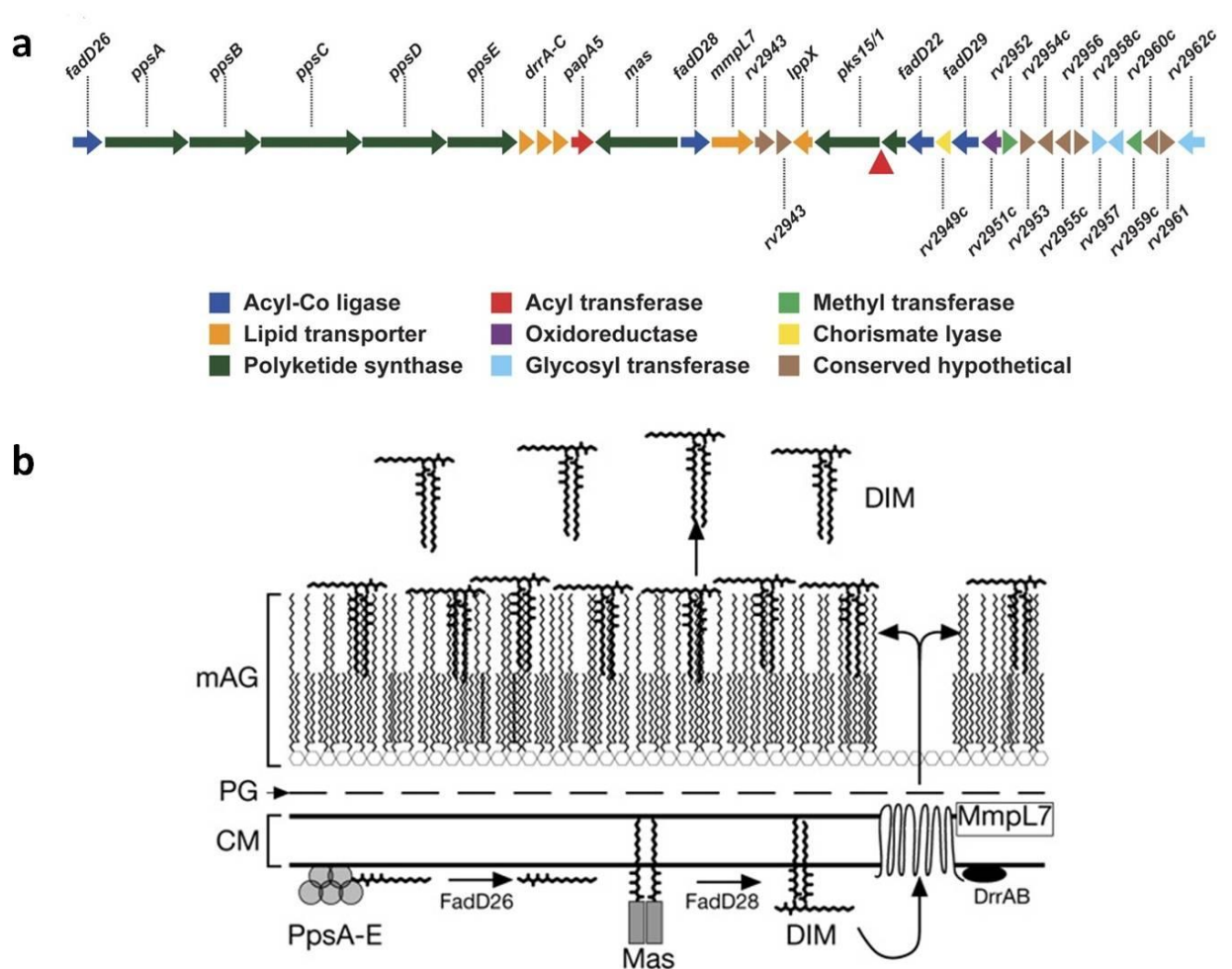


Fig. 8: PDIM operon and synthesis

a) All genes necessary for the synthesis and export of PDIM are encoded in a large ~50 kb locus. The PDIM locus is expressed as three transcriptional units. The first consists of the operon *fadD26-papA5*, the second consists of *mas* alone, and the third is a second operon consisting of *fadD28* and *mmpl7*. All Mtb strains produce PDIM. However, only a few produce the related lipid PGL due to a deletion in the gene *pks15/1* depicted by the red triangle. The genes upstream of *pks15/1* are all associated with the production of sugar groups to PGL. b) Schematic depiction of PDIM synthesis and export. The genes *pksA-E* and *mas* are responsible for the synthesis of the phthiocerol moiety and the mycocerosic acids respectively. *fadD26* and *fadD28* modify the short chain fatty acid starting material for recognition by *ppsA* and *mas*. The genes *drrA-C* and *mmpl7* export PDIM to the cell surface.

Adapted from (118,129)

established that Mtb makes significant use of host lipids as a carbon source during intracellular infection, particularly host cholesterol (92,131). Mtb grown with cholesterol or its catabolic by product propionate as a sole carbon source will increase production of PDIM (130). This is thought to be a result of metabolic flux to relieve the potential effects of propionate toxicity on the cell, which likely occurs during *in vivo* infections (131).

PDIM contributions to Mtb virulence

Since PDIM was first shown to be required for Mtb survival in the mouse model of infection, extensive research has been carried out to determine the exact role PDIM plays in virulence. Initial studies indicated that PDIM was required for Mtb survival in activated macrophages, while being dispensable for survival in resting macrophages (132). Killing of PDIM-deficient strains was believed to be the result of nitric oxide stress, as activated macrophages produce nitric oxide in abundance. Further, the group showed that infection of resting macrophages with PDIM-deficient Mtb resulted in increased production of the pro-inflammatory cytokines TNF α and Il-6 (132), suggesting a role of PDIM in inhibiting the inflammatory response in these cells. In somewhat contradictory findings, Kirksey and colleagues found that a PDIM-deficient Mtb strain survived as well as wild type Mtb in NOS2 knockout mice, which lack the ability to produce nitric oxide. They went on to show that PDIM deficiency renders Mtb attenuated in interferon-gamma knockout mice (129). This suggested that PDIM confers resistance to interferon-mediated immunity independent of nitric oxide production. To confuse the issue even further, another group found that while PDIM is essential for growth in wildtype mice, the lack of PDIM had no effect on growth in interferon, iNOS, or

phagocyte oxidase subunit p47 knockout mice (133). This indicated that Mtb strains lacking PDIM were susceptible to killing by an innate immune mechanism independent of reactive nitrogen, reactive oxygen, and interferon related immunity. While the involvement of these innate immune mechanisms remains elusive, what is clear is that PDIM-deficient Mtb strains consistently reside in more acidified phagosome as compared to wild type Mtb (134), suggesting a role for PDIM in the inhibition of phagosome acidification.

While it is clear PDIM has a multitude of roles establishing a favorable intracellular niche, it is also clear that PDIM plays an equally important role during the initial interaction of Mtb with macrophages. Infection of zebrafish with *M. marinum* deficient in PDIM resulted in the recruitment of iNOS expressing activated macrophages to the site of infection which were able to kill the pathogen. The authors suggested that PDIM functions to mask PAMPs on the surface of *M. marinum* from recognition by TLRs. PDIM also contributes directly to the invasion of macrophages by Mtb. Mtb deficient in PDIM synthesis consistently infected macrophages at a slower rate than wild type Mtb. This phenotype could be complemented by coating the PDIM-deficient strain with purified exogenous PDIM (135). Intriguingly, depletion of cholesterol from the macrophage membranes also ablated the infectivity deficiency of the PDIM mutants (135), suggesting PDIMs role in macrophage invasion is cholesterol dependent. In an elegant study, the same group showed using *M. bovis* BCG that the initial interaction of the bacterium with the macrophage results in a global decrease in membrane polarity that was dependent on PDIM (135). Further they showed that purified PDIM can insert into model membranes decreasing the fluidity of the membrane (135). While the contribution

of PDIM to Mtb virulence is obviously complex and multifaceted, the exact mechanism by which PDIM exerts its influence remains elusive.

1.7 Summary

Recently, our group described a hypervirulent mutant resulting from the deletion of the gene *Rv3167c*, a TetR-like family transcriptional regulator. Infection of macrophages with the *Rv3167c* deletion strain (*MtbΔRv3167c*) resulted in a significant increase in necrosis induction (136), an important step in Mtb dissemination (27,28,137). Further analysis revealed *MtbΔRv3167c* induced necrosis by a novel mechanism involving increased mitochondrial reactive oxygen species and reduced activation of the pro-survival protein kinase Akt. Additionally, it was discovered that *MtbΔRv3167c* induced higher levels of autophagy and escaped the phagosome earlier and in higher numbers than wild type Mtb (136).

Here, we further our understanding of *MtbΔRv3167c* effects on the host cell. Firstly, through the coordinated use of ChIP-seq and EMSA, we identify the direct regulatory sites of *Rv3167c* in the Mtb genome and assess their contribution to the *MtbΔRv3167c* necrotic phenotype. We follow by gaining an understanding of the global regulatory contributions of *Rv3167s* using RNAseq. Here, we identify the up-regulation of a subset of genes responsible for the synthesis of PDIM and show that these transcriptional changes manifest in an increase of PDIM in *MtbΔRv3167c*. Finally, we show that the increased PDIM is responsible for the increased necrosis of *MtbΔRv3167c* and demonstrate a role for PDIM in Mtb autophagy induction and phagosomal escape.

Chapter 2: Materials and Methods

Bacterial Strains and Growth Conditions

All *M. tuberculosis* cultures were grown at 37°C in 7H9 (broth) or on 7H11 (agar) media with 1x ADC enrichment (albumin-dextrose-Catalase), 0.5% glycerol and 0.05% Tween 80 (broth). *E. coli* cultures were grown in LB medium. Kanamycin, hygromycin, and zeocin were used at 40 µg/mL, 50 µg/mL, and 100 µg/mL respectively for Mtb cultures and 40 µg/mL, 150 µg/mL, and 100 µg/mL respectively for *E. coli*. For growth curves, bacteria were washed once in fresh 7H9 media and diluted to an OD₆₀₀=0.05 in a final volume of 10 mL. Antibiotics were added at the indicated concentrations. Bacterial growth was determined by measuring the OD₆₀₀ every 24 hours for one week.

Cell Culture and Infections

THP-1 cells from ATCC were maintained at 37°C and 5% CO₂ in RPMI (ATCC) supplemented with 10% heat inactivated FCS (growth media). THP-1 LC3-GFP cells were grown in growth media +100µg/mL G418 sulfate (CellGro). For infections THP-1 cells were treated with 20ng/mL Phorbol 12-myristate 13-acetate (PMA)(Sigma) for 24 hours to differentiate. Cells were washed twice in PBS and infected at an MOI of 3:1 in growth media + 5% Human Serum AB (Sigma). The infection was incubated at 37°C and 5% CO₂ for 4 hours followed by two more PBS washes and chased with growth media +100µg/mL gentamicin (Gibco). Time points indicated as 0 hours refer to immediately after 4 hour infection and washes while 24 hours refers to 24 hour chase period after 4 hour infection.

Cloning and construction of *M. tuberculosis* mutants

Recombinant DNA techniques were carried out following standard procedures. All restriction and modifying enzymes were purchased from Fermentas. Mtb mutants were constructed using a recombineering approach as previously described (138). Briefly, homology arms corresponding to regions up-stream and down-stream of the gene of interest were amplified and cloned into pSMG360. The completed plasmid was linearized and transformed into *E. coli* EL350/phAE87 and grown at 32°C. Phasmid was prepped and transformed into *M. smegmatis* which was mixed with top agar and plated for 2-3 days at 32°C. Individual plaques were picked from the plate and used to make high titer phage that was incubated with Mtb at 37°C overnight and plated on 7H11 media with appropriate antibiotics. The plates were incubated at 37°C for 3-4 weeks until colonies appeared. Knockouts were confirmed by PCR. Sequences of primers used can be found in appendix A. Knockouts were complemented by over-expression of a wild type copy of the gene in the mutant under control of a constitutively active promoter.

Protein Purification

Rv3167c was cloned into pET28c (Novagen) using the BamHI and NdeI restriction sites to generate an N-terminal 6x histidine tag. The cloned construct was transformed into *E. coli* BL21-DE3. BL21-DE3::pET28c-*Rv3167c* was grown in LB plus kanamycin to $OD_{600}=0.5$ after which expression of *Rv3167c* was induced with the addition of 1 mM IPTG for 5 hours. The culture was harvested, resuspended in PBS+200 mM NaCl and disrupted with sonication. Cellular debris was removed by spinning at 15,000 g for 30 min. The supernatant was applied to columns packed with His-Pur Cobalt Superflow Resin (Thermofisher) equilibrated with PBS+200 mM NaCl+10 mM

imidazole and incubated at 4°C for 1 hour rocking. The column was washed with 10 volumes of PBS+200 mM NaCl+30 mM imidazole. Rv3167c was eluted from the column with PBS+200 mM NaCl+250 mM imidazole. 10% glycerol was added and the purified protein was stored at 4°C until FPLC purification.

Fast Protein Liquid Chromatography (FPLC)

All FPLC experiments were carried out on a GE AKTA Explorer chromatography system. Gel filtration chromatography was carried out on a Superdex 75HR 10/30 column (GE Healthcare Life Science). Eluent was then further purified with ion exchange chromatography on a MonoQ 5/50 GL column (GE Healthcare Life Sciences). A LMW Gel Filtration calibration Kit (Amershan Biosciences) was used as standard for gel filtration chromatography determination of Rv3167c dimerization.

Isothermal Titration Calorimetry (ITC)

ITC was performed on a MicroCal iTC200 titration microcalorimeter with a starting protein concentration of 0.130 mM and a starting dsDNA concentration of 2.10 mM. Immediately before conducting the experiments, the protein was dialyzed against 10 mM phosphate (pH 7.2), 136 mM NaCl, and 4 mM KCl to remove glycerol. DNA oligos were annealed in the same buffer as the protein. Each titration experiment consisted of 2 μ L injections of dsDNA into protein at 25°C with a mixing speed of 1000 RPM. Data acquisition and analysis were performed with the software package ORIGIN according to a single-site binding model.

Electrophoretic Mobility Shift Assay (EMSA)

Two oligos per tested binding site were purchased from Operon corresponding to the plus and minus strand of each site. Sequences can be found in Appendix A. To

anneal, corresponding oligos were mixed at a 1:1 molar ratio and heated to 95°C for 10 minutes in a heat block after which the block was turned off and allowed to slowly cool to room temperature. Annealed oligos were mixed with purified Rv3167c at the indicated concentrations in a PBS+100mM NaCl +5mM MgCl₂ buffer and incubated on ice for 15 minutes. Samples were then separated on a 5% TBE PAGE gel (Bio-rad) at 150V for 1 hour at 4°C. The gel was then stained with SYBR Green (ThermoFisher) and imaged. Randomized oligos served as the negative control.

Propidium Iodide (PI) and LC3-GFP staining for Cell Death and Autophagy Analysis

For PI staining cells were harvested at the indicated time points and washed once in PBS and were then resuspended in PBS +5% FCS and 1 µg/mL PI and incubated for 10min. Percent PI positive cells was determined by flow cytometry (BD Accuri C6). Analysis of LC3-GFP expressing THP-1 cells was performed as described previously (158). At the indicated time points, cells were harvested and washed once with PBS. Cells were then permeabilized with 0.05% saponin for 5 minutes, after which they were washed once in PBS and resuspended in PBS+5% FCS. Percent autophagic cells was determined by flow cytometry (BD Accuri C6).

Mycobacterial Protein Fragment Complementation (MPFC)

MPFC was conducted as described in (139). Rv3167c was cloned into both pUAB300 and PUAB400 and constructs were co-transformed into *Mycobacterium smegmatis*. Transformants were then spotted with appropriate controls on 7H11 media supplemented with 50 µg/mL trimethoprim (Fisher) and grown at 37°C for 3 days.

FRET Assay for translocation of Mtb in host cell cytosol

To detect mycobacterial escape from the phagosome, the CCF4 FRET assay was performed as described previously (28). Briefly, cells were stained with 8 μ M of CCF4 (Invitrogen) in EM buffer (120mM NaCl, 7mM KCl, 1.8mM CaCl₂, 0.8mM MgCl₂, 5mM glucose, 25mM Hepes, pH7.3) containing 2.5 μ M of probenecid (Sigma-Aldrich) for 1.5 hours at room temperature. Live populations were distinguished from dead ones by addition of Live/Dead Fixable Red stain (Invitrogen) for 30 minutes at room temperature. Following staining, cells were fixed with 4% PFA overnight and analyzed by flow cytometry (BD FACSCanto).

RNA Isolation

M. tuberculosis cultures were grown in 7H9 until OD₆₀₀ = 0.6-0.8. Cultures were pelleted and resuspended in 1mL TRIzol (Ambion). RNA was extracted with chloroform, precipitated with 100% isopropanol, and washed with 70% ethanol. Purified RNA was treated with Turbo DNase (Ambion) for 1 hour. RNA was used right away or stored at -80°C.

RNAseq Library Preparation and Analysis

Ribosomal RNA was removed from samples using Epicentre Gram Positive RiboZero rRNA Magnetic Removal Kit. RNAseq libraries were prepared using Illumina ScriptSeq v2 Library Preparation Kit according to the manufacturer's protocol. Library quality was assayed by Bio-analyzer (Agilent) and quantified by qPCR (KAPA Biosystems). Libraries were run on an Illumina HiSeq1500 generating 100bp paired end reads at the UM-IBBR sequencing core. RNA-Seq read quality was verified using FastQC (140) and low-quality basepairs were trimmed using Trimmomatic (141). The *M*

tuberculosis H37Rv reference genome was downloaded from TB Database (142) and reads were mapped to the genome using TopHat2 (143). Count tables were generated using HTSeq (144) along with a custom GFF which includes features from both TB Database and Tuberculist (145). Count tables were loaded into R/Bioconductor (146), quantile normalized (147), and corrected for variance bias using Voom (148). Limma (149) was used to find genes that were differentially expressed between each of the pairs of sample conditions. A total of 442 genes were found to be both differentially expressed in the wildtype/mutant contrast and the mutant/complement contrast, and thus are potentially affected by Rv3167c regulation. This list of candidate regulated genes was checked for functional enrichment using Goseq (150) with multiple testing correction using the Benjamini and Hochberg method (151). All RNAseq analysis was carried out by Keith Hughitt and Dr. Najib El-Sayed.

Total Lipid Extraction and Thin Layer Chromatography (TLC)

Two independent cultures of Mtb, Mtb Δ Rv3167c, and Mtb Δ Rv3167c::*Comp* were grown in 7H9 broth in a volume of 50mL to an OD₆₀₀=0.8. Cultures were pelleted and resuspended in methanol:chloroform (2:1) and left at 4°C overnight. Samples were spun down and supernatant transferred to a glass beaker. The pellet was resuspended in methanol:chloroform (1:1) and left at room temperature for an hour. Samples were spun down and the supernatant removed. The process was repeated again with methanol:chloroform (1:2). All three fractions were pooled and the methanol and chloroform was allowed to evaporate overnight in a fume hood. The total lipid pellet was weighed and 300µg of total lipid was spotted on a TLC plate. The plate was resolved in a mobile phase of petroleum ether: diethyl ether (9:1). Lipid spots were revealed by

spraying the plate with a 3% cupric acetate in 8% phosphoric acid solution followed by baking at 140°C.

Immunoblotting

Bacteria were pelleted and resuspended in 25mM TrisHCl followed by bead beating to lyse cells. Lysate was cleared by spinning at 12,000 rpm for 5min. A Pierce BCA protein assay kit (Thermo Scientific) was used to measure protein concentrations. Antibody against EsxA was purchased from Santa Cruz Biotechnology Inc. and used at 1:200 dilution. Antibodies against FAP and GroEL were obtained from BEI Resources and used at 1:7500 and 1:50 dilution, respectively.

Statistical analysis

Statistical analysis was performed using GraphPad Prism version 6.0 software. Data is presented as mean \pm S.E.M. of three independent experiments and one-way ANOVA with Tukey post-test was used unless mentioned otherwise in the figure legends. p-value significance is indicated as follows—* \leq 0.05, ** \leq 0.01, *** \leq 0.001, **** \leq 0.0001.

Chapter 3: Rv3167 regulates the virulence lipid PDIM

3.1 Introduction

Recently, our group described a hypervirulent mutant resulting from the deletion of the gene *Rv3167c*, a proposed TFTR. Infection of macrophages with *MtbΔRv3167c* resulted in a significant increase in necrosis induction (136), an important step in *Mtb* dissemination (27,28,137). Additionally, it was discovered that *MtbΔRv3167c* induced higher levels of autophagy and escaped the phagosome earlier and in higher numbers than wild type *Mtb* (136). Since *Rv3167c* is annotated as a TFTR, we reasoned that the genes regulated by *Rv3167c*, as opposed to *Rv3167c* itself, are responsible for the increase necrosis, autophagy, and phagosomal escape observed in *MtbΔRv3167c*.

In this chapter, we describe the *Rv3167c* regulon using RNAseq. Further, we show that the *Rv3167c* is enriched in genes necessary for the synthesis and export of the *Mtb* cell wall lipid PDIM. Given its long association with *Mtb* virulence, PDIM represented an interesting target for follow up studies. By deletion of the PDIM membrane transporter encoded by *mmp17*, we show that PDIM was responsible for the increased necrosis in *MtbΔRv3167c*. Further, through the use of an *mmp17* single gene mutant, we implicate PDIM in *Mtb* autophagy induction and phagosomal escape.

3.2 Results

3.2.1 Establishing the Rv3167c regulon

In order to characterize the regulon of Rv3167c, we performed RNAseq on wildtype Mtb, Mtb Δ Rv3167c, and Mtb Δ Rv3167c complement (Mtb Δ Rv3167c::Comp) strains grown in standard growth media harvested during logarithmic growth. Our RNAseq data was highly reproducible as evidenced by the high degree of clustering between biological replicates and indicated that we are analyzing distinct transcriptional states (Figure 9a). That is to say biological replicates of each strain were more similar to each other than to that of other strains. Interestingly, clustering analysis indicated that Mtb Δ Rv3167c::Comp was more similar to Mtb Δ Rv3167c than to Mtb.

Principle component analysis confirmed this relationship (Figure 9b). This suggests that not all genes differentially expressed in Mtb Δ Rv3167c complement back to wild type expression levels. It is likely that some of the genes differentially expressed are independent of Rv3167c and are a result of polar effects from the construction of Mtb Δ Rv3167c.

The inclusion of Mtb Δ Rv3167c::Comp in our analysis provided a valuable internal control for determining the Rv3167c regulon. To do this, we determined genes differentially expressed in Mtb Δ Rv3167c as compared to Mtb as well as genes differentially expressed in Mtb Δ Rv3167c as compared to Mtb Δ Rv3167c::Comp. The criteria to be considered differentially expressed was an adjusted p-value <0.05 and a fold change of more than 1.5. We compared both gene sets (Figure 9c) and only considered genes differentially expressed in both contrasts as this gave us more confidence Rv3167c was involved in their regulation. In total, 442 genes were considered to be regulated by

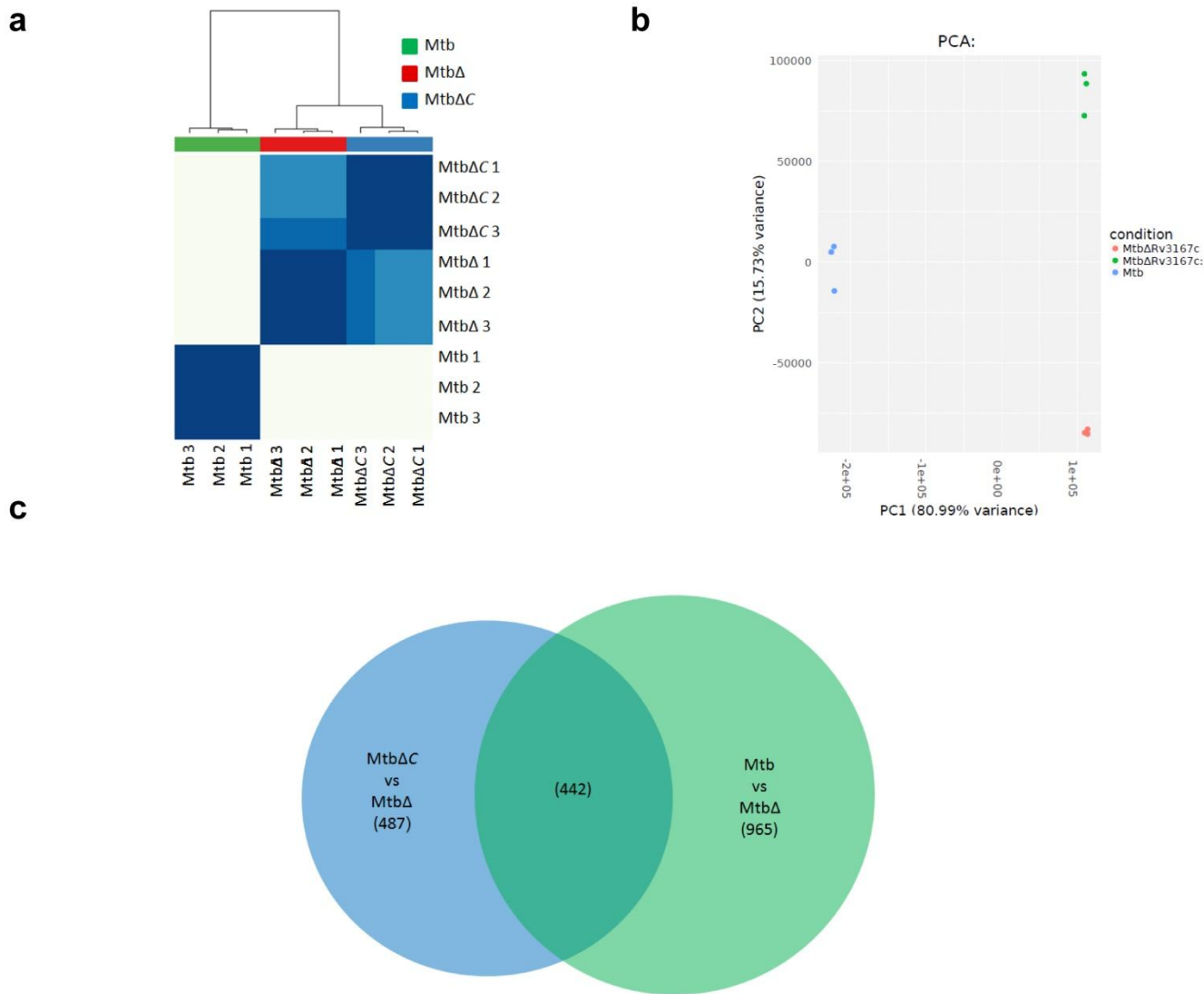


Fig. 9: RNAseq analysis reveals an extensive Rv3167c regulon

RNAseq analysis was performed on *in vitro* grown cultures of Mtb, MtbΔRv3167c (MtbΔ), and MtbΔRv3167c::Comp (MtbΔC) as described (n=3 per group). a) Pearson correlation was used to determine similarities between samples followed by biclustering to generate heat map depicting relationships between samples. Bottom and right axis are labeled with sample identifier. Top axis depicts relationship between sample groups. b) Principle component analysis (PCA) was conducted to visualize variation between samples. c) Venn diagram depicting scheme to determine Rv3167c regulated genes. Only genes in the overlap between Mtb/MtbΔ and MtbΔC/MtbΔ comparisons were considered. Numbers in parenthesis indicate number of genes de-regulated.

Rv3167c (Appendix B). The differential expression of such a number of genes indicates that Rv3167c has a relatively broad transcriptional impact.

3.2.2 RNAseq reveals up-regulation of PDIM synthesis genes in *MtbΔRv3167c*

Gene ontology (GO) enrichment analysis was conducted on the Rv3167c regulon and identified three GO terms (Table 2). Interestingly, all three GO terms are associated with fatty acid metabolism suggesting Rv3167c may play a role in cell wall processes. The GO term fatty acid biosynthetic processes contains many genes with proposed functions in fatty acid metabolism but as of yet are hypothetical. The GO term cell wall is a large ontology group containing 623 genes with diverse functions all thought to be involved in cell wall synthesis. Unfortunately, neither of these enriched GO terms provides much insight into the nature of Rv3167c role in inhibiting necrosis. However, the GO term DIM/DIP cell wall layer assembly, which encompasses genes associated with the synthesis and export of PDIM, was of particular interest considering PDIMs involvement in pathogenesis. Indeed, the entire PDIM operon was up-regulated in *MtbΔRv3167c* as compared to *Mtb*, while being mostly unchanged or even down-regulated in *MtbΔRv3167::Comp* compared to *Mtb*, indicating these genes do complement back to wild type levels (Figure 10a). Using thin layer chromatography, we showed that the transcriptional up-regulation manifested in an increase in PDIM lipid in *MtbΔRv3167c* (Figure 10b). As discussed in section 1.6.2, PDIM is a well known virulence factor of *Mtb* with a myriad of proposed functions and as such is an interesting target for follow up studies.

Table 2: GO term enrichment of *Mtb* Δ *Rv3167c* differentially regulated genes.

Category	Term	numDEInCat	numInCat	pval_adj
GO:0071770	DIM/DIP cell wall layer assembly	9	9	0.0000062
GO:0006633	Fatty acid biosynthetic process	6	7	0.0048904
GO:0005618	Cell wall	123	659	0.0045409

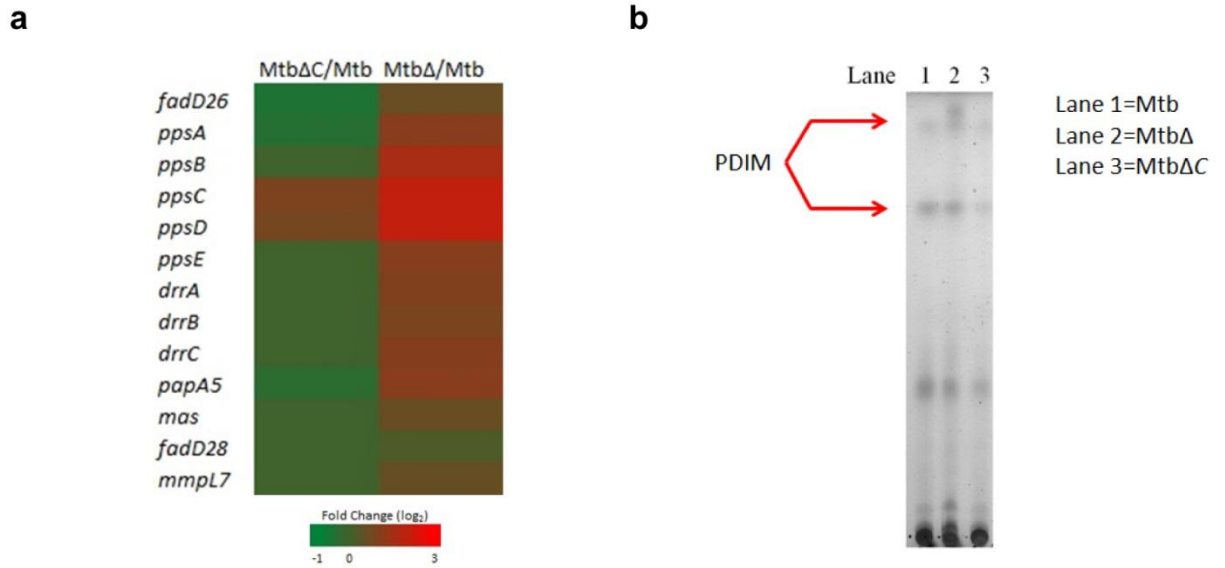


Fig. 10: *MtbΔRv3167c* over expresses the *Mtb* virulence lipid PDIM

a) Heat map depicting transcriptional fold changes of genes in the PDIM operon in *MtbΔC/Mtb* (first column) and *MtbΔ/Mtb* (second column). b) TLC analysis of PDIM production by *Mtb*, *MtbΔ*, and *MtbΔC*. 300μg total lipid was loaded in each lane. The plate was resolved in a mobile phase of petroleum ether: diethyl ether 9:1. Lipid spots were revealed by charring.

3.2.3 PDIM is responsible for the increased necrosis induction of *MtbΔRv3167c*

PDIM is synthesized completely in the cytosol and transported to the outer mycomembrane of *Mtb* by the membrane lipid transporter encoded by *mmp17*. Deletion of *mmp17* results in the failure of proper PDIM localization (118). To assess the role of PDIM in the necrosis induced by *MtbΔRv3167c*, we deleted *mmp17* in the *MtbΔRv3167c* background resulting in *MtbΔRv3167cΔmmp17* which was confirmed by PCR (Figure 11a). Infection of THP-1 macrophages with *MtbΔRv3167cΔmmp17* resulted in a significant decrease in cell death as compared to *MtbΔRv3167c* (Figure 12a). As discussed above, RNAseq analysis revealed more than 400 genes are differentially regulated in *MtbΔRv3167c*. Additionally, it was evident that a large portion of the genes differentially regulated did not complement. In an effort to minimize concerns about the contribution of other genes to the cell death phenotype and to assess whether PDIM alone was sufficient to modulate host cell death, we analyzed an *mmp17* single gene mutant in the *Mtb* CDC1551 strain (*Mtbmmp17::TN*). Analysis by real time PCR indicated that *Mtbmmp17::TN* did not express *mmp17* transcript (Figure 11b). The deletion of *mmp17* resulted in significantly less cell death as compared to CDC WT (*Mtb*). Complementation of *mmp17* back into *Mtbmmp17::TN* reverted the phenotype to levels similar to *Mtb* (Figure 12c).

Previous work has implicated PDIM in macrophage invasion (135) and in resistance to killing by an early innate immune response (129,132,133). However, we saw similar numbers of bacteria both initially after infection and at 24 hours post infection in *MtbΔRv3167cΔmmp17* (Figure 12b) and *Mtbmmp17::TN* (Figure 12d) as compared to wild type. This indicates that loss of PDIM expression on the cell surface in

either *Mtb* Δ *Rv3167c* Δ *mmp17* or *Mtbmmp17::TN* has no effect on these strains ability to infect macrophages or survive within the macrophages. These data demonstrate that the increased PDIM production by *Mtb* Δ *Rv3167c* is responsible for the increased necrosis seen in the mutant. This is a conserved function of PDIM as deletion of *mmp17* in the CDC background resulted in a reduction of necrosis induction as would be predicted.

3.2.4 PDIM contributes to autophagy induction and phagosomal escape in *Mtb*

As reviewed in section 1.4.1, autophagy is an evolutionarily conserved catabolic process that involves sequestration of cytosolic contents into *de novo* generated double membrane vesicles termed autophagosomes, which then get delivered to the lysosome for degradation. This process can be used to target and kill intracellular pathogens in a process termed xenophagy (48). Previous work in our lab demonstrated that in addition to increased necrosis induction, infection of cells with *Mtb* Δ *Rv3167c* resulted in increased induction of autophagy, but not autophagic death (136).

We wanted to determine whether PDIM played a role in *Mtb* induced autophagy in addition to induction of necrosis. To do this, we monitored the conversion of cytosolic LC3I to autophagosomal bound LC3II, a hallmark of autophagy using previously described methods (158). Briefly, LC3-GFP expressing THP-1's are infected for the indicated amount of time. After which the cells are permeabilized with saponin and washed. Cytosolic LC3I-GFP escapes the cell while autophagosomal bound LC3II is retained in the cell. An increase in autophagy results in an increase in GFP positive cells as measured by autophagy. A significant decrease in autophagy was seen in cells infected with *Mtbmmp17::TN* as compared to *Mtb* (Figure 13a) indicating PDIM plays a role in induction of autophagy in *Mtb*. Importantly, autophagy is restored to wildtype levels

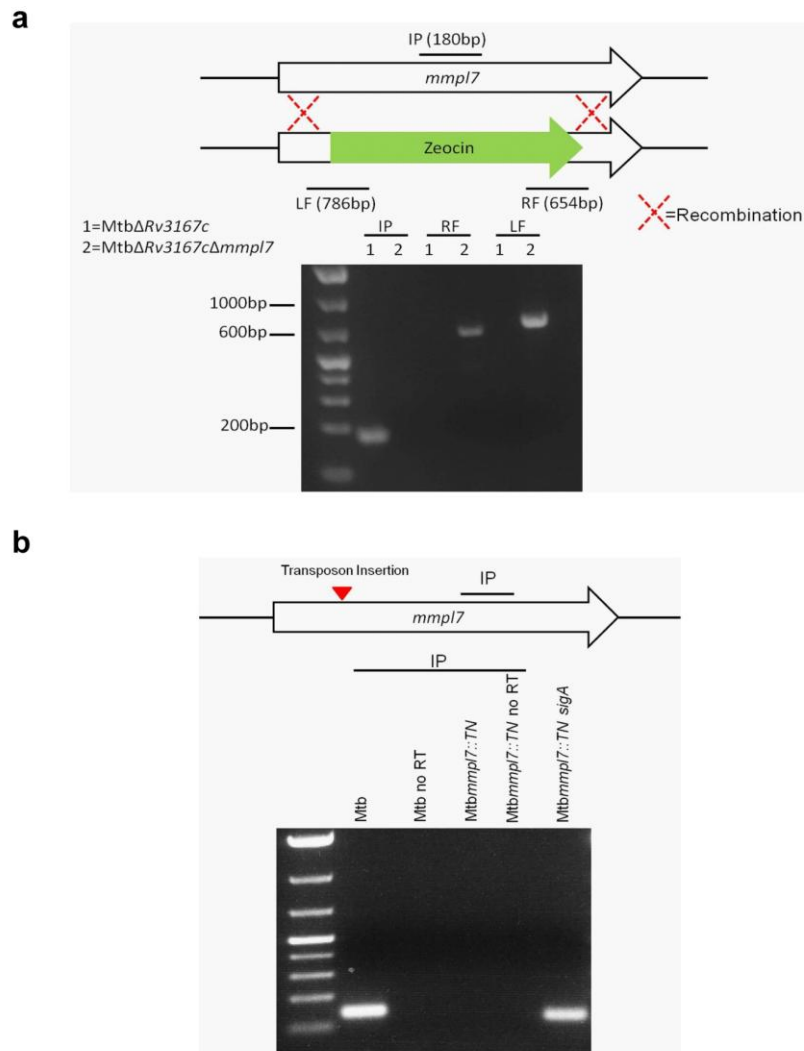


Fig. 11: PCR confirmation of *mmp17* knockouts.

a) depicts the strategy and confirmation of the recombination of zeocin marker in place of *mmp17*. Primer sets used to confirm knockout are labeled LF (Left Flank) and RF (Right Flank) which amplify the zeocin/gene junctions and only create a product if recombination was successful. Primer set labeled IP (Internal Priming) amplifies a region within *mmp17* and will not create a product if recombination was successful. Genomic DNA was used as template and PCR was carried out with standard methods. Reactions were run on a 1.5% agarose gel. PCR product sizes are given in parenthesis. b) Transposon insertion site is marked with a red arrow. RNA was collected from each strain grown in 7H9 to an $OD_{600}=0.8$ and cDNA was synthesized as described in methods. Presence of *mmp17* transcript was determined by PCR. IP (Internal Priming) primer set amplifies a region within *mmp17* downstream of transposon insertion site. No RT was used for control for genomic DNA contamination. To confirm presence and quality of RNA in *Mtbmmp17::TN*, *sigA* transcript was amplified.

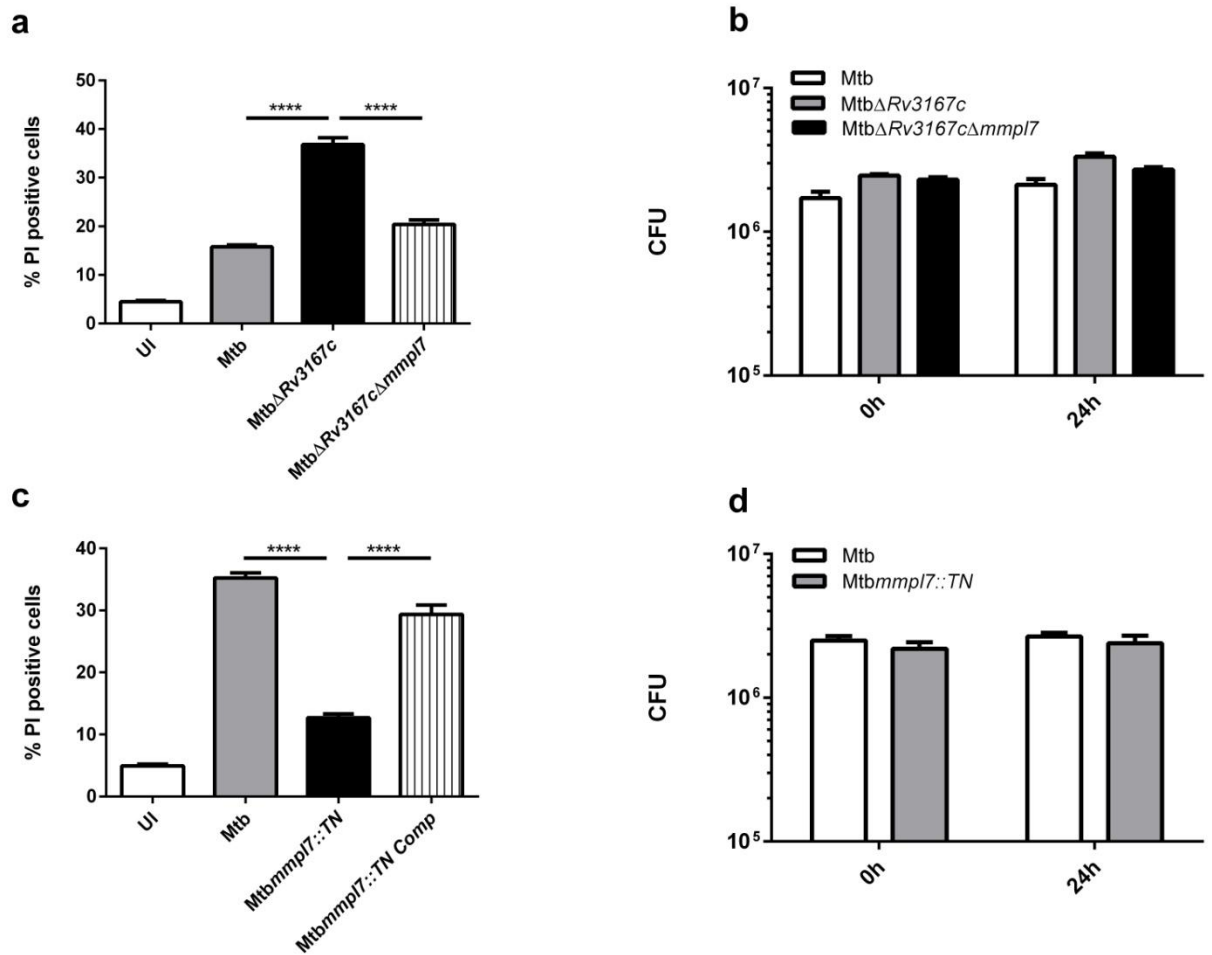


Fig. 12: PDIM contributes to induction of host cell necrosis by Mtb.

THP-1 cells were differentiated with PMA for 24h and were left uninfected (UI) or infected with indicated bacterial strains. **a, c**, Cells were harvested, stained with propidium iodide (PI) and analyzed by flow cytometry (n=5,000) at 24h post infection. **b, d**, Bacterial burden was determined by quantifying colony forming units (CFU) immediately following infection (0h) or 24h post infection (24h). Data are representative of three independent experiments. Data presented as mean \pm S.E.M. ****=p-value \leq 0.0001.

upon complementation.

Traditionally, Mtb was thought to reside completely in an early endosomal-like compartment for the duration of its intracellular lifecycle (26,159). Recently, this view has been challenged by studies demonstrating that Mtb can escape the phagosome (28,29,137) which is quickly followed by host cell necrosis induction (27,160). Our group previously demonstrated that *MtbΔRv3167c* accesses the cytosol earlier and to a higher extent than wild type Mtb (136). We hypothesized that PDIM contributes to phagosomal escape and that loss of PDIM would result in decreased access to the cytosol. To test this we made use of a FRET based assay described previously (28). Briefly, THP-1 cells differentiated for three days with PMA were loaded with CCF4-AM. Intact CCF4-AM emits green fluorescence (535nm) due to FRET between the fluorescent moieties. Cleavage of CCF4-AM by β -lactamase expressed by cytosolic bacteria leads to FRET loss and a shift in the emission wavelength to 450nm which can be monitored by flow cytometry.

Using this assay, we demonstrate that *Mtbmmp17::TN* accesses the cytosol to a lesser extent than Mtb and the *Mtbmmp17::TN* complemented strain (Figure 13b). Previous work has shown that Mtb escape is dependent on the ESX-1 secreted substrate EsxA (29). Given PDIMs location in the mycomembrane it could have indirect effects on the secretion of EsxA. It could be that *Mtbmmp17::TN* secretes less EsxA resulting in the decrease in escape and PDIM plays an indirect role in this process. However, we observed no difference in the secretion of EsxA in *Mtbmmp17::TN* compared to Mtb (Figure 14). This represents the first indication that PDIM influences Mtb phagosomal escape.

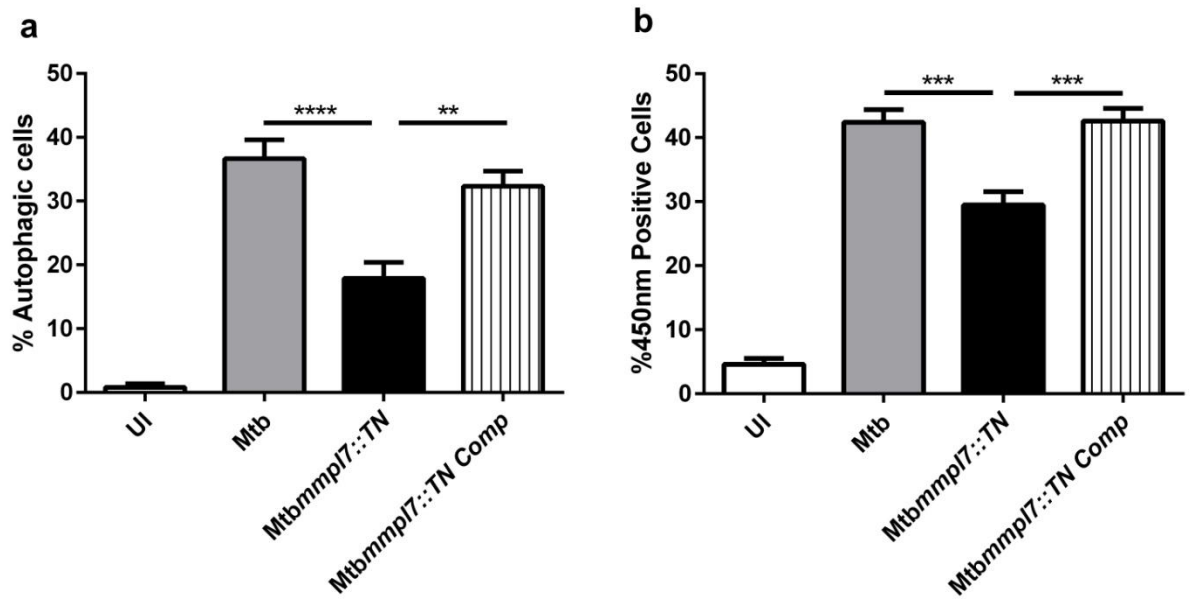


Fig. 13: PDIM is necessary for host cell autophagy induction and phagosomal escape of Mtb

a) Differentiated THP-1-LC3GFP were left uninfected (UI) or infected with indicated strains and cells were harvested 24h later. The fraction of autophagic cells out of 5,000 total cells was determined by gating on GFP-positive cells after mild detergent treatment by flow cytometry as described. b) The cleavage of CCF4-AM and increased fluorescence at 450nm is an indicator for Mtb in the host cell cytosol. THP-1 cells were infected with the indicated strains for 24h. Cells were then stained with CCF4-AM and the number of cells emitting at 450nm was determined by flow cytometry out of 5,000 total cells per condition. Data are representative of three independent experiments. Data presented as mean \pm S.E.M. p-value=** \leq 0.01-*** \leq 0.001-**** \leq 0.0001.

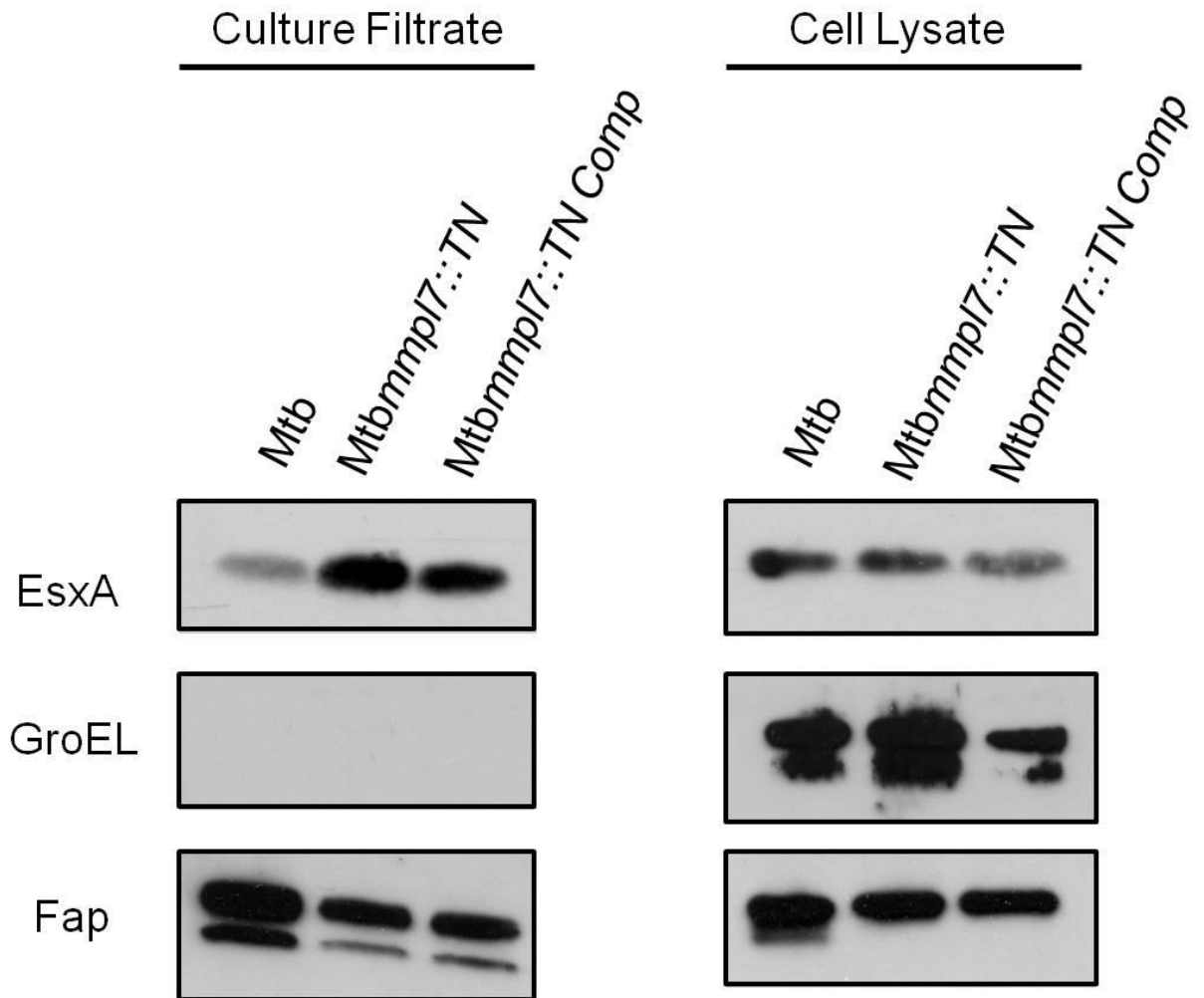


Fig. 14: EsxA secretion is maintained in *Mtbmmp17::TN*

Mtb, *Mtbmmp17::TN*, and *Mtbmmp17::TN Comp* were grown in 50mL Sauton's media to an $OD_{600}=0.7$. Bacteria were pelleted, the supernatant was removed, filtered, and concentrated (culture filtrate). The bacterial pellet was lysed by bead beating and filtered (cell lysate). 10 μ g total protein was run on an anyKd SDS-PAGE gel (Bio-Rad), transferred to a PVDF membrane (GE Healthcare) and blotted for EsxA, GroEL, or Fap. GroEL served as the lysis control. fap served as loading control. EsxA antibody was used as 1:200, GroEL antibody was used at 1:50, and Fap antibody was used at 1:7500.

3.3 Discussion

Analysis revealed that more than 400 genes were differentially regulated in *MtbΔRv3167c*. The differential expression of such a number of genes is unusual for a TFTR. While there are examples of TFTR serving as global regulators (156), typically their regulons contain a few genes. Insights into the prevalence of TFTR that function as global regulators are hindered by the lack of transcriptome analysis. Studies on TFTR typically focus on the regulation of genes in the immediate genomic vicinity of the TFTR studied. Additionally, most bacterial transcriptome analysis studies of mutants do not include a complemented strain. As such, it is unclear whether this is unique to *MtbΔRv3167c* or a more general characteristic of the construction of bacterial mutants. That being said, it is clear *Rv3167c* plays a much larger role in shaping the *Mtb* transcriptome than would be assumed and our confidence in this response is bolstered by the fact that these genes complement back to wild type levels.

Further analysis revealed that the *Rv3167c* regulon was enriched in genes for the synthesis and export of PDIM. We show that PDIM is indeed responsible for the increased necrosis seen in *MtbΔRv3167c* and further implicate PDIM in induction of autophagy as well as phagosomal escape by *Mtb*. Previous work has implicated PDIM in macrophage invasion (135) and in resistance to killing by an early innate immune response (129,132,133). It could be that the *mmp17* deletion strains were unable to infect macrophages with the same efficiency or they were killed by the innate immune response. However, we saw similar numbers of bacteria both initially after infection and at 24 hours post infection in *MtbΔRv3167cΔmmp17* (Figure 12b) and *Mtbmmp17::TN* (Figure 12a) as compared to wild type. While these findings are in disagreement with

those that are published, they can easily be explained by differences in infection protocols. The group that implicated PDIM in macrophage invasion used a one hour infection protocol. However, they noted that with extended periods of incubation, PDIM deficient mutants infected macrophages as well as wild type (135). The standard infection protocol we used includes a four hour incubation period, which likely explains why we didn't see any differences in infectivity at the 0 hour time point. Several groups also reported that PDIM is essential for resistance to an early innate immune response. However, they use interferon activated macrophages expressing reactive nitrogen intermediates. They go on to show PDIM is essential for resistance to reactive nitrogen species (129,133,132). Our infections were conducted with resting macrophages which explains why deletion of *mmpl7* did not result in killing of the bacteria at the 24 hour time point. The loss of PDIM on the cell surface does not result in a decrease in fitness of the *mmpl7* mutant.

Mtb phagosomal escape has been demonstrated to require the pore forming toxin EsxA (28, 29, 137). Interestingly, it appears PDIM plays a role in Mtb phagosomal escape is in some part independent of EsxA, as EsxA secretion was un-affected in *Mtbmmpl7::TN*, yet this strain still failed to escape the phagosome to the same extent as wild type. PDIM has been demonstrated to incorporate into host cell membranes as well as model membranes. Incorporation of PDIM into membranes results in a decrease in overall membrane fluidity (135). Establishing a causal relationship between PDIMs effects on membrane fluidity and Mtb phagosomal escape would prove difficult mostly because there are few methods to monitor or perturb membrane fluidity. A key step would be to establish that PDIM influences membrane fluidity during ex vivo infections.

There are several fluorescent probes available to monitor membrane fluidity and have been used to study PDIM (135). However, most of these studies monitor fluidity at the cell membrane. It's unclear whether these probes could be used to monitor the phagosomal membrane which is where we propose the effects of PDIM are most relevant. Another approach would be to manipulate macrophage membrane fluidity through addition of exogenous chemicals and monitoring Mtb escape. Treatment of cells with methyl- β -cyclodextrin (169), oleic acid (170), or the NSAID nimesulide (171) induce increases in membrane fluidity and would be expected to counter any decrease in fluidity as a result of PDIM insertion. Decreases in phagosomal escape by *Mtb* Δ *Rv3167c* infected cells treated with these drugs would hint that membrane fluidity perturbation plays a role in *Mtb* Δ *Rv3167c* virulence. However, this approach is not ideal as it would fail to implicate PDIM directly and would not provide any information about any targeted effects on the phagosomal membrane itself. Additionally, transmission electron microscopy could be used to assess the direct effects of PDIM on the phagosomal membrane in the absence of EsxA. This approach is not ideal given the need for large quantities of purified PDIM, which would undoubtedly be a laborious process.

In conclusion, this study identified a role of PDIM in Mtb-mediated necrosis and autophagy induction, as well as a role in Mtb phagosomal escape.

Chapter 4: Rv3167c is a TetR-like transcriptional regulator

4.1 Introduction

As reviewed in section 1.5.1, TFTR are one of the most abundant transcriptional regulators in bacteria and as such have been extensively studied (84). Classification as a TFTR is mostly through sequence homology of the N-terminal HTH DNA binding domain as well as overall structural homology. TFTR typically function as dimers, binding palindromic operator sequences to repress transcription. TFTR transcriptional repression is typically regulated by a small molecule ligand. Classical TFTRs are typically encoded in the genome in close proximity and in opposing orientation to the genes they regulate, which were traditionally thought to exclusively confer resistance to antibiotics (84). Rv3167c is annotated as a TFTR and as such would be expected to exhibit many of the qualities of a classical TFTR.

In this chapter we identify an Rv3167c palindromic binding site within the upstream promoter region of *Rv3167c*. Further, we implicate Rv3167c in the repression of the downstream genes *Rv3168* and *Rv3169*. Next, coordinately using ChIPseq and EMSA, we identify additional Rv3167c binding sites within the Mtb genome. Next, we assess the contribution of genes directly regulated by Rv3167c in the increased necrosis induction by *MtbΔRv3167c*. Finally, we analyzed the increased resistance of *MtbΔRv3167c* to aminoglycoside antibiotics. In summary, we establish Rv3167c as a classical TFTR.

4.2 Results

4.2.1 Rv3167c has the characteristics of a typical TetR-like transcriptional regulator

Rv3167c is annotated as a putative TetR-like transcriptional regulator. Indeed, 89% of the Rv3167c protein sequence can be modeled with 99.9% confidence using the highest scoring template TFR SCO0332, a TetR-like regulator of *Streptomyces coelicolor*, using Phyre2 software (www.sbg.bio.ic.ac.uk/phyre2/). Using the structural information from this search, a model of an Rv3167c homodimer was generated depicted in Figure 15a. The first subunit, colored in the image, depicts the typical N-terminal HTH DNA binding domain common to TFTR shown in blue with the C-terminal ligand binding and dimerization domain colored red. The second subunit of the homodimer is depicted as gray, interacting with the first subunit through its dimerization domain.

TFTR typically function as homodimers (84). To test whether Rv3167c can interact with itself, we made use of the Mycobacterial Protein Fragment Complementation Assay (M-PFC) described previously (139). In this assay the proteins of interest are fused independently to two domains of the enzyme dihydrofolate reductase (DHFR). If the proteins of interest interact it results in functional complementation of DHFR conferring resistance to the antibiotic trimethoprim. As shown in Figure 15b, growth is seen on plates containing trimethoprim when Rv3167c was expressed as both fusions in *Mycobacterium smegmatis* using the M-PFC system indicating that Rv3167c does interact with itself and likely forms a dimer. Additionally, using gel filtration chromatography, we were able to demonstrate that purified Rv3167c does indeed form a dimer. Using protein standards, we were able to show that purified Rv3167c, a monomer of which has a molecular weight of 24kDa, has the same elution volume as ovalbumin,

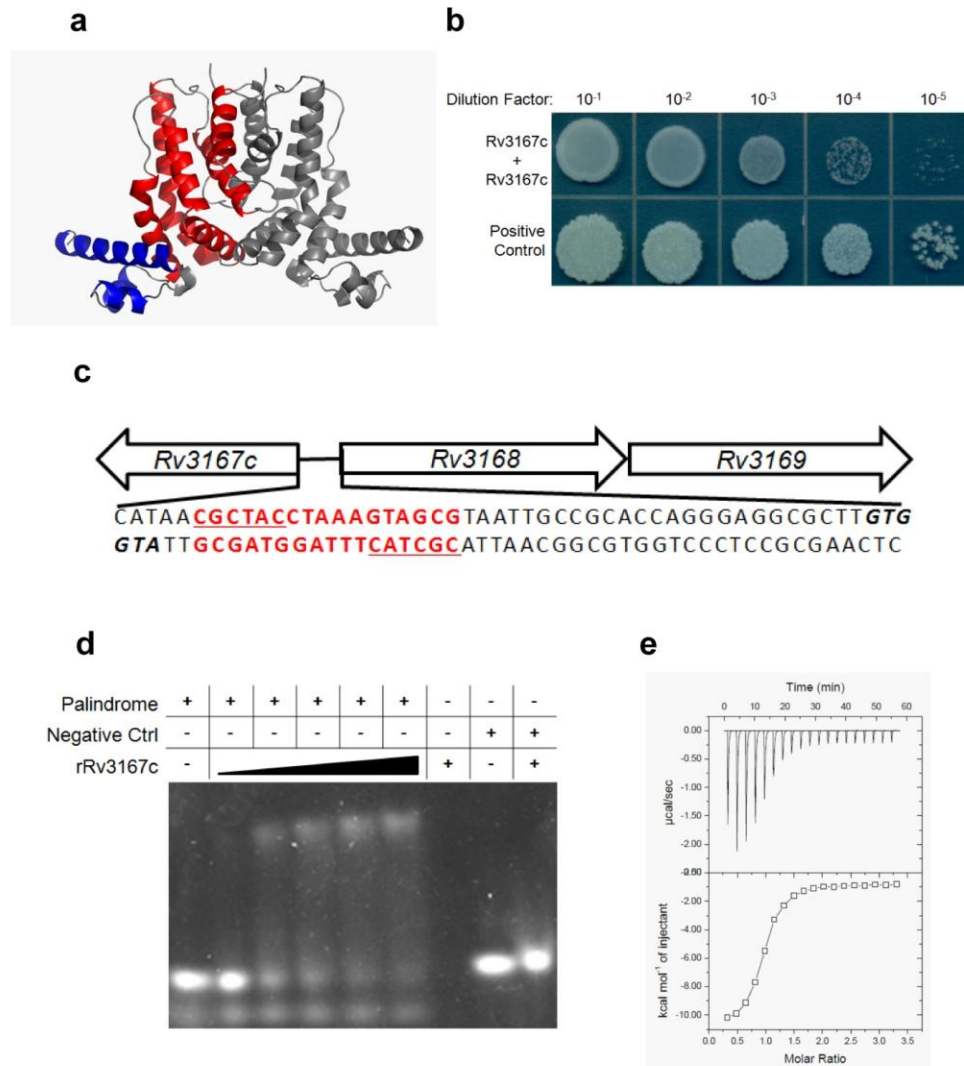


Fig. 15: Rv3167c is a TetR-like transcriptional regulator.

a) Phyre² predicted structure of Rv3167c modeled in PyMol. Helix-turn-helix DNA binding domain is colored blue. Ligand binding and dimerization domain is colored red. Second subunit of Rv3167c homodimer is colored gray. b) *Mycobacterium smegmatis* co-expressing Rv3167c/Rv3167c clones using the M-PFC system. c) Organization of the Rv3167c genomic locus depicting the intergenic region between Rv3167 and Rv3168. Putative palindromic Rv3167c binding site is in red (*palRv3167c*) with each arm of the palindrome underlined. Translational start of Rv3167c and Rv3168 are bolded and italicized. d) EMSA analysis of recombinant Rv3167c (rRv3167c) binding to *palRv3167c*. rRv3167c concentration ranged from 2µM-30µM. *palRv3167c* concentration was constant at 200nM. Randomized DNA served as negative control was used at 200nM with 30µM rRv3167c. Figure is representative of three independent experiments. e) ITC analysis of rRv3167c binding to *palRv3167c*. Figure is representative of three independent experiments. K_d of rRv3167c for *palRv3167c* is 12.3±3.2µM.

Table 3: Gel filtration chromatography analysis of Rv3167c dimerization.

	Elution Volume	VolumeElution/ Volume Void	Mw(kDa)
Albumin	10.91	1.283	67
Ovalbumin	11.66	1.371	43
Chymotrypsinogin A	13.62	1.602	25
Ribonuclease A	14.23	1.674	13.7
rRv3167c	11.66		

Albumin, Ovalbumin, Chymotrypsinogin A, and Ribonuclease A were from LMW Gel Filtration calibration Kit (Amershan Biosciences). Gel filtration was carried out on a GE AKTA Explorer chromatography system with a Superdex 75HR 10/30 column (GE Healthcare Life Science).

which has a molecular weight of 43kDa (Table 3). This indicated that purified Rv3167c exists as a dimer in solution.

Classical TFTRs are typically encoded in the genome in close proximity and in opposing orientation to the genes they regulate (84). Figure 15c depicts the genomic organization of the *Rv3167c* locus with the sequence of the intergenic region between *Rv3167c* and the adjacent genes *Rv3168* and *Rv3169*. The entire intergenic region is only 40 base pairs in length. While comparatively small, this is not out of the ordinary for TFTRs (152). The orientation and proximity of *Rv3168* and *Rv3169* to *Rv3167c* indicates these genes could potentially be regulated by Rv3167c. Indeed, RNAseq data indicates *Rv3168* and *Rv3169* are up-regulated in the *MtbΔRv3167c* (Figure 16) suggestive of direct regulation by Rv3167c. *Rv3168* is annotated as an aminoglycoside phosphotransferase and would be predicted to confer resistance to aminoglycoside antibiotics. This is intriguing as antibiotic resistance regulation was the first ascribed function to TFTR (84). *Rv3169* is annotated as a hypothetical unknown indicating no function has been assigned.

4.2.2 Identification of Rv3167c binding sites

TFTR are typically auto-regulatory and functioning as dimers to bind palindromic operator sequences (84). Interestingly, within the intergenic region between *Rv3167c* and *Rv3168* is a palindrome, highlighted in red in Figure 15c, referred to hereafter as *palRv3167c*. Given the location, this represents a likely Rv3167c binding site. EMSA was used to determine if recombinant Rv3167c could indeed bind this sequence. Complimentary oligonucleotides corresponding to both strands of the *palRv3167c* were annealed to form a double stranded product which was incubated with purified Rv3167c.

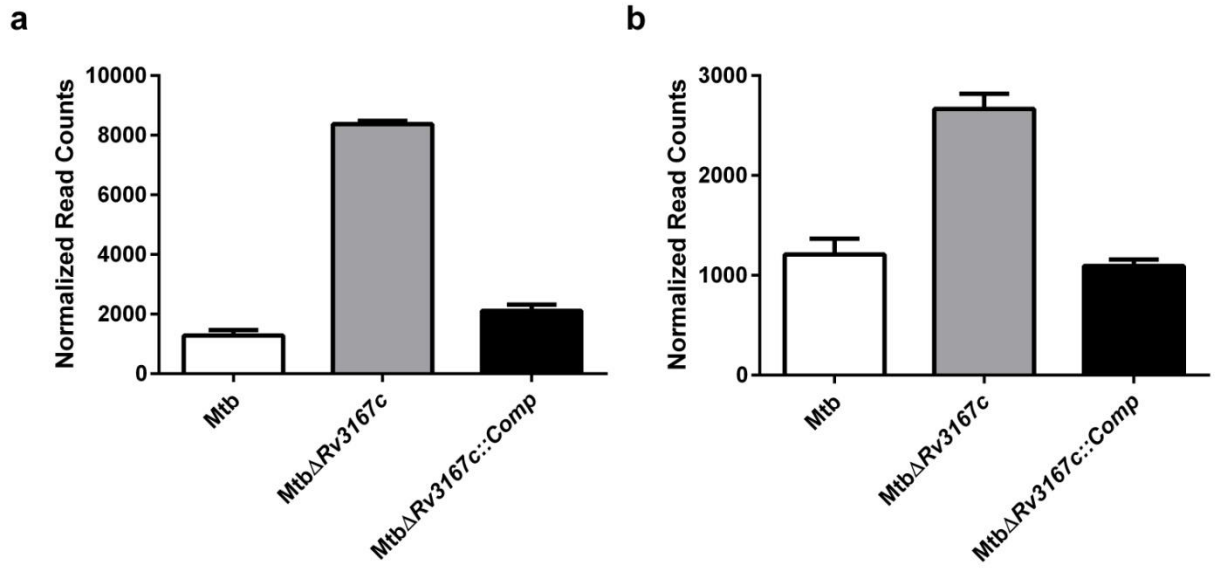


Fig. 16: *Rv3168* and *Rv3169* are up-regulated in *MtbΔRv3167c*

RNAseq mean quantile normalized read counts for a) *Rv3168* and b) *Rv3169* in *Mtb*, *MtbΔRv3167c*, and *MtbΔRv3167c::Comp*.

As shown in Figure 15d, incubating increasing concentrations of Rv3167c with *palRv3167c* results in an increasing shift indicating binding of Rv3167c to the sequence. Importantly, when Rv3167c is incubated with randomized double stranded DNA of similar size no shift is observed indicating Rv3167c's interaction with *palRv3167c* is specific. We further characterized Rv3167c interaction with *palRv3167c* using isothermal titration calorimetry (ITC). Using ITC we show that Rv3167c bound the *palRv3167c* in a 1:1 stoichiometry (protein:DNA) and had a dissociation constant of 12.3 ± 3.2 μ M. Figure 15e depicts a representative ITC experiment. Importantly, Rv3167c did not significantly interact with a negative control as measured by ITC again indicating the interacting between Rv3167c and *palRv3167c* is specific.

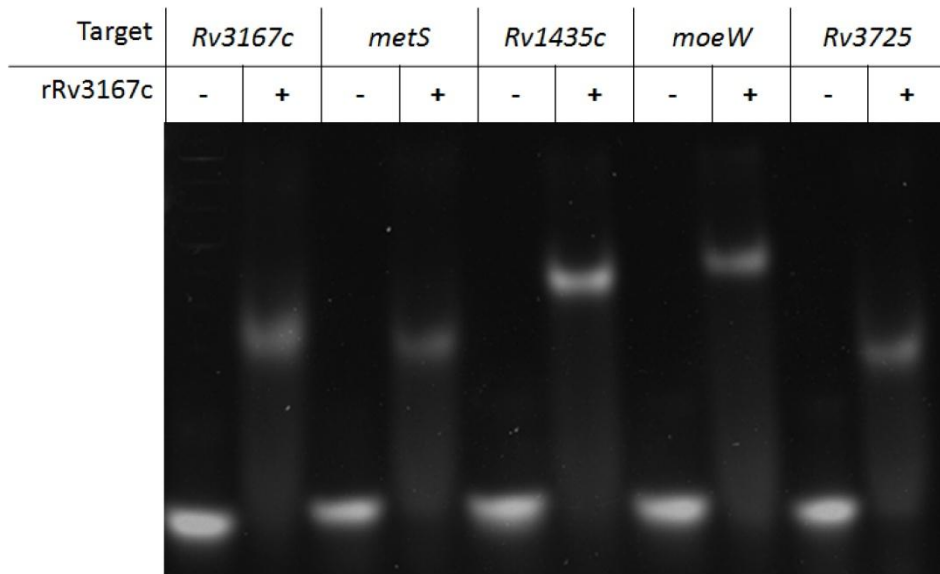
In an effort to better understand Mtb gene regulation, Dr. David Sherman and colleagues at Seattle Biomedical Research Institute undertook a study to identify the binding sites for all putative Mtb transcriptional regulators using ChIPseq (73). Dr. Sherman was kind enough to share the putative binding sites for Rv3167c from that work. We used EMSA to screen for Rv3167c binding to each of the 25 putative binding sites (Table 4). DNA probes were made by annealing oligonucleotides comprised of the 50 base pair region centered on the peak of binding as determined by ChIPseq. Figure 17a summarizes the results of the EMSA screen. Four binding sites were found in addition to the binding site identified in Figure 15d (Rv3167c in Figure 17a) for a total of five binding sites. Using the program MEME (<http://meme-suite.org/>), based on these five sites, we identified the palindromic 17 base pair consensus binding site for Rv3167c (Figure 17b). A summary of all Rv3167c binding sites including relation of binding site to nearest gene and regulatory effects are listed in Table 5. Two of the sites overlapped

Table 4: Putative Rv3167c binding sites as determined by ChIPseq

GENE	Function
Rv0003	recF, DNA replication and repair protein RecF
Rv0013	trpG, Possible anthranilate synthase component II TrpG
Rv0095c	Function unknown
Rv0166	Probable fatty-acid-CoA ligase FadD5
Rv0386	Probable transcriptional regulatory protein
Rv0487	Conserved hypothetical protein
Rv0501	Involved in galactose metabolism
Rv0691c	Probable transcriptional regulatory protein
Rv1007c	Methionyl-tRNA synthetase MetS
Rv1023	enolase eno
Rv1079	Cystathionine gamma-synthase MetB
Rv1212c	glgA, Putative glycosyl transferase GlgA
Rv1234	Probable transmembrane protein
Rv1435c	Unknown
Rv1795	ESX conserved component EccD5
Rv1895	Possible dehydrogenase
Rv2338c	Possible molybdopterin biosynthesis protein MoeW
Rv2941	fadD28, Involved in phthiocerol dimycocerosate
Rv3208	Probable transcriptional regulatory protein
Rv3349c	Probable transposase
Rv3412	Conserved hypothetical protein
Rv3428c	Transposase
Rv3725	Oxidoreductase
Rv3802c	Shown to have phospholipase and thioesterase activity
Rv3803c	fbpD, Involved in cell wall mycoloylation

Putative Rv3167c binding sites as provided by Dr. David Sherman of Seattle Biomedical Research Institute as part of the Mtb Consortium.

a



b

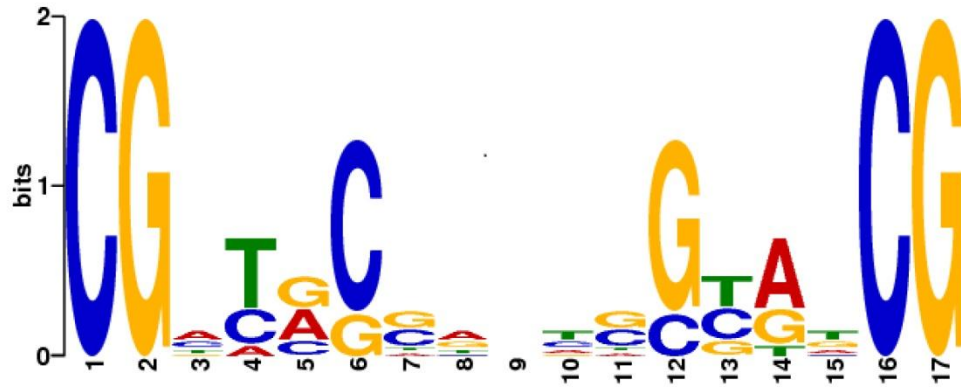


Fig. 17: Identification of additional Rv3167c binding sites

a) EMSA of additional Rv3167c binding sites in the Mtb genome. Figure is a consolidation of positive five hits from EMSA screen of potential binding sites identified through ChIPseq. Concentration of rRv3167c was 30uM and concentration of all oligos was 200nM. **b)** Rv3167c consensus binding sequence as determined by the program MEME (<http://meme-suite.org/>) based on the five identified Rv3167c binding sites.

Table 5: Summary of Rv3167c binding sites based on EMSA

Gene ID	Gene Name	EMSA Confirmed	Binding site relative to ATG	De-regulated in MtbΔRv3167c
<i>Rv1007c</i>	<i>metS</i>	Yes	Overlaps ATG	No
<i>Rv1435c</i>	<i>Rv1435c</i>	Yes	+329	No
<i>Rv2338c</i>	<i>moeW</i>	Yes	Overlaps ATG	No
<i>Rv3167c</i>	<i>Rv3167c</i>	Yes	Overlaps ATG	Yes (Rv3168 and Rv3169)
<i>Rv3725</i>	<i>Rv3725</i>	Yes	-385	No

Summary of Rv3167c binding sites including nearest gene to binding site, location of binding site to genes translational start, and differential expression of gene in MtbΔRv3167c.

with the translation start of the gene potentially indicating direct regulation. These sites were *metS* and *moeW*, annotated as a methionyl-tRNA synthetase and possible molybdopterin biosynthesis protein, respectively. However, neither of these genes are differentially regulated in *MtbΔRv3167c*. The other two binding sites were completely within the coding sequence of the gene, *Rv1435c*, or greater than 300 base pairs upstream of the coding sequence, *Rv3725*. Neither of these genes have an annotated function. Again, neither of these genes are differentially regulated in *MtbΔRv3167c* either. Considering that these binding sites do not fit the profile of a traditional TFTR and the genes are not differentially regulated in *MtbΔRv3167c*, we decided to no longer consider these sites for the time being. Even though *MetS* and *MoeW* showed no differential regulation in *MtbΔRv3167c*, the *Rv3167c* binding site in relation to the gene was similar to a traditional TFTR. As such, these genes were considered for future studies.

4.2.3 Identifying the *Rv3167c* inducing ligand

As reviewed in section 1.5.1, TFTR are fairly simplistic regulatory systems responding usually to small molecule ligands. Upon binding to their cognate ligand, repression is released and the genes regulated by the TFTR are expressed. Identifying the ligand or stimuli that causes the release of repression is a useful tool when studying TFTR as it provides insight into the function of the regulator. Considering the diverse functions of the genes regulated by *Rv3167c*, determining an inducing stimulus would provide insight into the function of *Rv3167c* as it relates to *Mtb* physiology. Identification of a stimulus would also be technically beneficial as it would allow for the study of *Rv3167c* gene regulation without having to infect macrophages. In an effort to determine the ligand/stimuli of *Rv3167c*, we utilized several *in vitro* approaches. The

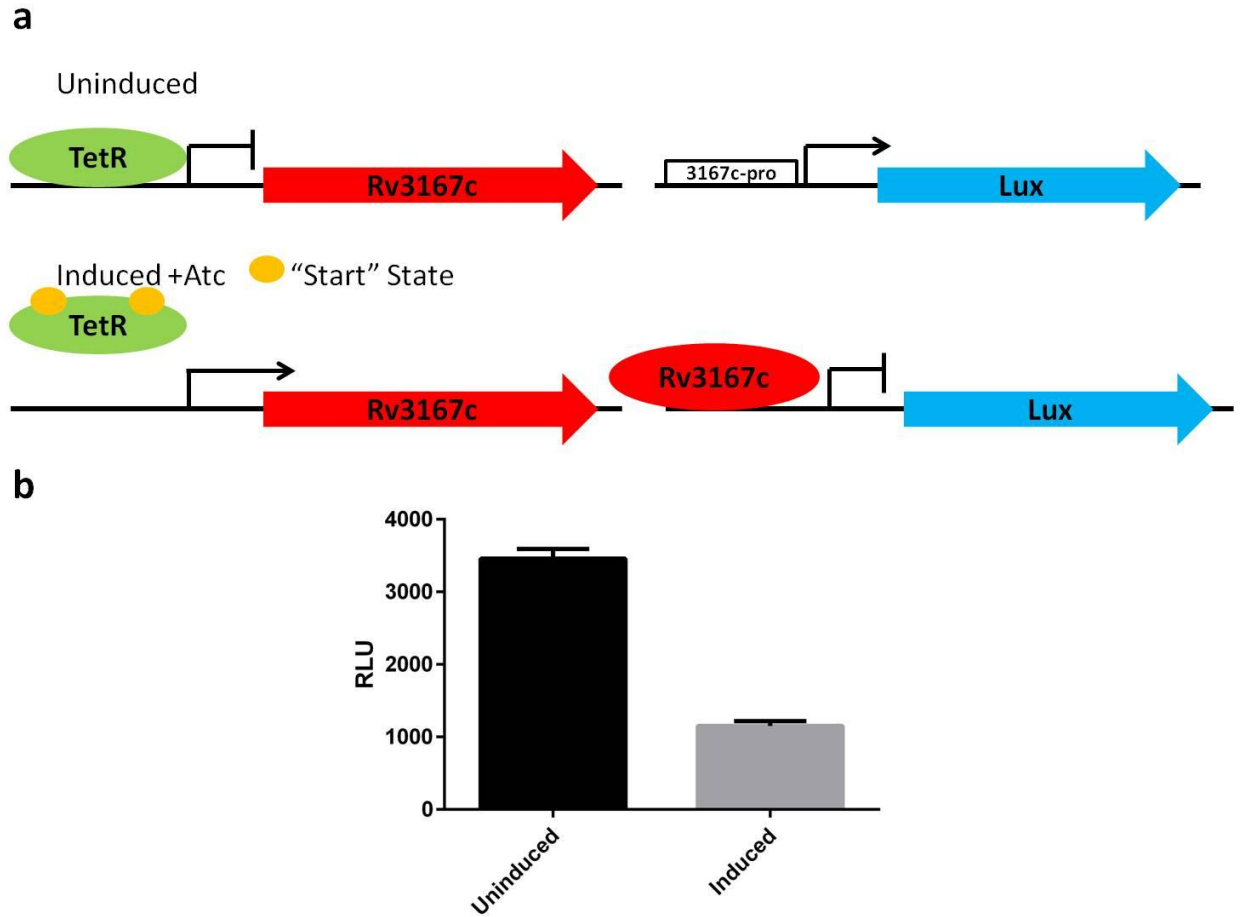


Fig. 18: Luciferase based reporter system to identify Rv3167c ligand

a) Schematic representation of luciferase based reporter system. Rv3167c expression is under control of *E. coli* TetR while the lux operon is under control of the Rv3167c promoter. When atc (anhydrotetracycline) is present Rv3167c expression is repressed and light is produced. This is the uninduced state. When atc is added, TetR releases repression and Rv3167c is expressed which binds to its own promoter repressing the lux operon reducing light production. This is induced state and is used to screen for Rv3167c ligands. b) Proof of concept showing that when atc is added to the system in the induced state, light production as measured by relative light units (RLU) is reduced.

first was a luciferase based reporter system used in *M. smegmatis* to facilitate high throughput screening of potential ligands. A plasmid encoding the bacterial *luxABCDE* operon was expressed in *M. smegmatis*. The substrate producing genes *luxCDE* were constitutively expressed, while *luxAB* were expressed from the Rv3167c native promoter. Additionally, Rv3167c was expressed in *M. smegmatis* under control of a tetracycline inducible promoter. When anhydrotetracycline (atc) is added, Rv3167c is expressed and represses light production (Figure 18b). This is considered the repressed, or off, state and is used to screen for ligands that then cause Rv3167c to release repression resulting in an increase in luminescence. In a complimentary approach, the expression of *Rv3168* was monitored by real time PCR of *in vitro* growth cultures treated with varying stimuli. Rv3167c directly regulates *Rv3168*. Release of DNA binding and repression by Rv3167c upon ligand interaction should result in up-regulation of *Rv3168*.

The first stimuli screened were those common to the phagosomal environment including reactive oxygen and nitrogen species, cell wall stressors, acid stress, and metabolic stress (Sauton's media). Because Rv3167c regulates *Rv3168*, an aminoglycoside phosphotransferase, several aminoglycoside antibiotics were tested. Additionally, the first line Mtb drugs were tested. Consolidated micro-array expression data at tbdb.org indicated that Rv3167c expression was induced when exogenous free fatty acids or the drug thioridazine are added to the media. These potential stimuli were tested as well. Summary of all stimuli tested and results are in Table 6. After thorough testing, none of these potential stimuli resulted in an increase in *Rv3168* expression or an increase in luminescence (Table 6).

Table 6: Summary of potential Rv3167c ligands tested

	Potential Stimuli	RT-PCR	Luciferase
Oxidative stress			
	H2O2	x	NT
	Superoxide	x	NT
	HOCl	x	NT
Nitrosative Stress			
	DETA-NO	x	x
Cell Surface Stress			
	SDS	x	x
	Triton	x	x
Metabolic Stress			
	Sauton's Media	x	x
Antibiotic Stress			
	Zeocin	NT	x
	Ethambutyl	NT	x
	Isoniazid	NT	x
	Rifampicin	NT	x
	Pyrazinamide	NT	x
pH Stress			
	pH=5.5	x	NT
	pH=5.0	x	NT
	pH=4.5	x	NT
Aminoglycoside Stress			
	Kanamycin	x	x
	Hygromycin	x	x
	Neomycin	x	x
	Parmomycin	x	x
	Streptomycin	x	x
	Gentamycin	x	x
Free Fatty Acids			
	Palmitic Acid	x	x
	Arachidonic Acid	x	x
	Oleic Acid	x	x
Miscellaneous			
	Thioridazine	x	x

Summary of stimuli tested as potential Rv3167c inducing ligands. Stimuli we tested *in vitro* either using real time PCR or a luciferase based reporter system. x=no phenotype, NT=not tested.

Because *Rv3167c* may play a role in the adaptation to the intracellular environment, expression of *Rv3168* was also monitored after *Mtb* infection of macrophages. Applying the same principle, if *Mtb* encounters the *Rv3167c* inducing ligand after infection it should result in an increase in *Rv3168* expression. THP-1 cells were infected and RNA samples were collected at 2hr, 1Day, 2Days, 3Days, and 4Days post infection. Again, no difference was seen in expression of *Rv3168* over the course of the infections.

4.2.4 Genes directly regulated by *Rv3167c* do not contribute to increased necrosis

DNA binding studies identified five *Rv3167c* binding sites in the *Mtb* genome. As discussed above, two of those binding sites, *Rv1435c* and *Rv3725*, are likely not functional binding sites and were not considered further. The three remaining binding sites would be expected to regulate four genes, *Rv3168*, *Rv3169*, *moeW*, and *metS*. Deletion of *Rv3167c* from the genome should result in up-regulation of these genes as *Rv3167c* is no longer present to repress transcription. As anticipated, *Rv3168* and *Rv3169* were up-regulated in the *MtbΔRv3167c*. However, *moeW* and *metS* were unchanged (Table 5). The *Rv3167c* binding site near *moeW* and *metS* overlapped the translational start of the genes, suggestive of direct regulation. Release of repression by *Rv3167c* may not be the only requirement for expression of these genes. It is likely they require an activator or alternative sigma factor not present under *in vitro* conditions for expression. Because of this, these genes, along with *Rv3168* and *Rv3169*, were selected for further analysis.

To determine the contribution of *Rv3168*, *Rv3169*, and *MoeW*, to the induction of necrosis we deleted these genes in the *MtbΔRv3167c* background to generate

MtbΔRv3167ΔRv3168ΔRv3169 (*MtbΔRv3167c-69*) and *MtbΔRv3167ΔmoeW*. *Rv3168* and *Rv3169* are proposed to form a two gene operon. As such, we opted to delete both genes simultaneously resulting in a triple gene knockout. Knockouts were confirmed by PCR analysis (Figure 19a and b). These mutants were used to infect THP-1 macrophages for 24 hours followed by staining with propidium iodide (PI) to measure cell membrane permeability. As shown in Figure 20a and b, *MtbΔRv3167c-69* and *MtbΔRv3167ΔmoeW* induce equivalent levels of cell death as compared to *MtbΔRv3167c* indicating these genes are not involved in necrosis induction by the mutant. Because *metS* is an essential gene, we were not able to create a double mutant. To assess its contribution to the death phenotype, *metS* was over expressed in *Mtb* (*Mtb::metS*). Over-expression was confirmed via western blotting (Figure 19c). We rationalized that over expression in wild type *Mtb* would result in increased PI staining if MetS were involved in inducing necrosis. However, *Mtb::metS* induced similar levels of necrosis as wild type *Mtb* in THP-1 cells at 24 hours post infection (Figure 20c). This suggests that MetS likely does not contribute to the increased necrosis seen in *MtbΔRv3167c*. However, this assumption is made with caution as over-expression is not always effective in replicating a phenotype.

4.2.5 *MtbΔRv3167c* is resistant to kanamycin

TFTR were traditionally thought to be exclusively involved in resistance to antibiotics, as is the case with the name sake of the family TetR from *E. coli*. As discussed above, as more TFTR began to be characterized, it became clear that regulating antibiotic resistance was just one of many functions of the TFTR family of regulators. That being said, at first glance *Rv3167c* appears to fit the mold of a TFTR that confers resistance to antibiotics. DNA binding and expression studies showed that *Rv3167c*

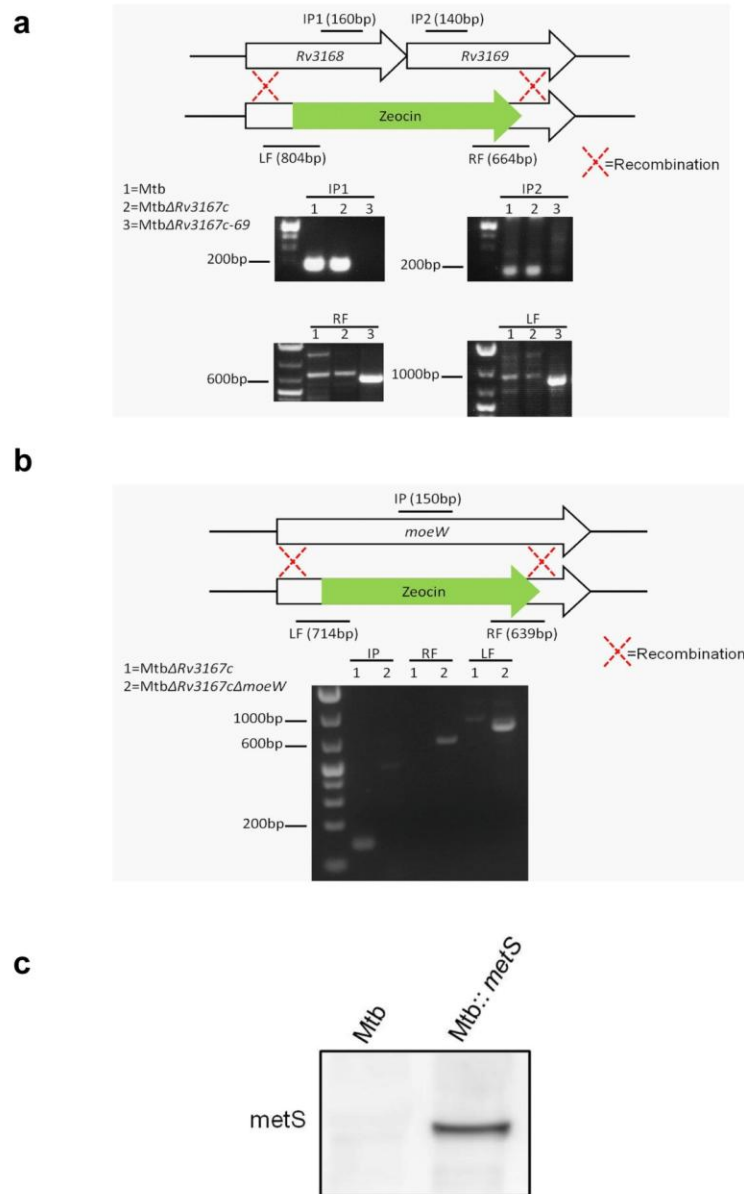


Fig. 19: Confirmation of *Rv3168-Rv3169* and *moeW* knockouts and MetS over expression

Strategy and confirmation of the recombination of zeocin marker in place of a) *Rv3168-Rv3169* or b) *moeW*. Primer sets used to confirm knockout are labeled LF (Left Flank) and RF (Right Flank) which amplify the zeocin/gene junctions and only create a product if recombination was successful. Primer set labeled IP (Internal Priming) amplifies a region within the genes deleted and will not create a product if recombination was successful. Genomic DNA was used as template and PCR was carried out with standard methods. Reactions were run on a 1.5% agarose gel. PCR product sizes are given in parenthesis. c) Western blot analysis confirming expression of MetS in Mtb::*metS*. A myc tagged version of MetS was expressed exogenously in Mtb. Lysates were prepared as described in methods. Anti-myc antibody was used at 1:50 dilution.

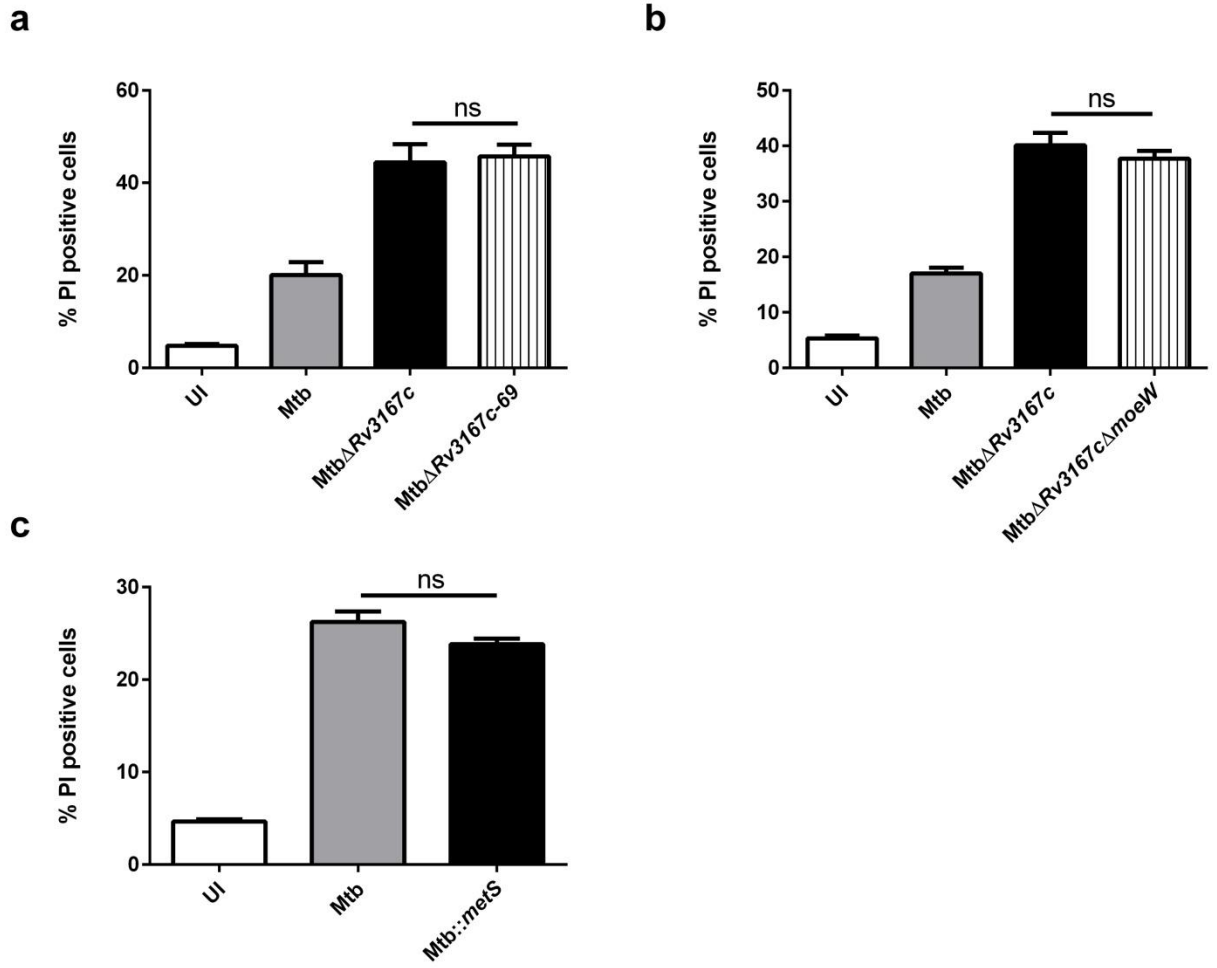


Fig. 20: Genes directly regulated by Rv3167c do not contribute to increased necrosis

THP-1 cells were differentiated with PMA for 24hours and were left uninfected or infected with Mtb, Mtb Δ Rv3167c and a) Mtb Δ Rv3167c-69, b) Mtb Δ Rv3167c Δ moeW or c) or Mtb::metS for 24hours followed by staining with propidium iodide (PI). Cell death was analyzed by flow cytometry. Data is representative of three independent experiments. Data presented as mean \pm S.E.M. ns=not significant.

regulates its neighboring gene Rv3168, a proposed aminoglycoside phosphotransferase. Rv3168 would be expected to confer resistance to aminoglycosides, such as kanamycin, by modifying them with a phosphate group so they can no longer bind their target, the ribosome. Given its proposed function and the fact that Rv3168 is up-regulated in *MtbΔRv3167c*, we wanted to test whether or not *MtbΔRv3167c* was more resistant than wildtype to kanamycin. Indeed, *MtbΔRv3167c* was able to grow in media containing kanamycin at the minimum inhibitory concentration (5 μg/mL) while wild type growth was arrested (Figure 21a). Next, *MtbΔRv3167c* was grown in media containing increasing concentrations of kanamycin to determine the extent of the aminoglycoside resistance. Unexpectedly, *MtbΔRv3167c* grew as well as the untreated control at kanamycin concentrations up to 1280μg/mL, the highest concentration of tested (Figure 21b). Additional testing indicated that *MtbΔRv3167c*'s antibiotic resistance was limited to the aminoglycosides (Table 7). Interestingly, *MtbΔRv3167c* was still susceptible to streptomycin. Although streptomycin is an aminoglycoside, it differs significantly in structure from other aminoglycosides which may explain this observation.

To determine whether Rv3168 was responsible for conferring the resistance to kanamycin in *MtbΔRv3167c*, we assessed whether the resistance phenotype was lost in *MtbΔRv3167c-69*, in which Rv3168 has been deleted. Unfortunately, *MtbΔRv3167c-69* exhibited resistance to kanamycin at MIC concentrations similar to the parental strain (Figure 21c) indicating that the over expression of Rv3168 is not responsible for the kanamycin resistance of *MtbΔRv3167c*. Owing to its position in the mycobacterial outer

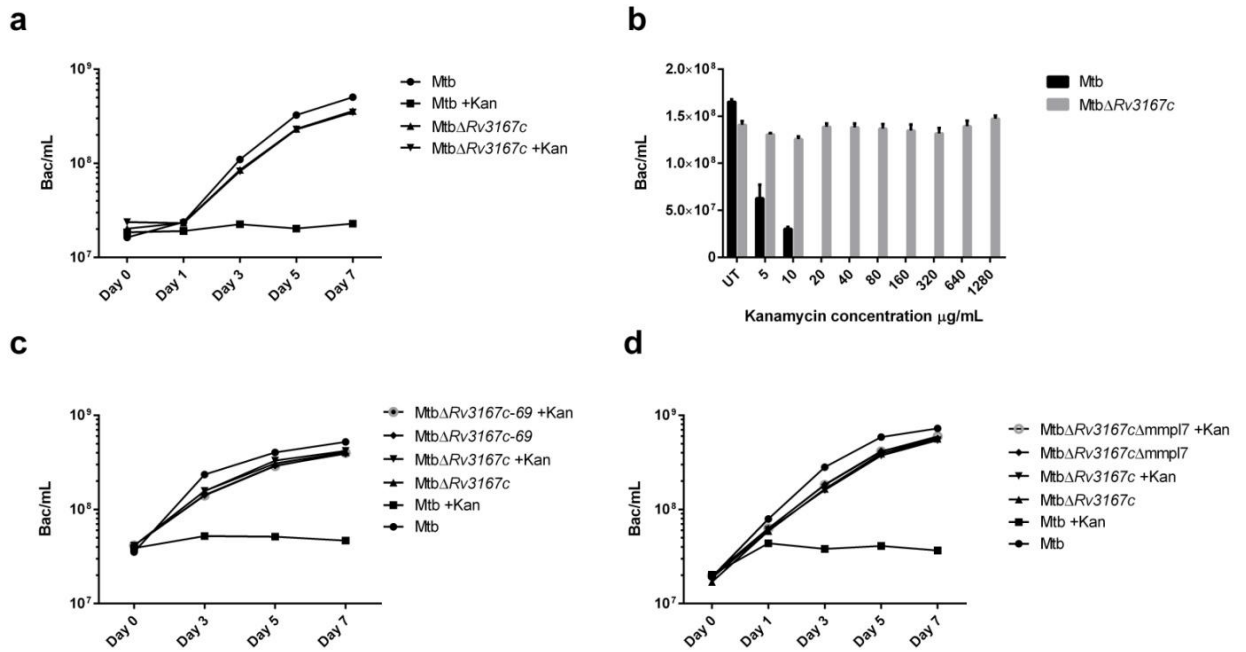


Fig. 21: *MtbΔRv3167c* demonstrates resistant to kanamycin

All growth curves were conducted in Middlebrook 7H9 broth at a starting OD₆₀₀~0.05. Unless otherwise noted, kanamycin was used at 5μg/mL. a) *Mtb* and *MtbΔRv3167c* grown in presence or absence of kanamycin. OD₆₀₀ readings were taken at days 0,1,3,5, and 7 and converted to bac/mL. b) Determination of maximum resistance of *MtbΔRv3167c* to kanamycin. Kanamycin concentrations range from 5-1280μg/mL. OD₆₀₀ measurements were taken at days 0,1,3,5, and 7. Graph depicts day 7 end point readings converted to bac/mL. *Mtb* was only tested at 5 and 10μg/mL to confirm kanamycin effectiveness. c) *Mtb*, *MtbΔRv3167c*, and *MtbΔRv3167c-69* grown in presence or absence of kanamycin. OD₆₀₀ readings were taken at days 0,1,5, and 7 and converted to bac/mL. d) *Mtb*, *MtbΔRv3167c*, and *MtbΔRv3167cΔmmp17* grown in presence or absence of kanamycin. OD₆₀₀ readings were taken at days 0,1,3,5, and 7 and converted to bac/mL.

Table 7: *MtbΔRv3167c* antibiotic resistance is limited to the aminoglycosides

Antibiotic	<i>MtbΔRv3167c</i>	
	Susceptible (S)	Resistant (R)
Aminoglycosides		
Kanamycin		R
Gentamicin		R
Neomycin		R
Parmomycin		R
Streptomycin		S
First Line Mtb Drugs		
Ethambutol		S
Isoniazid		S
Rifampicin		S
Pyrazinamide		S
General		
Zeocin		S
Vancomycin		S

membrane PDIM has long been associated with the Mtb permeability barrier. Mtb strains lacking the ability to synthesize PDIM are more susceptible to antibiotic stress (101). Considering this, an argument could be made that a strain over producing PDIM, such as *MtbΔRv3167c*, would be more resistant to antibiotics. However, *MtbΔRv3167cΔmmp17* maintains resistant to kanamycin at the MIC (Figure 21d). One caveat underlying interpretations of these results is that the kanamycin resistance does not revert in the *MtbΔRv3167c* complement strain making it hard to draw any significant conclusions. As it stands, the nature of the kanamycin resistance in *MtbΔRv3167c* remains a topic for future studies.

4.3 Discussion

In this chapter, we established Rv3167c as a traditional TFTR. We identified five total Rv3167c binding sites in the Mtb genome. Two of these sites, *Rv1435c* and *Rv3725*, we did not consider further given that the Rv3167c binding site relative to these genes was not in keeping to a traditional TFTR and neither gene was differentially regulated in *MtbΔRv3167c* (Table 5). There is the possibility that these binding sites are no longer functional in Mtb. The Mtb genome is roughly two mega base pairs smaller than that of the environmental *M. smegmatis*. Aside from some cases of horizontal gene transfer, the Mtb genome is considered to be a product of genetic reduction and specialization to the human host from a free living ancestor such as *M. smegmatis* (155).

Comparison of the genomic organization near these binding sites in Mtb with the genomic organization of the homologs of these genes in *M. smegmatis* suggests there was likely genomic re-organization at these sites in Mtb. For example, the gene upstream of *Rv1435c* (*Rv1433*) is divergently encoded in Mtb while in *M. smegmatis* the homologs of these same genes (*Msmeg_0673* and *Msmeg_0674*) are encoded in the same direction. Additionally, in Mtb there is a small open reading frame inserted between the genes (*Rv1434*) that does not have a homolog in *M. smegmatis*. There is evidence of genomic re-organization near the *Rv3725* binding site as well. While, *M. smegmatis* does not encode a homolog to *Rv3725*, the gene directly upstream, *cut5b*, does have a homolog, *Msmeg_5878*. Interestingly, in Mtb this gene is divided into two open reading frames, *cut5a* and *cut5b*, while in *M. smegmatis* it exists as a single open reading frame. It's possible that in *M. smegmatis* these represent functional binding sites for the *Rv3167c*

homolog *Msmeg_2043* while genomic evolution has rendered these sites non-functional or unnecessary in *Mtb*.

The other three *Rv3167c* binding sites would be expected to regulate four genes, *Rv3168*, *Rv3169*, *metS*, and *moeW*. Analysis revealed that these genes do not contribute to the necrosis induced by *MtbΔRv3167c* (Figure 20). It is possible that the sites we ruled out, *Rv1435* and *Rv3725*, are involved but this seems unlikely for the reasons outlined above. One caveat is that we were unable to delete *metS*; instead deciding to over express MetS in wild type *Mtb*. Over expression of a gene does not always replicate a phenotype. Additionally, MetS was expressed with an N-terminal myc tag which may interfere with its function. To completely rule out MetS, a conditional knockout approach would likely need to be used. However, this strain would undoubtedly suffer a fitness disadvantage making any effects on necrosis inducing after infection hard to interpret. There is the possibility we did not identify all *Rv3167c* binding sites. However, given the availability of ChIPseq data, this seems unlikely, especially considering the initial criteria were relaxed favoring false positives as oppose to false negatives. As it stands, none of the genes directly regulated by *Rv3167c* contribute to the increased necrosis induction observed in *MtbΔRv3167c*.

When considering the diverse functions of these genes, it is difficult to determine a conserved function for *Rv3167c*. The regulation of *Rv3168* suggests *Rv3167c* plays a role in antibiotic resistance. *Rv3168* is annotated as an aminoglycoside phosphotransferase and would be predicted to confer resistance to antibiotics such as kanamycin. We showed that *MtbΔRv3167c* is indeed resistant to kanamycin (Figure 21a). Confusingly, the increased resistance is not a function of over expression of *Rv3168* as

deletion of *Rv3168* in the *MtbΔRv3167c* background did not revert the resistance (Figure 21c). However, the regulation of *Rv3168* may still provide insight into *Rv3167c*'s function. *Rv3168* would be expected to confer resistance to kanamycin which inhibits the proof reading function of RNA polymerase resulting in aberrant and mis-folded protein (161). This may explain *Rv3167c* regulation of *metS*. As the only methionyl-tRNA synthetase encoded by *Mtb*, *metS* is essential as it is needed for the initiation of protein synthesis via n-formyl-methionine as well as protein elongation. A bacterium experiencing kanamycin stress would need to up-regulate protein synthesis to replace mis-folded protein with functional protein, a process of which *MetS* is essential. Additionally, prolonged exposure to kanamycin results in increased cell surface stress as a result of the incorporation of aberrant protein into the membrane (161). While *Rv3169* does not have an annotated function, it contains domain two attH-like domains, which are associated with import of lipids. Lipids imported by *Rv3169* may play a role in kanamycin resistance by being used to alleviate stress or repair the *Mtb* membrane. While their annotated functions on the surface seem incompatible, *Rv3168*, *Rv3169*, and *MetS* may all be associated with the *Mtb* response to aminoglycosides.

It is, unfortunately, hard to reconcile this proposed function with that of *MoeW*. Proposed to have a role in molybdenum co-factor (MoCo) biosynthesis, it is hard to imagine a direct role in resistance to aminoglycosides. MoCo is used by enzymes that make use of the redox properties of molybdenum to catalyze reaction in carbon, nitrogen, and sulfur metabolism (162). Interestingly, *Mtb* strains deficient in the production of MoCo are impaired in the ability to inhibit phagolysosome fusion as well as being attenuated in primate lungs (163,164) suggesting a role in intracellular survival. The

stresses associated with exposure to aminoglycosides are not that dissimilar to some of the stresses faced by Mtb in the intracellular environment, notably cell surface stress. With this in mind, it may be that Rv3167c is responsible for regulating Mtb general stress response and adaptation to the intracellular environment. Our RNAseq analysis lends credibility to this idea in that the Rv3167c regulon contains over 400 genes indicated a broad transcriptional response and is enriched for genes involved in lipid metabolism (Figure 9).

Extensive effort was made to identify an Rv3167c inducing stimuli using *in vitro* expression analysis and a luciferase based reporter system. Tested stimuli were selected in an effort to mimic the phagosomal environment (Table 6). Unfortunately, these efforts fell short which is perhaps unsurprising given the historical difficulty in identification of TFTR ligands. Additionally, we were unable to demonstrate that Rv3167c repression is relieved after ex vivo infection using quantitative PCR analysis between two hours and 3 days after infection. However, due to technical issues with ex vivo infections we may have missed the time point when Rv3167c encounters its cognate ligand. Additionally, using real time PCR has several drawbacks when analyzing bacterial gene expression after infection. The most important being the inability to correctly normalize gene expression as most genes in the Mtb genome experience some degree of differential regulation after infection, including the most commonly used normalization genes *sigA* and *16s* rRNA. To get around this problem and prove conclusively that Rv3167c responds to the intracellular environment, RNAseq analysis would have to be used to analyze varying time points after infection. RNAseq normalization is independent of the expression of any individual gene and would not be subject to the same shortfalls as

quantitative PCR. This all assumes that the Rv3167c inducing ligand is present during infection. There is the possibility that standard ex vivo infection protocols do not sufficiently mimic the *in vivo* environment to generate the Rv3167s inducing ligand, in which case RNAseq analysis on *in vivo* mouse infections would need to be conducted.

In this chapter we also showed that *MtbΔRv3167c* demonstrates increased resistance to kanamycin (Figure 21). In fact, *MtbΔRv3167c* is extremely resistant to kanamycin as growth is unaffected in media containing as much as 1280 μg/mL kanamycin (Figure 21b). Given that *Rv3168* is annotated as an aminoglycoside phosphotransferase, this is perhaps not surprising. However, the increased kanamycin resistance is independent of Rv3168 as deletion of *Rv3168* in *MtbΔRv3167c-69* did not restore kanamycin susceptibility (Figure 21c). Loss of PDIM has been implicated in increased susceptibility to vancomycin (101). Increased PDIM in *MtbΔRv3167c* could explain the increased kanamycin resistance. However, *MtbΔRv3167cΔmmp17* is as resistant to kanamycin as the *Rv3167c* mutant (Figure 21d). Considering the growth curves were conducted at MIC concentrations of kanamycin, it is possible that deletion of *Rv3168* or *mmp17* made *MtbΔRv3167c* more susceptible to kanamycin, just not as susceptible as wild type. There could be synergy between Rv3168 and PDIM in the mutant as well, which could only be revealed with a triple mutant. Kanamycin requires active transport into the cell to reach its target. Given that *MtbΔRv3167c* resistance appears limited to the aminoglycosides (Table 7), it could be that the pore required to transport kanamycin into the cell is expressed at lower levels in *MtbΔRv3167c*. Given the extreme level of resistance, it is likely that all of these factors play a role in *MtbΔRv3167c* kanamycin resistance.

In conclusion, we demonstrate here that Rv3167c is a classical TFTR. We further identified the Rv3167c binding sites in the Mtb genome. However, the genes directly regulated by Rv3167c do not contribute to the increased necrosis observed in *Mtb* Δ *Rv3167c* infected cells.

Chapter 5: Discussion and Future Directions

Mtb has a complex relationship with host cell death induction. The prevailing model is that Mtb inhibits apoptosis at early stages of the infection, favoring replication, but induces necrosis at later stages in order to exit the host cell (58). Recently, our group described an Mtb mutant resulting from the deletion of the gene *Rv3167c*, a putative member of the TFTR family of transcriptional regulators. Infection of macrophages with *MtbΔRv3167c* resulted in a significant increase in phagosomal escape, autophagy, and host cell necrosis when compared to wild-type infected cells (136). In this dissertation we establish *Rv3167c* as a member of the TFTR and define its core regulon. We go on to show that *MtbΔRv3167c* produces increased amounts of the virulence associated glycolipid PDIM. Further, we show that the increased PDIM is responsible for the increased necrosis of *MtbΔRv3167c* and demonstrate a role for PDIM in Mtb autophagy induction and phagosomal escape.

5.1 *Rv3167c* regulation of the PDIM operon

Analysis of the genes directly regulated by *Rv3167c* indicated these genes were not involved in the induction of cell death in *MtbΔRv3167c* (Figure 20). RNAseq analysis identified the up-regulation of the PDIM synthesis cluster (Figure 10) in the mutant and subsequent studies established PDIM as responsible for the increased necrosis, autophagy, and phagosomal escape of *MtbΔRv3167c* (Figure 12 and 13). What is unclear is the nature of *Rv3167c* regulatory control on the PDIM operon. *Rv3168*, *Rv3169*, *MetS*, and *MoeW* would not be expected to have any direct transcriptional activity. As such it is unlikely that they represent nodes in a transcriptional hierarchy beginning at *Rv3167c* and leading to PDIM regulation. The fact that these genes do not

influence *MtbΔRv3167c* necrosis induction is indirect evidence that they are unlikely to be involved in PDIM regulation. However, directly assessing PDIM gene expression in *MtbΔRv3167c-69*, *MtbΔRv3167ΔmoeW*, and *Mtb::mets* would be needed to completely rule out this possibility. There is the possibility that *Rv3167c* directly regulates the PDIM operon. In the initial ChIPseq data there was a putative *Rv3167c* binding site within the PDIM operon but this site was ruled out during follow up studies. Of course there is always the possibility that an *Rv3167c* binding site was not identified. However, given the availability of ChIPseq data, this possibility seems unlikely. Our RNAseq data indicated greater than 400 genes are differentially expressed in *MtbΔRv3167c*. There are several known regulators of PDIM biosynthesis such as *rpoB* (124), *pknH* (125), and *espR* (123). However, none of these genes are differentially regulated in *MtbΔRv3167c* and they themselves indirectly regulate PDIM synthesis. Closer inspection of our RNAseq data reveals differential regulation of several RNA polymerase sigma factors, including *sigE* and *sigB*. Differential expression of these global regulators could explain the high degree of gene regulation we see in *MtbΔRv3167c*. However, it is unclear from available data whether the PDIM operon is under regulatory control of these sigma factors. The PDIM operon is predicted to have a promoter regulated by *sigL* (74). Unfortunately, *sigL* is not differentially regulated in *MtbΔRv3167c*. Deletion of these sigma factors in *MtbΔRv3167c* and assessment of PDIM production would need to be conducted to verify if these sigma factors do indeed have a role in PDIM regulation.

It has been shown that PDIM production is increased when *Mtb* is grown on cholesterol as its sole carbon source. Cholesterol is believed to be the primary carbon source used for energy production by intracellular *Mtb* (131). The increase in PDIM was

proposed to be the result of metabolic flux from increased propionate as a result of cholesterol catabolism (130). However, this study did not determine whether growth on cholesterol resulted in increased transcription of PDIM synthesis genes or whether the increase in PDIM was a result of protein already present. PDIM synthesis and export genes are large modular proteins that are energetically expensive to synthesize and as a result *in vitro* grown Mtb typically lose surface PDIM with extended passaging (122). It is likely then that growth on cholesterol results in the up-regulation of PDIM synthesis genes followed by increase PDIM production to alleviate the increase in propionate. It is interesting to think that Rv3167c may influence PDIM regulation through metabolic flux. One caveat is that our RNAseq analysis was conducted on cultures grown with glycerol as the sole carbon source, degradation of which does not produce propionate. However, analysis revealed enrichment of three gene ontology categories all associated with lipid metabolism. All three of these categories include genes involved in beta oxidation and break down of lipids which would ultimately lead to increases in propionate concentrations in the cell. It would be interesting to analyze production of propionate in Mtb Δ Rv3167c by liquid chromatography coupled to mass spectrometry. Ultimately, without a better understanding of the transcriptional regulation of the PDIM operon itself, which is lacking in the field, it will continue to be difficult to explain Rv3167c transcriptional effects on the operon.

5.2 PDIM contribution to Mtb phagosomal escape

Previous work in our lab established that Mtb Δ Rv3167c induces increased necrosis, increased autophagy, and increased phagosomal escape in infected macrophages (136). Here, we demonstrate that all three of these phenotypes are a result of the

increased production of PDIM by the mutant. Necrosis and autophagy, while both mechanisms of cell death, are separate distinct processes requiring specialized cellular machinery. Additionally, our previous work demonstrated that the induction of necrosis was independent of all known programmed necrosis pathways and that the induction of autophagy was independent of necrosis induction in infected cells (136).

It has been established that after gaining access to the cytosol, Mtb induces necrosis in order to exit the infected cell and disseminate (27,160). Autophagy, specifically xenophagy, can be considered a form of cytosolic surveillance. Increased presents of cytosolic bacteria would inevitably engage autophagic machinery in the cytosol. It seems unlikely that PDIM directly affects two distinct cell death pathways while also contributing to escape of Mtb from the phagosome. We propose that PDIM contributes primarily to the escape of Mtb from the phagosome and the increased cytosolic bacteria induce host cell necrosis and autophagy. Establishing whether or not this hierarchy exists, that increased phagosomal escape leads to increased necrosis and autophagy, would be difficult to do given that PDIM is essential to all three phenotypes. Ultimately, we would have to establish a PDIM deficient mutant that readily escapes the phagosome and assess the effects on necrosis and autophagy. One possible way to do this is by overexpressing the Mtb pore forming toxin EsxA, which is also essential for phagosomal escape, in a PDIM deficient mutant. The hope would be that this mutant still efficiently exits the phagosome at which point we could assess any effects on necrosis and autophagy. Another possibility would be to conduct infections of macrophages with polystyrene beads coated in purified PDIM and assess any effects on cell death. This

approach would essentially establish whether PDIM alone is sufficient to induce all three phenotypes.

Our previous findings demonstrated that induction of necrosis and autophagy by *Mtb* Δ *Rv3167c* was dependent on increases in mitochondrial reactive oxygen species (136). PDIM has the ability to insert into host membranes decreasing their fluidity (135). It has been demonstrated that *Mtb* lipids can be trafficked within endosomal membranes (110). While it has not been shown that PDIM traffics in endosomal compartments, direct effects of PDIM on the mitochondrial membrane could also explain the increased necrosis and autophagy in *Mtb* Δ *Rv3167c*. After escape to the cytosol, it is possible that PDIM continues to be shed by *Mtb* and inserts directly into the mitochondrial membrane. Once inserted, PDIM may exert the same effects on the mitochondrial membrane as it does on the phagosomal membrane, leading to mitochondrial membrane damage, increased mitochondrial ROS, and subsequent necrosis.

Mtb escape is dependent on the pore forming type VII secreted substrate EsxA (29,137). PDIM may work synergistically with EsxA to help *Mtb* escape the phagosome. It was shown previously that EsxA favors association with liposomes containing phosphatidylcholine and cholesterol (63). While these lipids are not essential for insertion of EsxA (165,166), it is an enticing idea that EsxA may show preference for certain membrane compositions. Cholesterol is a critical component of mammalian cellular membranes as it provides the membrane rigidity necessary for signaling events (167). Certain biophysical properties, such as membrane fluidity, may promote insertion of EsxA into host membranes. Preference for certain membrane compositions is not unheard of in bacterial virulence. Cholesterol dependent cytolysins are bacterial pore forming

toxins with varying contributions to virulence. Examples include listerolysin O from *L. monocytogenes* that is required for phagosomal exit and streptolysin O from *S. pyogenes* required for delivery of toxins to the host cell cytosol (168). PDIM has the ability to insert into host membranes decreasing their fluidity (135) a characteristic shared with cholesterol. While not necessary for EsxA pore formation, insertion of PDIM into phagosomal membranes may alter the biophysical properties of the membrane to favor further EsxA insertion as demonstrated in Figure 22a. Testing synergistic effects of EsxA and PDIM during *ex vivo* infection would prove difficult given there are very few methods available to monitor phagosomal membrane fluidity or damage in real time. Synergy could be tested in principle with a more realistic *in vitro* approach such as a red blood cell (RBC) lysis assay. It has already been established that EsxA can insert into RBC membranes causing lysis and release of heme which can be monitored by absorbance at 405nm (64). It would be interesting to test whether inclusion of purified PDIM enhances the ability of EsxA to lyse RBC.

There is also the possibility that EsxA and PDIM work independently towards the same goal. While EsxA is essential for gaining access to the host cell through membrane pore formation, PDIM may insert and weaken the phagosomal membrane favoring bacterial escape (Figure 22b). While PDIMs effects on membrane fluidity may not aid EsxA function, it may still favor bacterial escape by interfering with membrane repair or various signaling events. It is important to note as well that the Mtb containing phagosome is not a static structure. Even when contained in an early endosomal like structure, Mtb continues to shape its environment through manipulation of surface markers (22). Membrane fluidity is an essential component of proper signaling in

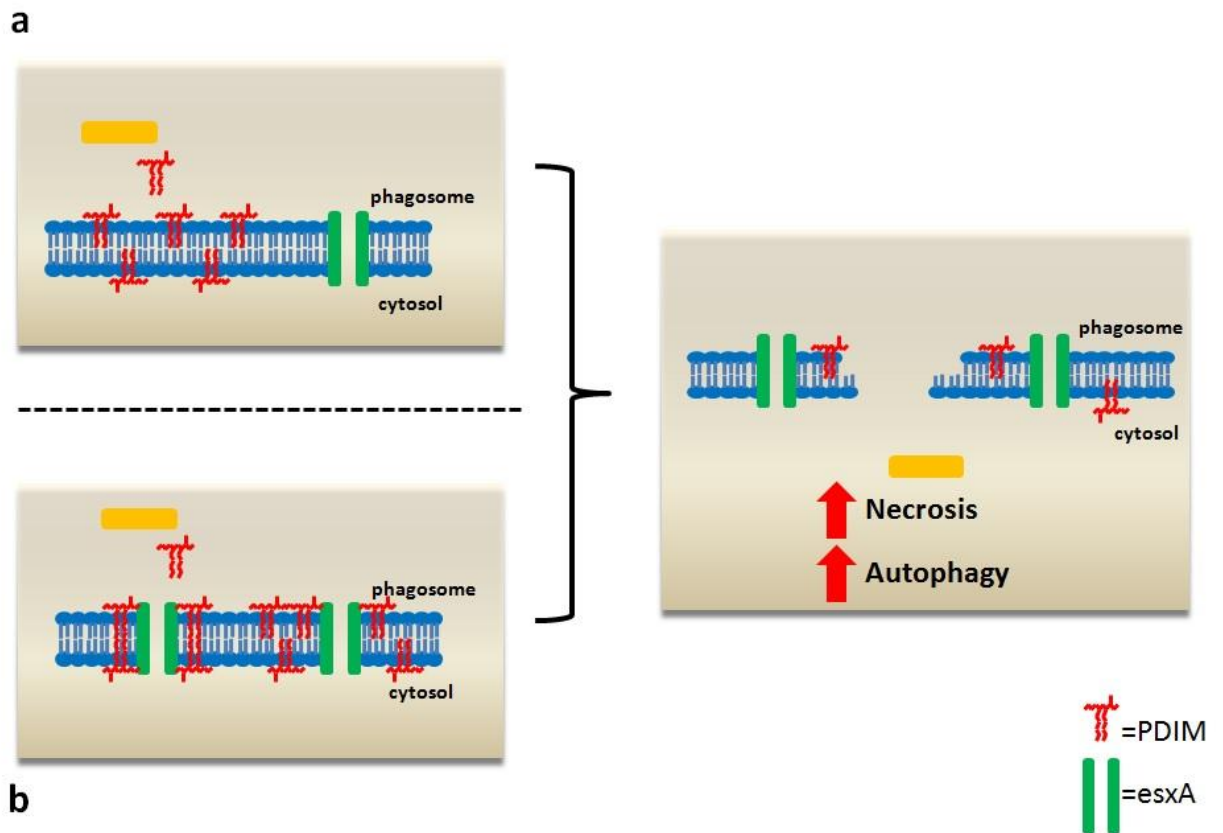


Fig. 22: Possible mechanisms of PDIM contribution to Mtb phagosomal escape

PDIM is shed from Mtb within the phagosome. PDIM then inserts into the phagosomal membrane inducing changes in membrane fluidity. In **a**, PDIM functions independently of EsxA to damage or weaken the phagosomal membrane. In **b**, PDIM and EsxA have a synergistic relationship resulting in damage to the phagosomal membrane. Damage to the phagosomal membrane by PDIM and EsxA results in increased Mtb phagosomal escape shown in the right panel. Increased presence of Mtb in the host cell cytosol leads to induction of necrosis and autophagy leading to Mtb dissemination.

eukaryotic cells. PDIMs manipulation of fluidity could have broad effects on signaling events occurring at the phagosomal membrane. Immunofluorescence microscopy could be used to determine if PDIM levels have any impact on recruitment and retention of early endosomal markers such as rab5 and EEA1. The established role of PDIM in Mtb virulence is multifaceted. This work expands on those previous findings to establish a new role for PDIM in Mtb phagosomal escape. As more work continues to elucidate how Mtb escapes the phagosome, it is abundantly clear that exit into the host cell cytosol induces host cell necrosis and is vital for bacterial dissemination and re-infection. Further work to elucidate the relationship between PDIM and Mtb escape will no doubt lead to valuable insights into understanding this important human pathogen.

References

1. Hershkovitz, I. *et al.* Detection and Molecular Characterization of 9000-Year-Old *Mycobacterium tuberculosis* from a Neolithic Settlement in the Eastern . *PLoS ONE* **3**, e3426 (2008).
2. Dutta, N. K., Mehra, S. & Kaushal, D. A *Mycobacterium tuberculosis* Sigma Factor Network Responds to Cell-Envelope Damage by the Promising Anti-Thioridazine. *PLoS ONE* **5**, e10069 (2010).
3. Ottenhoff, T. H. M. & Kaufmann, S. H. E. Vaccines against Tuberculosis: Where Are We and Where Do We Need to Go? *PLoS Pathogens* **8**, e1002607 (2012).
4. Rastogi, N., Legrand, E. & Sola, C. The mycobacteria: an introduction to nomenclature and pathogenesis. *Revue Scientifique Et Technique- ...* **20**, 21 (2001).
5. Cambier, C. J. *et al.* Mycobacteria manipulate macrophage recruitment through coordinated use of membrane lipids. doi:10.1038/nature12799
6. Roca, F. J. & Ramakrishnan, L. TNF Dually Mediates Resistance and Susceptibility to Mycobacteria via Mitochondrial Reactive Oxygen Species. *Cell* **153**, 521 (2013).
7. Volkman, H. E., Pozos, T. C., Zheng, J. & Davis, J. M. Tuberculous granuloma induction via interaction of a bacterial secreted protein with host epithelium. (2010).
8. Galagan, J. E. Genomic insights into tuberculosis. *Nature Reviews Genetics* **15**, 307 (2014).
9. Russell, D. G. Who puts the tubercle in tuberculosis? *Nature Reviews Microbiology* **5**, 39 (2006).
10. Repasy, T., Lee, J., Marino, S. & Martinez, N. Intracellular bacillary burden reflects a burst size for *Mycobacterium tuberculosis in vivo*. *PLoS Pathogens* **9**, e1003190 (2013).
11. Orme, I. M. & Basaraba, R. J. The formation of the granuloma in tuberculosis infection. *Seminars in Immunology* **26**, 601 (2014).
12. Dietrich, J. & DOHERTY, T. Interaction of *Mycobacterium tuberculosis* with the host: consequences for vaccine development. *Apmis* **117**, 440 (2009).
13. Dorhoi, A., Reece, S. T. & Kaufmann, S. For better or for worse: the immune response against *Mycobacterium tuberculosis* balances pathology and protection. *Immunological reviews* (2011).
14. Zumla, A., Nahid, P. & Cole, S. T. Advances in the development of new tuberculosis drugs and treatment regimens. *Nature Reviews Drug Discovery* (2013).
15. Udawadia, Z. F., Amale, R. A. & Ajbani, K. K. Totally drug-resistant tuberculosis in India. *Clinical Infectious ...* (2012).
16. Gheorgiu, M. *Antituberculosis BCG Vaccine: Lessons from the Past*. (2011). doi:10.1007/978-1-4419-1339-5_7
17. Stanley, S. A. & Cox, J. S. *Host-Pathogen Interactions During Mycobacterium tuberculosis infections*. (2013). doi:10.1007/82_2013_332
18. Tuberculosis Pathogenesis and Immunity. *Annual Review of Pathology: Mechanisms of Disease* **7**, 353 (2012).

19. Flynn, J., Goldstein, M. M., Chan, J., Triebold, K. J. & Pfeffer, K. Tumor necrosis factor- α is required in the protective immune response against *Mycobacterium tuberculosis* in mice. *Immunity* **2**, 561 (1995).
20. Mayer, K. D. Cutting edge: caspase-1 independent IL-1 β production is critical for host resistance to *Mycobacterium tuberculosis* and does not require TLR signaling *in vivo*. *The Journal of Immunology* **184**, 3326 (2010).
21. Lambeth, J. D. NOX enzymes and the biology of reactive oxygen. *Nature Reviews Immunology* **4**, 181 (2004).
22. Forrellad, M. A. *et al.* Virulence factors of the *Mycobacterium tuberculosis* complex. *Virulence* **4**, 3 (2013).
23. Jayachandran, R., Sundaramurthy, V. & Combaluzier, B. Survival of mycobacteria in macrophages is mediated by coronin 1-dependent activation of calcineurin. *Cell* (2007).
24. Puri, R. V., Reddy, P. V. & Tyagi, A. K. Secreted Acid Phosphatase (SapM) of *Mycobacterium tuberculosis* Is Indispensable for Arresting Phagosomal Maturation and Growth of the Pathogen in Guinea Pig Tissues. *PLoS ONE* **8**, e70514 (2013).
25. Levitte, S. *et al.* Mycobacterial Acid Tolerance Enables Phagolysosomal Survival and Establishment of Tuberculous Infection *In vivo*. *Cell Host & Microbe* **20**, 250 (2016).
26. Welin, A. & Lerm, M. Inside or outside the phagosome? The controversy of the intracellular localization of *Mycobacterium tuberculosis*. *Tuberculosis* (2012).
27. Simeone, R. *et al.* Phagosomal Rupture by *Mycobacterium tuberculosis* Results in Toxicity and Host Cell Death. *PLoS Pathogens* **8**, e1002507 (2012).
28. Simeone, R. *et al.* Cytosolic Access of *Mycobacterium tuberculosis*: Critical Impact of Phagosomal Acidification Control and Demonstration of Occurrence *In vivo*. *PLoS Pathogens* **11**, e1004650 (2015).
29. Houben, D. *et al.* ESX-1-mediated translocation to the cytosol controls virulence of mycobacteria. *Cellular Microbiology* **14**, 1287 (2012).
30. Russell, D. G. The ins and outs of the *Mycobacterium tuberculosis*-containing vacuole. *Cellular Microbiology* **18**, 1065 (2016).
31. Jamwal, S. V., Mehrotra, P., Singh, A., Siddiqui, Z. & Basu, A. Mycobacterial escape from macrophage phagosomes to the cytoplasm represents an alternate adaptation mechanism. *Scientific Reports* **6**, 23089 (2016).
32. Watson, R. O., Manzanillo, P. S. & Cox, J. S. Extracellular *M. tuberculosis* DNA targets bacteria for autophagy by activating the host DNA-sensing pathway. *Cell* (2012).
33. Stamm, L. M. *et al.* *Mycobacterium marinum* Escapes from Phagosomes and Is Propelled by Actin-based Motility. *The Journal of Experimental Medicine* **198**, 1361 (2003).
34. Hybiske, K. & Stephens, R. S. Exit strategies of intracellular pathogens. *Nature Reviews Microbiology* **6**, 99 (2008).
35. Briken, V. 'With a Little Help from My Friends': Efferocytosis as an Antimicrobial Mechanism. *Cell Host & Microbe* (2012).
36. Srinivasan, L. & Ahlbrand, S. Interaction of *Mycobacterium tuberculosis* with host cell death pathways. *Cold Spring ...* **4**, a022459 (2014).

37. Vandenabeele, P., Declercq, W., Van Herreweghe, F. & Berghe, T. V. The Role of the Kinases RIP1 and RIP3 in TNF-Induced Necrosis. *Science Signaling* **3**, re4 (2010).
38. Galluzzi, L., Vitale, I., Abrams, J. M. & Alnemri, E. S. Molecular definitions of cell death subroutines: recommendations of the Nomenclature Committee on Cell Death 2012. *Cell Death & ...* **19**, 107 (2012).
39. Duprez, L., Wirawan, E., Berghe, T. V. & Vandenabeele, P. Major cell death pathways at a glance. *Microbes and Infection* **11**, 1050 (2009).
40. Mukae, N. Identification and Developmental Expression of Inhibitor of Caspase-activated DNase (ICAD) in *Drosophila melanogaster*. *Journal of Biological Chemistry* **275**, 21402 (2000).
41. Lamkanfi, M. & Dixit, V. M. Manipulation of host cell death pathways during microbial infections. *Cell Host & Microbe* (2010).
42. Krysko, D. V., Berghe, T. V., Parthoens, E. & D'Herde, K. Methods for distinguishing apoptotic from necrotic cells and measuring their clearance. *Methods in ...* (2008).
43. Xu, G. & Shi, Y. Apoptosis signaling pathways and lymphocyte homeostasis. *Cell research* **17**, 759 (2007).
44. Codogno, P. & Mehrpour, M. Canonical and non-canonical autophagy: variations on a common theme of self-eating? ... *reviews Molecular cell ...* (2012). doi:10.1038/nrm3249
45. Huang, J. & Brumell, J. H. Bacteria-autophagy interplay: a battle for survival. *Nature Reviews Microbiology* **12**, 101 (2014).
46. He, C. & Klionsky, D. J. Regulation mechanisms and signaling pathways of autophagy. *Annual review of genetics* **43**, 67 (2009).
47. Boyle, K. B. & Randow, F. The role of 'eat-me' signals and autophagy cargo receptors in innate immunity. *Current Opinion in Microbiology* (2013).
48. Deretic, V. Autophagy: An Emerging Immunological Paradigm. *The Journal of Immunology* **189**, 15 (2012).
49. Zullo, A. J. & Lee, S. Mycobacterial induction of autophagy varies by species and occurs independently of mammalian target of rapamycin inhibition. *Journal of Biological Chemistry* **287**, 12668 (2012).
50. Biswas, D., Qureshi, O. S. & Lee, W. Y. ATP-induced autophagy is associated with rapid killing of intracellular mycobacteria within human monocytes/macrophages. *BMC ...* (2008).
51. Yuk, J. M. *et al.* Vitamin D3 induces autophagy in human monocytes/macrophages via cathelicidin. *Cell host & ...* (2009).
52. Gutierrez, M. G., Master, S. S., Singh, S. B. & Taylor, G. A. Autophagy is a defense mechanism inhibiting BCG and *Mycobacterium tuberculosis* survival in infected macrophages. *Cell* (2004).
53. Shin, D. M., Yuk, J. M., Lee, H. M., Lee, S. H. & Son, J. W. Mycobacterial lipoprotein activates autophagy via TLR2/1/CD14 and a functional vitamin D receptor signalling. *Cellular Microbiology* **12**, 1648 (2010).
54. Shin, D.-M. *et al.* *Mycobacterium tuberculosis* Eis Regulates Autophagy, Inflammation, and Cell Death through Redox-dependent Signaling. *PLoS Pathogens* **6**, e1001230 (2010).

55. Vandenabeele, P., Galluzzi, L. & Berghe, T. V. Molecular mechanisms of necroptosis: an ordered cellular explosion. ... *reviews Molecular cell ...* **11**, 700 (2010).
56. Molloy, A. & Laochumroonvorapong, P. Apoptosis, but not necrosis, of infected monocytes is coupled with killing of intracellular bacillus Calmette-Guerin. *The Journal of ...* **180**, 1499 (1994).
57. Pan, H., Yan, B. S., Rojas, M., Shebzukhov, Y. V. & Zhou, H. Ipr1 gene mediates innate immunity to tuberculosis. *Nature* **434**, 767 (2005).
58. Behar, S. M., Divangahi, M. & Remold, H. G. Evasion of innate immunity by *Mycobacterium tuberculosis*: is death an exit strategy? *Nature Reviews Microbiology* (2010).
59. Bafica, A., Scanga, C. A. & Serhan, C. Host control of *Mycobacterium tuberculosis* is regulated by 5-lipoxygenase-dependent lipoxin production. *The Journal of ...* **115**, 1601 (2005).
60. Divangahi, M., Chen, M., Gan, H. & Desjardins, D. *Mycobacterium tuberculosis* evades macrophage defenses by inhibiting plasma membrane repair. *Nature Immunology* **10**, 899 (2009).
61. Gan, H., Lee, J., Ren, F., Chen, M. & Kornfeld, H. *Mycobacterium tuberculosis* blocks crosslinking of annexin-1 and apoptotic envelope formation on infected macrophages to maintain virulence. *Nature Immunology* **9**, 1189 (2008).
62. Hsu, T. & Hingley, S. M. The primary mechanism of attenuation of bacillus Calmette–Guerin is a loss of secreted lytic function required for invasion of lung interstitial tissue. *Proceedings of the National Academy of Sciences* **100**, 12420 (2003).
63. de Jonge, M. I. *et al.* ESAT-6 from *Mycobacterium tuberculosis* Dissociates from Its Putative Chaperone CFP-10 under Acidic Conditions and Exhibits Membrane-Lysing Activity. *Journal of Bacteriology* **189**, 6028 (2007).
64. Smith, J. *et al.* Evidence for Pore Formation in Host Cell Membranes by ESX-1-Secreted ESAT-6 and Its Role in *Mycobacterium marinum* Escape from the Vacuole. *Infection and Immunity* **76**, 5478 (2008).
65. Abdallah, A. M., Bestebroer, J. & Savage, N. Mycobacterial secretion systems ESX-1 and ESX-5 play distinct roles in host cell death and inflammasome activation. *The Journal of ...* (2011).
66. Kaku, T., Kawamura, I. & Uchiyama, R. RD1 region in mycobacterial genome is involved in the induction of necrosis in infected RAW264 cells via mitochondrial membrane damage and ATP *FEMS Microbiology Letters* **274**, 189 (2007).
67. Tundup, S., Mohareer, K. & Hasnain, S. E. *Mycobacterium tuberculosis* PE25/PPE41 protein complex induces necrosis in macrophages: Role in virulence and disease reactivation? *FEBS open bio* (2014).
68. Cadieux, N. *et al.* Induction of cell death after localization to the host cell mitochondria by the *Mycobacterium tuberculosis* PE_PGRS33 protein. *Microbiology* **157**, 793 (2010).
69. Danilchanka, O. *et al.* An outer membrane channel protein of *Mycobacterium tuberculosis* with exotoxin activity. *Proceedings of the National Academy of Sciences* **111**, 6750 (2014).

70. Balleza, E. *et al.* Regulation by transcription factors in bacteria: beyond description. *FEMS Microbiology Reviews* **33**, 133 (2009).
71. Schnappinger, D. *et al.* Transcriptional Adaptation of *Mycobacterium tuberculosis* within Macrophages. *The Journal of Experimental Medicine* **198**, 693 (2003).
72. Minch, K. J. *et al.* The DNA-binding network of *Mycobacterium tuberculosis*. *Nature Communications* **6**, 5829 (2015).
73. Galagan, J. E. *et al.* The *Mycobacterium tuberculosis* regulatory network and hypoxia. *Nature* **499**, 178 (2013).
74. Flentie, K., Garner, A. L. & Stallings, C. L. *Mycobacterium tuberculosis* Transcription Machinery: Ready To Respond to Host Attacks. *Journal of Bacteriology* **198**, 1360 (2016).
75. Sachdeva, P., Misra, R., Tyagi, A. K. & Singh, Y. The sigma factors of *Mycobacterium tuberculosis*: regulation of the regulators. *FEBS Journal* **277**, 605 (2009).
76. Sun, R. *et al.* *Mycobacterium tuberculosis* ECF sigma factor sigC is required for lethality in mice and for the conditional expression of a defined gene set. *Molecular Microbiology* **52**, 25 (2004).
77. Raman, S., Hazra, R., Dascher, C. C. & Husson, R. N. Transcription Regulation by the *Mycobacterium tuberculosis* Alternative Sigma Factor SigD and Its Role in Virulence. *Journal of Bacteriology* **186**, 6605 (2004).
78. Chen, P., Ruiz, R. E., Li, Q., Silver, R. F. & Bishai, W. R. Construction and Characterization of a *Mycobacterium tuberculosis* Mutant Lacking the Alternate Sigma Factor Gene, sigF. *Infection and Immunity* **68**, 5575 (2000).
79. Dainese, E. *et al.* Posttranslational Regulation of *Mycobacterium tuberculosis* Extracytoplasmic-Function Sigma Factor L and Roles in Virulence and in Global Regulation of Gene Expression. *Infection and Immunity* **74**, 2457 (2006).
80. Wehenkel, A. *et al.* Mycobacterial Ser/Thr protein kinases and phosphatases: Physiological roles and therapeutic potential. *Biochimica et Biophysica Acta (BBA) - Proteins and Proteomics* **1784**, 193 (2008).
81. Sharma, K., Gupta, M., Krupa, A., Srinivasan, N. & Singh, Y. EmbR, a regulatory protein with ATPase activity, is a substrate of multiple serine/threonine kinases and phosphatase in *Mycobacterium tuberculosis*. *FEBS Journal* **273**, 2711 (2006).
82. Jayakumar, D., Jacobs, W. R. & Narayanan, S. Protein kinase E of *Mycobacterium tuberculosis* has a role in the nitric oxide stress response and apoptosis in a human macrophage model of infection. *Cellular Microbiology* **0**, 070925015921001 (2007).
83. Balhana, R. J. C., Singla, A., Sikder, M. H., Withers, M. & Kendall, S. L. Global analyses of TetR family transcriptional regulators in mycobacteria indicates conservation across species and diversity in regulated functions. *BMC Genomics* **16**, (2015).
84. Cuthbertson, L. & Nodwell, J. R. The TetR Family of Regulators. *Microbiology and Molecular Biology Reviews* **77**, 440 (2013).
85. Ramos, J. L. *et al.* The TetR Family of Transcriptional Repressors. *Microbiology and Molecular Biology Reviews* **69**, 326–356 (2005).

86. Yu, Z., Reichheld, S. E., Savchenko, A., Parkinson, J. & Davidson, A. R. A Comprehensive Analysis of Structural and Sequence Conservation in the TetR Family Transcriptional Regulators. *Journal of Molecular Biology* **400**, 847 (2010).
87. Hillen, W. & Wissmann, A. *Tet repressor-tet operator interaction. Protein-Nucleic Acid Interaction* (1989). doi:10.1007/978-1-349-09871-2_7
88. Goeke, D. *et al.* Short Peptides Act as Inducers, Anti-Inducers and Corepressors of Tet Repressor. *Journal of Molecular Biology* **416**, 33 (2012).
89. Kendall, S. L. *et al.* Cholesterol utilization in mycobacteria is controlled by two TetR- type transcriptional regulators: kstR and kstR2. *Microbiology* **156**, 1362 (2010).
90. Baulard, A. R. Activation of the pro-drug ethionamide is regulated in mycobacteria. *Journal of Biological Chemistry* (2000). doi:10.1074/jbc.m003744200
91. Bolla, J. R. *et al.* Structural and functional analysis of the transcriptional regulator Rv3066 of *Mycobacterium tuberculosis*. *Nucleic Acids Research* **40**, 9340 (2012).
92. Wipperfurth, M. F., Sampson, N. S. & Thomas, S. T. Pathogen lipid usage: Cholesterol utilization by *Mycobacterium tuberculosis*. *Critical Reviews in Biochemistry and Molecular Biology* **49**, 269 (2014).
93. Santangelo, M. D. L. P. *et al.* Mce3R, a TetR-type transcriptional repressor, controls the expression of a regulon involved in lipid metabolism in *Mycobacterium tuberculosis*. *Microbiology* **155**, 2245 (2009).
94. Chou, T.-H. *et al.* Crystal structure of the *Mycobacterium tuberculosis* transcriptional regulator Rv0302. *Protein Science* **24**, 1942 (2015).
95. Kieser, K. J. & Rubin, E. J. How sisters grow apart: mycobacterial growth and division. *Nature Reviews Microbiology* **12**, 550 (2014).
96. Jamet, S. *et al.* Evolution of Mycolic Acid Biosynthesis Genes and Their Regulation during Starvation in *Mycobacterium tuberculosis*. *Journal of Bacteriology* **197**, 3797 (2015).
97. Brown, L., Wolf, J. M. & Prados, R. Through the wall: extracellular vesicles in Gram- positive bacteria, mycobacteria and fungi. *Nature Reviews ...* (2015).
98. Mishra, A. K., Driessen, N. N., Appelmek, B. J. & Besra, G. S. Lipoarabinomannan and related glycoconjugates: structure, biogenesis and role in *Mycobacterium tuberculosis* physiology and host–pathogen interaction. *FEMS Microbiology Reviews* **35**, 1126 (2011).
99. De Libero, G. & Mori, L. The T-Cell Response to Lipid Antigens of *Mycobacterium tuberculosis*. *Frontiers in Immunology* **5**, (2014).
100. Belardinelli, J. M. *et al.* Biosynthesis and Translocation of Unsulfated Acyltrehaloses in *Mycobacterium tuberculosis*. *Journal of Biological Chemistry* **289**, 27952 (2014).
101. Soetaert, K. *et al.* Increased Vancomycin Susceptibility in Mycobacteria: a New Approach To Identify Synergistic Activity against Multidrug-Resistant Mycobacteria. *Antimicrobial Agents and Chemotherapy* **59**, 5057 (2015).
102. Liu, J., Barry, C. E. & Nikaido, H. *Cell Wall: Physical Structure and Permeability. Mycobacteria* doi:10.1002/9781444311433.ch12

103. Fukuda, T. *et al.* Critical Roles for Lipomannan and Lipoarabinomannan in Cell Wall Integrity of Mycobacteria and Pathogenesis of Tuberculosis. *mBio* **4**, e00472–12 (2013).
104. Ouellet, H., Johnston, J. B. & de Montellano, P. Cholesterol catabolism as a therapeutic target in *Mycobacterium tuberculosis*. *Trends in Microbiology* (2011).
105. Vergne, I., Gilleron, M. & Nigou, J. M. Manipulation of the endocytic pathway and phagocyte functions by *Mycobacterium tuberculosis* lipoarabinomannan. *Frontiers in Cellular and Infection Microbiology* **4**, (2015).
106. Briken, V., Porcelli, S. A., Besra, G. S. & Kremer, L. Mycobacterial lipoarabinomannan and related lipoglycans: from biogenesis to modulation of the immune response. *Molecular Microbiology* **53**, 391 (2004).
107. Maiti, D., Bhattacharyya, A. & Basu, J. Lipoarabinomannan from *Mycobacterium tuberculosis* Promotes Macrophage Survival by Phosphorylating Bad through a Phosphatidylinositol 3-Kinase/Akt Pathway. *Journal of Biological Chemistry* **276**, 329 (2000).
108. Vergne, I., Fratti, R. A., Hill, P. J. & Chua, J. *Mycobacterium tuberculosis* phagosome maturation arrest: mycobacterial phosphatidylinositol analog phosphatidylinositol mannoside stimulates early *Molecular Biology of the Cell* **15**, 751 (2004).
109. Welin, A. *et al.* Incorporation of *Mycobacterium tuberculosis* Lipoarabinomannan into Macrophage Membrane Rafts Is a Prerequisite for the Phagosomal Maturation Block. *Infection and Immunity* **76**, 2882 (2008).
110. Beatty, W. L. *et al.* Trafficking and Release of Mycobacterial Lipids from Infected Macrophages. *Traffic* **1**, 235 (2000).
111. Indrigo, J. Cord factor trehalose 6,6'-dimycolate (TDM) mediates trafficking events during mycobacterial infection of murine macrophages. *Microbiology* **149**, 2049 (2003).
112. Hunter, R. L., Olsen, M., Jagannath, C. & Actor, J. K. Trehalose 6,6'-Dimycolate and Lipid in the Pathogenesis of Caseating Granulomas of Tuberculosis in Mice. *The American Journal of Pathology* **168**, 1249 (2006).
113. Saita, N., Fujiwara, N., Yano, I., Soejima, K. & Kobayashi, K. Trehalose 6,6'-Dimycolate (Cord Factor) of *Mycobacterium tuberculosis* Induces Corneal Angiogenesis in Rats. *Infection and Immunity* **68**, 5991 (2000).
114. Gilmore, S. A. *et al.* Sulfolipid-1 Biosynthesis Restricts *Mycobacterium tuberculosis* Growth in Human Macrophages. *ACS Chemical Biology* **7**, 863 (2012).
115. Converse, S. E. *et al.* MmpL8 is required for sulfolipid-1 biosynthesis and *Mycobacterium tuberculosis* virulence. *Proceedings of the National Academy of Sciences* **100**, 6121 (2003).
116. Goren, M. B., Brokl, O. & Schaefer, W. B. Lipids of putative relevance to virulence in *Mycobacterium tuberculosis*: phthiocerol dimycocerosate and the attenuation indicator lipid. *Infection and Immunity* (1974).
117. Camacho, L. R., Ensergueix, D. & Perez, E. Identification of a virulence gene cluster of *Mycobacterium tuberculosis* by signature-tagged transposon mutagenesis. *Molecular ...* (1999).

118. Cox, J. S., Chen, B., McNeil, M. & Jacobs, W. R. Complex lipid determines tissue-specific replication of *Mycobacterium tuberculosis* in mice. *Nature* (1999).
119. Onwueme, K. C., Vos, C. J., Zurita, J. & Ferreras, J. A. The dimycocerosate ester polyketide virulence factors of mycobacteria. *Progress in Lipid Research* **44**, 259 (2005).
120. Constant, P. Role of the pks15/1 Gene in the Biosynthesis of Phenolglycolipids in the *Mycobacterium tuberculosis* Complex. EVIDENCE THAT ALL STRAINS SYNTHESIZE GLYCOSYLATED p-HYDROXYBENZOIC METHYL ESTERS AND THAT STRAINS DEVOID OF PHENOLGLYCOLIPIDS HARBOR A FRAMESHIFT MUTATION IN THE pks15/1 GENE. *Journal of Biological Chemistry* **277**, 38148 (2002).
121. Arbues, A., Lugo-Villarino, G., Neyrolles, O., Guilhot, C. & Astarie-Dequeker, C. Playing hide-and-seek with host macrophages through the use of mycobacterial cell envelope phthiocerol dimycocerosates and phenolic glycolipids. *Frontiers in Cellular and Infection Microbiology* **4**, (2014).
122. Domenech, P. & Reed, M. B. Rapid and spontaneous loss of phthiocerol dimycocerosate (PDIM) from *Mycobacterium tuberculosis* grown *in vitro*: implications for virulence studies. *Microbiology* **155**, 3532 (2009).
123. Blasco, B. *et al.* Virulence Regulator EspR of *Mycobacterium tuberculosis* Is a Nucleoid-Associated Protein. *PLoS Pathogens* **8**, e1002621 (2012).
124. Bisson, G. P. *et al.* Upregulation of the Phthiocerol Dimycocerosate Biosynthetic Pathway by Rifampin-Resistant, rpoB Mutant *Mycobacterium tuberculosis*. *Journal of Bacteriology* **194**, 6441 (2012).
125. Gomez-Velasco, A. *et al.* Disruption of the serine/threonine protein kinase H affects phthiocerol dimycocerosates synthesis in *Mycobacterium tuberculosis*. *Microbiology* **159**, 726 (2013).
126. Converse, P. J. *et al.* The Impact of Mouse Passaging of *Mycobacterium tuberculosis* Strains prior to Virulence Testing in the Mouse and Guinea Pig Aerosol Models. *PLoS ONE* **5**, e10289 (2010).
127. Camacho, L. R. *et al.* Analysis of the Phthiocerol Dimycocerosate Locus of *Mycobacterium tuberculosis*. *Journal of Biological Chemistry* **276**, 19845 (2001).
128. Yu, J. *et al.* Both Phthiocerol Dimycocerosates and Phenolic Glycolipids Are Required for Virulence of *Mycobacterium marinum*. *Infection and Immunity* **80**, 1381 (2012).
129. Kirksey, M. A. *et al.* Spontaneous Phthiocerol Dimycocerosate-Deficient Variants of *Mycobacterium tuberculosis* Are Susceptible to Gamma Interferon-Mediated Immunity. *Infection and Immunity* **79**, 2829 (2011).
130. Jain, M. *et al.* Lipidomics reveals control of *Mycobacterium tuberculosis* virulence lipids via metabolic coupling. *Proceedings of the National Academy of Sciences* **104**, 5133 (2007).
131. Russell, D. G. *et al.* *Mycobacterium tuberculosis* Wears What It Eats. *Cell Host & Microbe* **8**, 68 (2010).
132. Rousseau, C. *et al.* Production of phthiocerol dimycocerosates protects *Mycobacterium tuberculosis* from the cidal activity of reactive nitrogen

- intermediates produced by macrophages and modulates the early immune response to infection. *Cellular Microbiology* **6**, 277 (2004).
133. Day, T. A. *et al.* *Mycobacterium tuberculosis* Strains Lacking Surface Lipid Phthiocerol Dimycocerosate Are Susceptible to Killing by an Early Innate Host Response. *Infection and Immunity* **82**, 5214 (2014).
 134. Passemar, C. *et al.* Multiple deletions in the polyketide synthase gene repertoire of *Mycobacterium tuberculosis* reveal functional overlap of cell envelope lipids in host-pathogen interactions. *Cellular Microbiology* **16**, 195 (2013).
 135. Astarie-Dequeker, C. *et al.* Phthiocerol Dimycocerosates of *M. tuberculosis* Participate in Macrophage Invasion by Inducing Changes in the Organization of Plasma Membrane Lipids. *PLoS Pathogens* **5**, e1000289 (2009).
 136. Lalitha Srinivasan, S. A. G. B. E. H. J. L. M. P. C. K. V. B. Identification of a Transcription Factor That Regulates Host Cell Exit and Virulence of *Mycobacterium tuberculosis*. doi:10.1371/journal
 137. van der Wel, N. *et al.* *M. tuberculosis* and *M. leprae* Translocate from the Phagolysosome to the Cytosol in Myeloid Cells. *Cell* **129**, 1287 (2007).
 138. Bardarov, S. & Bardarov, S., Jr. Specialized transduction: an efficient method for generating marked and unmarked targeted gene disruptions in *Mycobacterium tuberculosis*, *M. bovis* BCG and *M. ...* (2002).
 139. Singh, A., Mai, D. & Kumar, A. Dissecting virulence pathways of *Mycobacterium tuberculosis* through protein-protein association. *Proceedings of the ...* (2006).
 140. Andrews, S. *FastQC: A quality control tool for high throughput sequence data. Reference Source, 2010* (2010).
 141. Bolger, A. M., Lohse, M. & Usadel, B. Trimmomatic: a flexible trimmer for Illumina sequence data. *Bioinformatics* (2014).
 142. Galagan, J. E., Sisk, P., Stolte, C., Weiner, B. & Koehrsen, M. TB database 2010: overview and update. *Tuberculosis* (2010).
 143. Kim, D., Pertea, G. & Trapnell, C. TopHat2: accurate alignment of transcriptomes in the presence of insertions, deletions and gene fusions. *Genome ...* (2013).
 144. Anders, S., Pyl, P. T. & Huber, W. HTSeq—a Python framework to work with high-throughput sequencing data. *Bioinformatics* (2014).
 145. Nicolas, P. *et al.* Condition-Dependent Transcriptome Reveals High-Level Regulatory Architecture in *Bacillus subtilis*. *Science* **335**, 1103 (2012).
 146. Gentleman, R. C. & Carey, V. J. Bioconductor: open software development for computational biology and bioinformatics. *Genome ...* (2004).
 147. Bullard, J. H. & Purdom, E. Evaluation of statistical methods for normalization and differential expression in mRNA-Seq experiments. *BMC ...* (2010).
 148. Law, C. W., Chen, Y. & Shi, W. Voom: precision weights unlock linear model analysis tools for RNA-seq read counts. *Genome ...* (2014). doi:10.3410/f.718262366.793491184
 149. Gentleman, R., Carey, V., Huber, W., Irizarry, R. & Dudoit, S. *Bioinformatics and computational biology solutions using R and Bioconductor*. (2006).
 150. Young, M. D. & Wakefield, M. J. Gene ontology analysis for RNA-seq: accounting for selection bias. *Genome ...* (2010).

151. Benjamini, Y. & Hochberg, Y. Controlling the false discovery rate: a practical and powerful approach to multiple testing. *Journal of the royal statistical society Series B* (... (1995).
152. Ahn, S. K., Cuthbertson, L. & Nodwell, J. R. Genome Context as a Predictive Tool for Identifying Regulatory Targets of the TetR Family Transcriptional Regulators. *PLoS ONE* **7**, e50562 (2012).
153. Chiu, H.-J. *et al.* Structure of the first representative of Pfam family PF09410 (DUF2006) reveals a structural signature of the calycin superfamily that suggests a role in lipid metabolism. *Acta Crystallographica Section F Structural Biology and Crystallization Communications* **66**, 1153 (2009).
154. Flower, D. R. The lipocalin protein family: structure and function. *Biochemical Journal* **318**, 1 (1996).
155. Reva, O., Korotetskiy, I. & Ilin, A. Role of the horizontal gene exchange in evolution of pathogenic Mycobacteria. *BMC Evolutionary Biology* **15**, S2 (2015).
156. Palanca, C. & Rubio, V. Structure of AmtR, the global nitrogen regulator of *Corynebacterium glutamicum*, in free and DNA-bound forms. *FEBS Journal* **283**, 1039 (2016).
157. Manzanillo, P. S., Ayres, J. S., Watson, R. O. & Collins, A. C. The ubiquitin ligase parkin mediates resistance to intracellular pathogens. *Nature* (2013).
158. izushima, N., Yoshimori, T. & Levine, B. Methods in mammalian autophagy research. *Cell* (2010).
159. Russell, D. G. *Mycobacterium tuberculosis* and the intimate discourse of a chronic infection. *Immunological reviews* (2011).
160. Abdallah, A. M., Savage, N. & van Zon, M. The ESX-5 secretion system of *Mycobacterium marinum* modulates the macrophage response. *The Journal of ...* (2008).
161. Tanaka, N. *Mechanism of Action of Aminoglycoside Antibiotics*. *Handbook of Experimental Pharmacology* (1982). doi:10.1007/978-3-642-68579-8_5
162. Iobbi-Nivol, C. & Leimkühler, S. Molybdenum enzymes, their maturation and molybdenum cofactor biosynthesis in *Escherichia coli*. *Biochimica et Biophysica Acta (BBA) - Bioenergetics* **1827**, 1086 (2013).
163. Williams, M. J., Kana, B. D. & Mizrahi, V. Functional Analysis of Molybdopterin Biosynthesis in Mycobacteria Identifies a Fused Molybdopterin Synthase in *Mycobacterium tuberculosis*. *Journal of Bacteriology* **193**, 98 (2010).
164. Wang, F. *et al.* Identification of a small molecule with activity against drug-resistant and persistent tuberculosis. *Proceedings of the National Academy of Sciences* **110**, E2510 (2013).
165. Ma, Y., Keil, V. & Sun, J. Characterization of *Mycobacterium tuberculosis* EsxA Membrane Insertion. *Journal of Biological Chemistry* **290**, 7314 (2015).
166. De Leon, J. *et al.* *Mycobacterium tuberculosis* ESAT-6 Exhibits a Unique Membrane-interacting Activity That Is Not Found in Its Ortholog from Non-pathogenic *Mycobacterium smegmatis*. *Journal of Biological Chemistry* **287**, 44184 (2012).
167. Spector, A. A. & Yorek, M. A. Membrane lipid composition and cellular function. *Journal of lipid research* (1985).

168. Reboul, C. F., Whisstock, J. C. & Dunstone, M. A. A new model for pore formation by cholesterol-dependent cytolysins. *PLoS Comput Biol* **10**, e1003791 (2014).
169. Mahammad, S. & Parmryd, I. *Cholesterol Depletion Using Methyl- β -cyclodextrin*. *Methods in Molecular Biology* (2014). doi:10.1007/978-1-4939-1752-5_8
170. Yang, X., Sheng, W. & Sun, G. Y. Effects of fatty acid unsaturation numbers on membrane fluidity and α -secretase-dependent amyloid precursor protein processing. *Neurochemistry International* **58**, 321 (2011).
171. Sousa, C., Nunes, C., Lúcio, M. & Ferreira, H. Effect of nonsteroidal anti-inflammatory drugs on the cellular membrane fluidity. *Journal of ...* (2008).

Appendix A

Primers used in this study

Primer Name	Primer Sequence 5'-3'
EMSA	
<i>palRv3167c+</i>	TAACGCTACCTAAAGTAGCGTAA
<i>palRv3167c-</i>	TTACGCTACTTTAGGTAGCGTTA
<i>Negative+</i>	AGCCTTGCAGGCTAATCGGTAGCTA
<i>Negative-</i>	TAGTACCGATTAGCTGCAAGGCT
EMSA Screen	
Rv0003-	CGTCGTGAATACCACAGTGCCTCAATAAGATTTCGTCTTACCATAACCGT
Rv0003+	ACGGTTATGGTAAGACGAATCTTATTGAGGCACTGTGGTATTTCGACGACG
Rv0013-	GTGAAGGGATCCGGAAGCCCTTGTAGCACACCGACATTGGTGTGGAATAC
Rv0013+	GTATTCCACACCAATGTCCGGTGTGCTACAAGGGCTCCGGATCCCTTCAC
Rv0095-	CTCGTAGGATCTGGGTAAATCCCTTGTGTCACCTTCAGTTTCACGGTTATC
Rv0095+	GATAACCGTGAAACTGAAGTGACACAAGGGATTTACCCAGATCCTACGAG
Rv0166-	TTTTCCCTTCTCTCCGTGAAACCAGCTGATGCAGAACGTCTTTCAACATT
Rv0166+	AATGTTGAAAGACGTTCTGCATCAGCTGGTTTCACGGAGAGAAGGGAAAA
Rv0386-	CAGGTGCACCGGAAGACCATGGGCCACATCGTCATTGGCCACCCGCAGCG
Rv0386+	CGCTGCGGGTGGCCAATGACGATGTGGCCCATGGTCTCCGGTGCACCTG
Rv0487-	CGACGACCGAAATCCCAACTCCAACAACGCATTGAAGTCCGAATCCACCA
Rv0487+	TGGTGGATTTCGGACTTCAATGCGTTGTTGGAGTTGGGATTTCCGGTCGTCG
Rv0501-	CGGCGTGCACCACCGTGTCCACCTCGCCATTGCGAATCACCTTGGCGATG
Rv0501+	CATCGCCAAGGTGATTTCGCAATGGCGAGGTGGACACGGTGGTGCACGCCG
Rv0691c-	GACGCGTTGCGCGCAGCGCTGTTGGCCTTCAACACCTTTGACGAATCCGA
Rv0691c+	TCGGATTTCGTCAAAGGTGTTGAAGGCCAACAGCGCTGCGCGCAACGCGTC
Rv1007c-	TCGAAATGAAGCCCTATTACGTCACCACCGCGATCGCATATCCCAACGCT
Rv1007c+	AGCGTTGGGATATGCGATCGCGGTGGTACGTAATAGGGCTTCATTTGCA
Rv1023-	TCGCACGCGAACCAGGAAATGCCAGGTCGCCCCGCTAGCGGGCCGCGTC
Rv1023+	GACGCGGCCCGCTACGCGGGCGACCTGGCATTTCCTCGTTTCGCGTGCGA
Rv1079-	GTGAGGCAAAGGTATTGTCCACCAATACTTTTGGCGATCTGTCTGTGCC
Rv1079+	GGGCACAGACAGATCGGCAAAAGTATTGGTGGACAATACCTTTGCCTCAC
Rv1212c-	CAACTACGAGAAATACTTTCCGGCAGCAACAGTTTTTCGTGTGCCCGTCGGT
Rv1212c+	ACCGACGGGCACACGAAAAGTGTGCTGCCGAAAGTATTTCTCGTAGTTG
Rv1234-	CATGGTCGAGCTGAAATCCCTTGTGCCGCGAGCCATTGCGTACGGCACTG
Rv1234+	CAGTGCCGTACGCAATGGCTCGCGGCACAAGGGATTTACGCTCGACCATG
Rv1435c-	GGACCGGTACCGATACCGGGCGCACCGGTACCGGTACCCGCCGTTCCGGC
Rv1435c+	GCCGGAACGGCGGGTACCGGTACCGGTGCGCCCCGGTATCGGTACCGGTCC
Rv1795-	TGCTCAAATTTGTTGTTGTACTTCGGGTTTCACGCCCTGGCGTCATACTC
Rv1795+	GAGTATGACGCCAGGGCGTGAAACCCGAAGTACAACAACAAATTTGAGCA
Rv1895-	GCGTTTGAACGTGGTGAACGGCGGGCCGGCAATCCGAGACTCGGCATAG
Rv1895+	CTATGCCGAGTCTCGGAATTGCCGGCCCCGCCGTTACCACGTTCAAACGC

Rv2338c-	GCGATGCGAGCCGGTGCGGATGCCCCGACTCTGGACGGGTGAAAGAAAG
Rv2338+	CTTTCTTTCACCCGTCCAGAGTCGGGGGCATCCGCACCGGCTCGCATCGC
Rv2941-	ATGCGGGCACCCGAAATAATTGCGGTGCAACGGATGTAGTGCTTCGTGGC
Rv2941+	GCCACGAAGCACTACATCCGTTGCACCGCAATTATTTTCGGTGCCCGCAT
Rv3208-	GCTCGAAAAATGTTGATACAGAACGGGTTTACTGACTCCCGCCGATCCG
Rv3208+	CGGATCGGGCGGGAGTCAGTAAACCCGTTCTGTATCAACATTTTTTCGAGC
Rv3349c-	CGAAGACCGCATCATGGTGCCTGGAACAAAATTCGCTGGCGATGCCGAG
Rv3349c+	CTCGGCATCGCCAGCAATTTTGTCCAGCGCACCATGATGCGGTCTTCG
Rv3412-	ACACTACAAGTCCACGAATTCCTTGTGCGCCAACAGAGCTTCGTATACG
Rv3412+	CGTATACGAAGCTCTGTTGGCGCACAAGGGAATTCGTGGACTTGTAGTGT
Rv3428c-	TGTGTCAGCGGTCACGTATTTCCCCAGGTTTGAGGGGTTGTCCGTCACGT
Rv3428c+	ACGTGACGGACAACCCCTCAAACCTGGGGAAATACGTGACCGCTGACACA
Rv3725-	ATTGACTGGATATGAGAGCCCGCGTCGCGAATTCGTCGATGACCGTCTT
Rv3725+	AAGACGGTCATCGACGGAATTCGCGACGCGGGCTCTCATATCCAGTCAAT
Rv3802c-	GTTTCCGAAGCGTTGCTGCTCAAGGTAACGGCCGATCGCCAGCAAT
Rv3802c+	ATTGCTGGGCGATCGGCCAGTTACCTTGAGCAGCAACGCCTTCGGAAAC
Rv3803c-	CGATGAACACGTTGGCGGGCAAGGGGATTCGGTGGTGGCACC GGCCGGT
Rv3803c+	ACCGGCCGGTGCCACCACCGAAATCCCCTTGCCCGCCAACGTGTTTCATCG

M-PFC

3167-pUAB300For	TTTGATCCGGGATGAAAGCAGACCTGCCCTCCC
3167-pUAB300Rev	TTGATCGATGGGTGACGACACTGCCGCCAGGAG
3167-pUAB400For	GGGAAGCTTGGGATGAAAGCAGACCTGCCCTCCCTTG
3167-pUAB400Rev	GAAGTTAACAGGTCAGACGACACTGCCGCCAGGAG

Knockout generation

mmp17KOLFFor	AATTCAGATCTCGGTAGTCCGGCTGGCCGTC
mmp17KOLFRev	TTGAAGCTTGAGCATGGCCGTAGCGGAG
mmp17KORFFor	AAGTCTAGAGAACGGCTGTCCGCGATGCC
mmp17KORFRev	TTTGGTACCTTTGCCCTGGCGTGGTCGGAAGC

Gene Complementation

mmp17For	TTGAAGCTTAACATGCCTAGTCCGGCTGGCCGTC
mmp17Rev	TTTAAGCTTTCCTCACAGGTCCTCCTCGTGATCAGCTTCTGCTCACGCCGCCCTGGCG

Protein over expression

3167-pet28cFor	GGGCATATGGGTATGAAAGCAGACCTGCCCTCCCTTG
3167-pet28cRev	TTTGATCCGGGTCAGACGACACTGCCGCCAGGAG

Knockout confirmation

zeo-fwdout	GCACTTCGTGGCCGAGGAG
zeo-revout	GGAACGGCACTGGTCAACTTGG
mmp17KOLFFor	AATTCAGATCTCGGTAGTCCGGCTGGCCGTC

mmp17KORFRev	TTTGGTACCTTTGCCCTGGCGTGGTCGGAAGC
mmp17IPFor	CAGTTACCGGCACCAACCAC
mmp17IPRev	CGCATCCCGATGATGGGTAG
mmp17qPCRFor	CAGTTACCGGCACCAACCAC
mmp17qPCRRev	CGCATCCCGATGATGGGTAG
sigAqPCRFor	CGTCAAGCACGCAAGGA
sigAqPCRRev	TCGCTAAGCTCGGTCAT

Appendix B
Genes differentially expressed in *MtbΔRv3167c* that complement
As determined by RNAseq, Figure 9 overlap region (442 genes)

Gene ID	logFC	AveExpr	adj.P.Val	Gene Name
Rv0001	-0.74	9.469027534	0.000383435	dnaA
Rv0014c	0.30	8.49598068	0.015811343	pknB
Rv0018c	0.36	8.369868445	0.004840445	pstP
Rv0020c	0.20	10.13613496	0.041828008	fhaA
Rv0053	-0.45	6.825524815	0.011254122	rpsF
Rv0058	-0.28	9.141264265	0.029957534	dnaB
Rv0059	-0.36	6.170797004	0.026031886	Rv0059
Rv0075	0.27	7.160733224	0.046102084	Rv0075
Rv0079	1.39	7.032268559	0.001988719	Rv0079
Rv0082	0.65	6.675668342	0.005569836	Rv0082
Rv0084	0.40	6.008178652	0.041244156	hycD
Rv0086	0.56	7.544076578	0.018631548	hycQ
Rv0108c	-1.12	5.651697581	8.23E-05	Rv0108c
Rv0118c	-1.13	6.214345549	0.000193903	oxcA
Rv0119	-0.96	5.278068501	0.000462976	fadD7
Rv0120c	-0.63	7.089264189	0.000410625	fusA2
Rv0134	0.39	7.280231917	0.005042075	ephF
Rv0140	-3.05	5.25851271	4.40E-07	Rv0140
Rv0146	0.48	6.828530357	0.019775614	Rv0146
Rv0165c	-1.59	6.450885297	5.26E-05	mce1R
Rv0166	-1.08	9.415747097	1.16E-05	fadD5
Rv0167	-1.07	7.313045002	0.000118807	yrbE1A
Rv0168	-1.01	7.144301922	9.60E-06	yrbE1B
Rv0169	-0.94	9.119011527	2.66E-06	mce1A
Rv0173	-0.87	8.912686677	2.01E-05	lprK
Rv0179c	0.46	8.132483724	0.004976222	lprO
Rv0188	-0.27	6.682451031	0.043768827	Rv0188
Rv0192	0.35	5.743136909	0.026362248	Rv0192
Rv0196	1.14	3.468154854	0.007686438	Rv0196
Rv0197	1.07	5.728520184	0.000210344	Rv0197
Rv0208c	-0.48	7.784331846	0.006314419	Rv0208c
Rv0210	0.68	4.502595581	0.005438349	Rv0210
Rv0211	0.67	9.615354372	0.000565443	pckA
Rv0233	-1.30	7.236127448	2.09E-05	nrdB
Rv0235c	0.78	5.324571983	0.003241562	Rv0235c
Rv0236c	1.41	7.135845433	0.00095648	aftD
Rv0244c	-1.43	7.275465849	8.53E-06	fadE5
Rv0249c	-0.38	8.51480346	0.008587941	Rv0249c

Rv0251c	-3.29	10.4634887	2.00E-08	hsp
Rv0252	0.54	6.438729513	0.00135286	nirB
Rv0274	0.57	5.662611275	0.035249976	Rv0274
Rv0275c	0.55	4.808413026	0.0263571	Rv0275c
Rv0280	-0.79	5.345343969	0.006191796	PPE3
Rv0282	0.34	10.64335485	0.005465455	eccA3
Rv0284	0.50	9.835890641	0.001774348	eccC3
Rv0287	0.28	8.679929505	0.018685163	esxG
Rv0338c	0.21	10.45781776	0.042104479	Rv0338c
Rv0339c	0.43	6.613097147	0.008665751	Rv0339c
Rv0341	1.51	7.967332158	5.18E-05	iniB
Rv0350	-1.85	12.68916998	8.57E-07	dnaK
Rv0351	-2.03	11.5480541	2.69E-06	grpE
Rv0352	-1.74	10.57359343	1.43E-07	dnaJ1
Rv0353	-1.85	8.452917298	5.18E-06	hspR
Rv0356c	0.73	3.69482976	0.010569222	Rv0356c
Rv0361	0.47	6.614316485	0.02090826	Rv0361
Rv0362	0.98	4.998437823	8.81E-05	mgtE
Rv0383c	-0.31	8.508100419	0.012933582	Rv0383c
Rv0384c	-3.07	9.676341797	3.84E-08	clpB
Rv0405	0.34	9.952813998	0.021055971	pk6
Rv0418	0.26	8.143600385	0.032906715	lpqL
Rv0440	-2.05	12.901398	2.72E-08	groEL2
Rv0456B	0.97	2.898525553	0.021131898	mazE1
Rv0457c	0.78	5.65877132	0.000398454	Rv0457c
Rv0458	-0.50	7.364912798	0.005077163	Rv0458
Rv0459	-0.81	5.052613343	0.004511768	Rv0459
Rv0464c	-0.32	7.395790124	0.034053821	Rv0464c
Rv0467	-0.90	7.383983361	0.001289494	icl1
Rv0470A	0.85	4.622647405	0.005395874	Rv0470A
Rv0472c	0.30	7.294210641	0.02090826	Rv0472c
Rv0474	-0.70	7.839127838	8.73E-05	Rv0474
Rv0475	-0.28	9.526078802	0.031751124	hbhA
Rv0483	1.02	7.719983484	0.000455641	lprQ
Rv0485	0.76	7.959554014	0.000352206	Rv0485
Rv0515	0.84	5.584821158	0.000249838	Rv0515
Rv0519c	0.58	5.587731534	0.014907295	Rv0519c
Rv0531	0.75	3.15936714	0.027429707	Rv0531
Rv0538	1.10	5.731003543	9.95E-05	Rv0538
Rv0542c	0.98	5.185862316	0.002357354	menE
Rv0544c	1.63	4.15103248	0.000618002	Rv0544c
Rv0563	-1.57	6.555561514	1.18E-06	htpX
Rv0570	0.63	6.244805201	0.044817776	nrdZ

Rv0577	-0.37	7.941860698	0.015987637	TB27.3
Rv0613c	0.52	8.589901849	0.000738361	Rv0613c
Rv0633c	0.37	6.369975354	0.021055971	Rv0633c
Rv0640	0.31	11.1675544	0.01234695	rplK
Rv0646c	0.79	6.358469829	0.001407875	lipG
Rv0649	2.15	-2.242484826	0.032461827	fabD2
Rv0658c	0.49	6.620320146	0.010419703	Rv0658c
Rv0668	0.76	12.59468046	0.000113356	rpoC
Rv0684	0.25	12.1038145	0.034764128	fusA1
Rv0688	-0.58	7.553565606	0.001533208	Rv0688
Rv0695	1.08	6.95386961	2.09E-05	Rv0695
Rv0696	0.38	6.911856246	0.017762704	Rv0696
Rv0698	0.49	4.838881225	0.008204772	Rv0698
Rv0707	0.26	10.60162439	0.015559411	rpsC
Rv0710	0.80	11.59248526	0.000211879	rpsQ
Rv0749A	-0.52	3.771671349	0.025067595	Rv0749A
Rv0751c	-0.52	6.010389936	0.020199545	mmsB
Rv0752c	-1.00	7.287801607	0.00024828	fadE9
Rv0753c	-1.11	7.858567144	0.000155969	mmsA
Rv0822c	1.01	7.932161077	2.25E-06	Rv0822c
Rv0823c	0.60	9.2923997	0.000184207	Rv0823c
Rv0824c	1.01	11.84867232	2.66E-06	desA1
Rv0831c	0.27	9.568846025	0.027533885	Rv0831c
Rv0847	-1.24	3.714738882	0.000757822	lpqS
Rv0853c	-0.36	5.673231676	0.028467164	pdc
Rv0854	-0.43	5.592671957	0.014664097	Rv0854
Rv0859	-1.14	7.875452588	0.0003213	fadA
Rv0860	-1.05	9.810811709	6.50E-05	fadB
Rv0867c	1.50	7.712693512	0.001116444	rpfA
Rv0869c	0.70	5.231534987	0.000410625	moaA2
Rv0878c	0.53	6.562058248	0.013473284	PPE13
Rv0885	-1.43	6.490337378	6.73E-06	Rv0885
Rv0886	-0.48	6.566809126	0.025773721	fprB
Rv0888	-0.71	6.765584429	0.003093792	Rv0888
Rv0890c	0.27	6.984359908	0.041274177	Rv0890c
Rv0896	0.97	10.55211852	6.45E-05	gltA2
Rv0905	0.62	7.496633449	0.000822359	echA6
Rv0906	1.14	5.685611795	0.000100548	Rv0906
Rv0908	0.39	7.640848346	0.003966362	ctpE
Rv0931c	0.47	10.32437211	0.00135702	pknD
Rv0932c	0.52	10.63240054	0.000276845	pstS2
Rv0951	0.61	9.982395677	0.003206709	sucC
Rv0952	0.51	7.787528779	0.005553871	sucD

Rv0953c	-0.91	3.545166839	0.003193447	Rv0953c
Rv0972c	-0.67	6.308355936	0.000579391	fadE12
Rv0973c	-0.70	4.982909059	0.008394297	accA2
Rv0974c	-1.15	4.16581073	0.010587544	accD2
Rv0976c	-1.16	4.091227261	0.003193447	Rv0976c
Rv0990c	-1.95	3.001900505	0.000165702	Rv0990c
Rv0991c	-3.09	7.281050649	1.43E-07	Rv0991c
Rv0999	0.52	4.712055846	0.007998177	Rv0999
Rv1013	-0.33	7.12209282	0.03915985	pks16
Rv1020	0.83	7.540986236	5.26E-05	mfd
Rv1038c	-0.94	3.781754881	0.00632084	esxJ
Rv1057	2.71	3.843609177	7.72E-05	Rv1057
Rv1061	0.30	6.679996873	0.045235091	Rv1061
Rv1067c	2.11	1.426473994	0.00095648	PE_PGRS19
Rv1073	-2.81	9.626183198	6.66E-09	Rv1073
Rv1092c	1.06	6.29639731	0.003022166	coaA
Rv1094	0.92	12.26387559	6.34E-05	desA2
Rv1107c	0.58	8.08376771	0.003030281	xseB
Rv1115	0.57	4.230445404	0.024128262	Rv1115
Rv1134	1.69	2.321250106	0.009372238	Rv1134
Rv1148c	-0.78	7.377639739	0.0053092	Rv1148c
Rv1172c	-0.52	8.395996067	0.000349831	PE12
Rv1175c	-0.37	7.240156826	0.020071903	fadH
Rv1177	0.59	9.104570885	0.004719992	fdxC
Rv1185c	0.53	11.07392492	0.000420597	fadD21
Rv1229c	0.33	8.49131474	0.005077163	mrp
Rv1242	-0.54	3.717313457	0.036142366	vapC33
Rv1279	-0.58	7.605377378	0.001048965	Rv1279
Rv1280c	-0.26	7.670597552	0.023822051	oppA
Rv1285	-4.44	6.250228956	6.17E-08	cysD
Rv1286	-4.57	7.346828651	6.66E-09	cysN
Rv1290c	1.09	5.445120888	2.14E-05	Rv1290c
Rv1292	0.35	6.972528426	0.031287276	argS
Rv1295	0.51	8.615953639	0.003040495	thrC
Rv1308	0.31	11.29414868	0.004440889	atpA
Rv1324	0.24	9.222076633	0.038753472	Rv1324
Rv1326c	0.38	7.492655595	0.003651545	glgB
Rv1327c	0.31	8.057705199	0.026393543	glgE
Rv1363c	0.68	7.017113145	0.027904744	Rv1363c
Rv1378c	1.27	5.820080492	0.001414404	Rv1378c
Rv1385	0.79	3.435263471	0.007448015	pyrF
Rv1391	0.99	9.243134259	8.23E-05	dfp
Rv1392	0.38	9.476446246	0.002976299	metK

Rv1394c	-0.70	4.744613533	0.012184982	cyp132
Rv1411c	0.37	9.497439404	0.002040868	lprG
Rv1415	0.51	9.194412703	0.00770378	ribA2
Rv1450c	1.02	3.759273001	0.010664993	PE_PGRS27
Rv1460	0.73	4.08727292	0.035612896	Rv1460
Rv1475c	-0.59	9.774554762	0.000189481	acn
Rv1481	0.48	8.740559563	0.000352206	Rv1481
Rv1485	0.74	6.24184855	0.000330159	hemZ
Rv1490	0.66	4.784439918	0.010468352	Rv1490
Rv1504c	0.43	5.865716455	0.021496508	Rv1504c
Rv1505c	0.59	7.009616074	0.000672632	Rv1505c
Rv1529	-0.88	6.14524087	0.000369556	fadD24
Rv1535	-1.31	6.162462311	0.000334418	Rv1535
Rv1536	-0.73	8.560151905	9.30E-05	ileS
Rv1553	-1.55	1.184768829	0.044934347	frdB
Rv1563c	0.40	5.023662015	0.019019312	treY
Rv1564c	0.32	8.042144868	0.019644861	treX
Rv1565c	0.44	7.469228691	0.005047259	Rv1565c
Rv1573	1.02	3.657882314	0.001358282	Rv1573
Rv1596	-0.53	9.440572126	0.000384723	nadC
Rv1622c	-0.72	6.937459459	0.000210344	cydB
Rv1635c	0.80	5.944929563	0.001101911	Rv1635c
Rv1636	0.47	8.584857416	0.001227317	TB15.3
Rv1639c	-0.37	7.665228808	0.028319302	Rv1639c
Rv1642	0.59	11.70862964	0.010162158	rpml
Rv1661	0.29	8.289766837	0.025067595	pks7
Rv1676	0.40	7.522561473	0.003966362	Rv1676
Rv1680	0.70	6.183874504	0.000787914	Rv1680
Rv1691	0.77	5.760679213	0.01050485	Rv1691
Rv1696	0.62	6.487304344	0.000405706	recN
Rv1702c	1.30	6.85113984	0.000108193	Rv1702c
Rv1710	0.34	7.016927285	0.038753472	scpB
Rv1712	0.63	6.258697851	0.005077163	cmk
Rv1732c	0.55	5.977530689	0.008204772	Rv1732c
Rv1738	0.90	8.535881355	0.038082325	Rv1738
Rv1751	0.48	8.480435808	0.007012566	Rv1751
Rv1752	0.74	5.012343728	0.002826678	Rv1752
Rv1759c	0.67	3.381429981	0.020085672	wag22
Rv1778c	0.85	4.717349163	0.004345916	Rv1778c
Rv1779c	2.11	6.953621587	4.55E-06	Rv1779c
Rv1780	0.43	5.750515784	0.01159208	Rv1780
Rv1792	-0.28	10.09735558	0.016439913	esxM
Rv1806	-1.27	3.876950893	0.002215327	PE20

Rv1807	-1.24	3.495255693	0.001652256	PPE31
Rv1813c	-1.03	6.443062099	0.024397804	Rv1813c
Rv1837c	0.40	10.70456375	0.002702336	glcB
Rv1842c	0.56	6.508928723	0.001955344	Rv1842c
Rv1854c	0.87	7.220210913	0.000189481	ndh
Rv1856c	-1.73	6.473872383	1.30E-07	Rv1856c
Rv1857	-1.49	6.851292109	2.01E-05	modA
Rv1869c	0.36	9.540455974	0.007527442	Rv1869c
Rv1875	-1.24	5.035016893	0.000181251	Rv1875
Rv1883c	-0.36	8.614114947	0.014154417	Rv1883c
Rv1895	1.42	5.275333234	1.50E-06	Rv1895
Rv1898	0.57	6.928371066	0.015502508	Rv1898
Rv1905c	0.68	6.668911392	0.000875911	aao
Rv1907c	-1.06	5.610852726	0.000156027	Rv1907c
Rv1908c	-1.00	8.815431066	5.23E-06	katG
Rv1925	1.06	10.57000061	0.000299529	fadD31
Rv1932	0.38	8.070832077	0.009467309	tpx
Rv1945	-0.45	4.872062423	0.031661953	Rv1945
Rv1954A	-0.73	6.445797898	0.000881263	Rv1954A
Rv1955	-0.88	6.356802187	0.000815922	higB
Rv1987	0.39	8.317925409	0.01248116	Rv1987
Rv1989c	-0.80	4.809105133	0.0039803	Rv1989c
Rv1990c	-0.72	6.58767983	0.001809807	Rv1990c
Rv1994c	-0.59	5.822720907	0.017398366	cmtR
Rv1996	1.59	8.008819908	0.001701187	Rv1996
Rv2016	-2.73	6.043518971	1.40E-07	Rv2016
Rv2024c	-0.37	6.75921396	0.019954439	Rv2024c
Rv2034	-1.25	2.380467807	0.011095371	Rv2034
Rv2035	-1.47	4.761892051	4.51E-05	Rv2035
Rv2036	-1.07	4.322522802	0.000348473	Rv2036
Rv2092c	0.54	9.016812144	0.000155366	helY
Rv2095c	1.21	5.64720705	0.001752757	paFC
Rv2100	0.65	4.234495825	0.028467164	Rv2100
Rv2107	0.60	4.025907869	0.016439913	PE22
Rv2115c	-0.26	9.879955456	0.024128262	mpa
Rv2130c	0.55	7.782043861	0.002654387	mshC
Rv2144c	-0.31	8.733923206	0.008616683	Rv2144c
Rv2145c	0.44	10.57475487	0.005465455	wag31
Rv2150c	0.36	10.31311532	0.02041452	ftsZ
Rv2151c	0.63	5.720727143	0.001358282	ftsQ
Rv2178c	0.24	8.110652477	0.031181191	aroG
Rv2187	-0.47	7.629870404	0.008913645	fadD15
Rv2215	0.41	9.232746091	0.001426775	dlaT

Rv2222c	0.26	9.084380979	0.031196414	glnA2
Rv2230c	0.68	5.996030147	0.000738361	Rv2230c
Rv2241	0.48	9.909111255	0.001983813	aceE
Rv2273	1.34	2.28635669	0.003030281	Rv2273
Rv2332	0.45	5.307644304	0.021075378	mez
Rv2334	0.34	7.917830144	0.019231938	cysK1
Rv2335	0.68	6.29466816	0.000473356	cysE
Rv2339	0.31	8.566730265	0.011463064	mmpL9
Rv2346c	-0.59	9.613577538	0.001935871	esxO
Rv2347c	-0.43	10.6571761	0.002702336	esxP
Rv2348c	-0.37	11.16104339	0.007487376	Rv2348c
Rv2352c	-0.62	7.608236499	0.003241562	PPE38
Rv2358	1.40	4.503695257	0.004853781	smtB
Rv2364c	0.50	6.684527389	0.005293222	era
Rv2365c	1.50	2.688272169	0.00125857	Rv2365c
Rv2378c	0.55	5.412374491	0.016439913	mbtG
Rv2380c	1.07	6.57852011	7.30E-06	mbtE
Rv2390c	-0.36	5.628200394	0.03492054	Rv2390c
Rv2398c	-0.75	5.779387845	0.000827043	cysW
Rv2400c	-0.70	6.524310335	0.000131643	subI
Rv2406c	-0.63	5.200387422	0.008204772	Rv2406c
Rv2410c	-0.53	6.85139083	0.004129618	Rv2410c
Rv2424c	0.77	3.292287137	0.028467164	Rv2424c
Rv2428	0.90	6.055490931	0.005425527	ahpC
Rv2429	0.65	4.716134457	0.01368368	ahpD
Rv2432c	-0.41	7.531182233	0.034281286	Rv2432c
Rv2436	1.36	3.38616015	0.004673928	rbsK
Rv2438c	0.33	8.880250208	0.005378755	nadE
Rv2444c	0.46	11.06027351	0.000463217	rne
Rv2450c	3.63	3.261089258	0.000109606	rpfE
Rv2454c	-0.44	7.648067909	0.009229805	Rv2454c
Rv2455c	0.31	9.807297838	0.020071903	Rv2455c
Rv2456c	0.41	6.588431192	0.011489859	Rv2456c
Rv2459	-0.75	6.723127983	0.001698093	Rv2459
Rv2463	0.26	8.445632287	0.020900924	lipP
Rv2466c	-4.10	5.679324383	1.14E-08	Rv2466c
Rv2476c	0.31	10.03533196	0.007775872	gdh
Rv2483c	-0.65	8.097618235	0.001222535	plsC
Rv2484c	-0.37	8.024687991	0.021195145	Rv2484c
Rv2485c	-1.48	4.932885674	0.007443607	lipQ
Rv2504c	-0.68	7.003454099	0.003744394	scoA
Rv2516c	-1.89	6.283053021	4.34E-07	Rv2516c
Rv2519	0.46	7.603455068	0.005955103	PE26

Rv2524c	0.55	11.36763428	0.003182764	fas
Rv2531c	0.27	7.990165552	0.025067595	Rv2531c
Rv2542	-0.42	5.906707509	0.040883521	Rv2542
Rv2550c	0.69	4.981465926	0.025003845	vapB20
Rv2579	-0.76	4.738120454	0.003279259	dhaA
Rv2620c	-2.38	6.177109743	6.52E-08	Rv2620c
Rv2632c	-0.69	7.432800964	0.000704862	Rv2632c
Rv2641	-0.59	4.488870228	0.038082325	cadI
Rv2643	-2.16	4.162144421	1.19E-05	arsC
Rv2672	0.40	6.349415837	0.016039326	Rv2672
Rv2676c	0.57	6.846870936	0.006198992	Rv2676c
Rv2707	-0.59	7.694543236	0.002034114	Rv2707
Rv2708c	0.59	9.557679723	0.00391406	Rv2708c
Rv2710	-1.76	10.95743642	1.40E-07	sigB
Rv2719c	0.57	6.001682647	0.008616683	Rv2719c
Rv2724c	-0.82	7.562474494	0.001237416	fadE20
Rv2744c	-2.08	9.254182792	6.45E-08	35kd_ag
Rv2745c	-2.23	9.965354909	2.24E-07	Rv2745c
Rv2782c	0.84	8.603348416	5.18E-05	pepR
Rv2792c	0.48	8.222887116	0.015585329	Rv2792c
Rv2816c	0.56	5.294004818	0.02102767	Rv2816c
Rv2819c	-0.31	6.154746	0.041082507	Rv2819c
Rv2846c	-0.46	9.193030695	0.001245419	efpA
Rv2858c	0.61	6.234442645	0.001952561	aldC
Rv2860c	0.53	5.826701944	0.007588665	glnA4
Rv2913c	-2.60	6.796639614	7.19E-07	Rv2913c
Rv2929	-0.37	5.424148831	0.040351523	Rv2929
Rv2930	0.65	9.576108307	0.0047719	fadD26
Rv2931	1.15	10.1958592	4.93E-05	ppsA
Rv2932	1.67	9.421367729	4.69E-06	ppsB
Rv2933	2.07	9.677442679	2.66E-06	ppsC
Rv2934	2.06	8.960643225	6.22E-08	ppsD
Rv2935	1.09	9.665149631	3.09E-05	ppsE
Rv2936	1.04	8.112512339	4.22E-06	drrA
Rv2937	0.93	6.234287393	0.001308771	drrB
Rv2938	1.10	6.715822553	0.000220532	drrC
Rv2939	1.14	8.534824046	3.73E-06	papA5
Rv2940c	0.64	11.79727421	0.000255705	mas
Rv2942	0.60	9.802161832	0.000200567	mmpL7
Rv2946c	1.15	10.60005402	9.43E-05	pkS1
Rv2949c	0.33	10.11820974	0.016101381	Rv2949c
Rv2987c	-2.34	8.615245336	3.35E-06	leuD
Rv3032	1.00	5.910420333	0.002784102	Rv3032

Rv3047c	-1.32	5.773411145	5.94E-05	Rv3047c
Rv3053c	-0.79	9.881604514	4.71E-05	nrdH
Rv3054c	-3.12	4.287530998	1.50E-06	Rv3054c
Rv3060c	-0.58	6.254383261	0.001955344	Rv3060c
Rv3061c	-0.88	7.376419156	0.000127231	fadE22
Rv3064c	-0.95	2.208533614	0.016439913	Rv3064c
Rv3083	-0.91	8.822163414	0.007555027	Rv3083
Rv3086	-0.56	8.468565167	0.008501841	adhD
Rv3092c	0.83	7.097312473	0.001075901	Rv3092c
Rv3093c	2.04	6.111097887	0.000297512	Rv3093c
Rv3094c	1.18	5.242639701	0.000762962	Rv3094c
Rv3098c	-0.80	3.643912325	0.008501841	Rv3098c
Rv3101c	-0.28	7.384510108	0.036705232	ftsX
Rv3103c	0.53	4.780811397	0.016287812	Rv3103c
Rv3130c	1.13	9.807780402	0.009236126	tgs1
Rv3131	1.12	8.245803362	0.01771258	Rv3131
Rv3139	0.65	9.125130148	0.000858331	fadE24
Rv3140	0.42	9.110596956	0.008587941	fadE23
Rv3146	-0.29	8.449999081	0.023952641	nuoB
Rv3161c	-0.68	7.251005559	0.000519253	Rv3161c
Rv3168	2.72	8.315261777	1.24E-08	Rv3168
Rv3169	2.24	7.78700103	2.39E-08	Rv3169
Rv3170	1.10	5.455208198	4.71E-05	aofH
Rv3182	-0.51	4.031398022	0.040071594	Rv3182
Rv3197A	-1.63	5.433277893	1.02E-05	whiB7
Rv3202c	0.44	5.916954093	0.025067595	Rv3202c
Rv3206c	-0.89	8.247049421	2.60E-05	moeB1
Rv3229c	-4.79	9.483635988	3.35E-06	desA3
Rv3230c	-1.75	7.003253697	2.01E-05	Rv3230c
Rv3232c	-0.59	8.027051965	0.002417221	ppk2
Rv3237c	-0.76	6.754278438	0.000762771	Rv3237c
Rv3265c	0.43	6.908482778	0.025019682	wbbL1
Rv3289c	-1.87	4.264361825	7.16E-06	Rv3289c
Rv3290c	-1.93	7.722252037	6.46E-07	lat
Rv3336c	0.35	7.28463209	0.009836564	trpS
Rv3338	-0.93	4.638205939	0.002049407	Rv3338
Rv3339c	0.36	7.491275856	0.014907295	icd1
Rv3343c	0.43	7.4053274	0.005077163	PPE54
Rv3370c	0.89	4.403634656	0.036903537	dnaE2
Rv3382c	0.40	6.121354804	0.032572578	lytB1
Rv3390	-0.97	6.732890317	0.00125857	lpqD
Rv3395c	1.23	4.686237236	0.000155366	Rv3395c
Rv3396c	0.39	7.897764589	0.003030281	guaA

Rv3413c	0.81	6.959196046	0.000110118	Rv3413c
Rv3417c	-2.40	10.63131511	1.14E-08	groEL1
Rv3418c	-2.76	11.0546563	6.66E-09	groES
Rv3427c	0.71	5.776677183	0.007048177	Rv3427c
Rv3456c	0.26	10.89515626	0.025019682	rplQ
Rv3467	0.55	4.436252893	0.045660636	Rv3467
Rv3477	-0.53	10.66143599	0.009417375	PE31
Rv3484	0.44	7.711612044	0.008188992	cpsA
Rv3485c	0.57	6.696606949	0.00361171	Rv3485c
Rv3490	0.20	9.261384606	0.039683417	otsA
Rv3524	0.37	6.958190476	0.015559411	Rv3524
Rv3526	-1.45	9.125610999	6.05E-05	kshA
Rv3534c	-1.19	4.910782164	5.54E-05	hsaF
Rv3544c	-0.78	5.436096951	0.000356281	fadE28
Rv3547	-0.58	5.815195782	0.001823464	ddn
Rv3569c	-1.45	5.760805937	4.73E-06	hsaD
Rv3570c	-1.42	7.140229991	5.89E-05	hsaA
Rv3596c	0.24	12.34875111	0.022069771	clpC1
Rv3610c	0.42	9.279807602	0.009836564	ftsH
Rv3612c	-2.38	5.664458147	1.24E-07	Rv3612c
Rv3613c	-2.31	6.712940803	3.90E-07	Rv3613c
Rv3614c	-2.27	10.31201516	9.36E-07	espD
Rv3615c	-2.43	7.975674669	3.74E-06	espC
Rv3616c	-2.05	10.75114322	7.17E-07	espA
Rv3618	-1.48	4.219198446	0.000306562	Rv3618
Rv3624c	0.30	5.965976938	0.041144093	hpt
Rv3625c	1.54	4.307355544	0.00344428	mesJ
Rv3629c	-0.69	4.688568374	0.003469403	Rv3629c
Rv3633	-1.01	6.596792822	0.000133817	Rv3633
Rv3645	0.91	6.827040942	3.57E-05	Rv3645
Rv3711c	0.37	6.071679292	0.009807115	dnaQ
Rv3719	0.28	8.855916676	0.022266906	Rv3719
Rv3720	0.26	7.671143905	0.032788724	Rv3720
Rv3733c	-0.79	6.098355961	0.003651545	Rv3733c
Rv3734c	-0.80	6.793861641	0.000324032	tgs2
Rv3753c	-0.66	5.05264134	0.016463686	Rv3753c
Rv3759c	0.31	6.923594395	0.02102767	proX
Rv3763	-0.73	7.661651336	0.000142346	lpqH
Rv3769	0.39	5.863271194	0.043930996	Rv3769
Rv3775	0.54	5.73100955	0.005086391	lipE
Rv3805c	0.51	8.946481531	0.000432147	aftB
Rv3807c	0.68	7.176149155	0.00093371	Rv3807c
Rv3812	0.38	5.706780936	0.021055971	PE_PGRS62

Rv3823c	-0.48	9.429228357	0.002305812	mmpL8
Rv3825c	-0.41	10.60329107	0.006336635	pks2
Rv3828c	-0.45	5.961556422	0.014127026	Rv3828c
Rv3830c	-0.91	2.873908526	0.007487376	Rv3830c
Rv3852	0.63	10.54509372	0.012866179	hns
Rv3862c	1.03	2.603203942	0.025067595	whiB6
Rv3869	0.57	8.558735561	0.001432876	eccB1
Rv3870	0.36	10.08024045	0.007443607	eccCa1
Rv3873	0.51	8.764332197	0.013473284	PPE68
Rv3903c	0.39	6.173952471	0.04753363	Rv3903c
Rv3907c	0.33	7.315318985	0.019448194	pcnA
Rv3910	0.35	8.372159285	0.009741057	Rv3910
Rv3917c	0.59	9.242411279	0.000274255	parB
Rv3918c	0.42	7.933305257	0.009042966	parA
Rv3919c	0.41	9.200841193	0.003425156	gid
Rv3920c	0.55	11.46778945	0.000483987	Rv3920c
Rv3921c	0.71	11.23121312	5.84E-05	Rv3921c